Food and Agriculture Organization of the United Nations

Indian Ocean Tuna Commission
Commission des Thons de l'Ocean Indien
iotc ctoi

IOTC-2026-WPB24-27

STOCK ASSESSMENT OF INDIAN OCEAN SWORDFISH (*XIPHIAS GLADIUS*) USING STOCK SYNTHESIS (2026)

GENEVIEVE A.C. PHILLIPS

Discussions, Feedback, Recommendations, and Decisions:

This report presents an integrated stock assessment for *X. gladius* in the Indian Ocean in 2026, using data up to the end of 2024 (31st December 2024). The stock assessment is based on an update of the 2023 model and is a spatially structured, sex-based, age-structured integrated model that uses catch rate indices, length-compositions, catch data to inform estimates of spawning stock biomass (SSB) and fishing mortality (F), relative to estimated maximum sustainable yield (MSY).

The assessment was completed using Stock Synthesis 3.30.25.1 and incorporates all newly available data since the previous assessment.

This assessment provides information on stock status, but is not used for management advice, as there is a management procedure in place for *X. gladius* (Resolution 24/08).

The report is the first iteration of the assessment and requires members of the Working Party on Billfish to read the report and agree or provide additional advice on the grid / model ensemble, so that the assessment can be finalised during the meeting.

Abstract

Indian Ocean swordfish (*Xiphias gladius*) are a large pelagic species, broadly distributed throughout the Indian Ocean to a southern limit of 50°south. Swordfish are highly fecund, migratory fish that grow quickly when young, and reach maximum size at approximately 15 yrs of age. Swordfish have a wider geographical distribution than other billfish and routinely move between surface waters and the deep seas. They are not known to form schools. Female swordfish are thought to grow faster and live longer than males and may have different spatial distributions depending on body size.

This report presents an integrated stock assessment for *X. gladius* in the Indian Ocean in 2026, using data up to the end of 2024 (31st December 2024). The stock assessment is based on an update of the 2023 model and is a spatially structured, sex-based, age-structured integrated model that uses catch rate indices, length-compositions and catch data to inform estimates of spawning stock biomass (SSB) and fishing mortality (F), relative to estimated maximum sustainable yield (MSY).

The Stock Synthesis 3.30 (SS3.30.25.1) assessment model covers the period 1950-2024 and assumes that the Indian Ocean swordfish constitutes a single genetic stock, modelled as four spatially disaggregated regions, with 15 fishing fleets. Standardised catch per unit effort (CPUE) series from the main longline fleets from Japan, Taiwan (China), European Union (Portugal; Spain' Réunion), South Africa, and Indonesia were available for the assessment. The reference model included Japanese longline CPUE only.

In 2026, the overall stock status for Indian Ocean swordfish is that the stock is **not overfished** and **not subject to overfishing** with a likelihood of 100 % over an ensemble of 48 models that encompass the main uncertainties within the model.

This assessment provides information on stock status, but is not used for management advice, as there is a management procedure in place for *X. gladius* (Resolution 24/08).

IOTC-2026-WPB24-27

Stock assessment of Indian Ocean Swordfish (*Xiphias gladius*) using Stock Synthesis (2026)

Genevieve A.C. Phillips[1]

1. Indian Ocean Tuna Commission Secretariat, FAO

CONTENTS

LIST OF FIGURES

LIST OF TABLES

EXECUTIVE SUMMARY

Introduction

Indian Ocean swordfish (*Xiphias gladius*) are a large pelagic species, broadly distributed throughout the Indian Ocean to a southern limit of 50°south. Swordfish are highly fecund, migratory fish that grow quickly when young, and reach maximum size at approximately 15 yrs of age. Swordfish have a wider geographical distribution than other billfish and routinely move between surface waters and the deep seas. They are not known to form schools. Female swordfish are hypothesised to grow faster and live longer than males and likely have different spatial distributions that change depending on body size.

This report presents an integrated stock assessment for *X. gladius* in the Indian Ocean in 2026, using data up to the end of 2024 (31st December 2024). The stock assessment is based on an update of the 2023 model and is a spatially structured, sex-based, age-structured integrated model that uses catch rate indices, length-compositions and catch data to inform estimates of spawning stock biomass (SSB) and fishing mortality (F), relative to estimated maximum sustainable yield (MSY).

The assessment was completed using Stock Synthesis 3.30.25.1 and incorporates all newly available data since the previous assessment.

This assessment provides information on stock status, but is not used for management advice, as there is a management procedure in place for *X. gladius* (Resolution 24/08).

Methods

The Stock Synthesis 3.30 (SS3.30.25.1) assessment model covers the period 1950-2024 and assumes that the Indian Ocean swordfish constitutes a single genetic stock. The population is modelled as four spatially disaggregated regions, with 15 fishing fleets distributed among these regions. Standardised catch per unit effort (CPUE) series from the main longline fleets from Japan, Taiwan (China), the European Union (Portugal; Spain; Réunion Island), South Africa, and Indonesia were available for the assessment. The reference model included the Japanese longline CPUE only.

It was assumed that CPUE indices were proportional to the regional abundance of swordfish.

Sensitivity scenarios were run to explore the effects of alternative model assumptions with alternative CPUE configurations (inclusion of Japanese/Portuguese/South African indices, or Japanese/Taiwanese (Chinese) /Indonesian indices). After sensitivity analyses, and running of diagnostics, including running retrospectives, jitter analyses, and age-structured production models (ASPM), a biologically relevant, and internally consistent model was chosen as a base model, and the grid run using this model (“**4_update_rec**”).

To account for uncertainty within specific model parameters, several model options were then run using the base model in a ‘grid’ or ensemble of models using a combination of plausible options for various, mainly biological, parameters. This included: three options for the steepness parameter (h = 0.7, 0.8, 0.9); two options for variation in mean recruitment (σ_R = 0.2, 0.4); three options for the instantaneous rate of natural mortality (M); and two options for likely abundance indices (CPUE indices). The model ensemble (a total of 48 models) therefore encompasses a reasonable range of uncertainty, and stock trajectories. Estimates of stock status were combined across the 48 models and incorporate uncertainty estimates from both within and across the model ensemble.

Results

In 2026, the overall stock status for Indian Ocean swordfish is that the stock is **not overfished** and **not subject to overfishing** with a likelihood of 100 % (Figure i, Table i) over an ensemble of 48 models that encompass the main uncertainties within the model. The base model in the figure is **‘SWO_h80_Gold_fixed_r2_JP’.**

Table i: STOCK STATUS INDICATORS FROM MODEL ENSEMBLE

Catch in 2024:	28112
Average catch 2019–2024:	27076
MSY (1000 t) (plausible range):	39 (32-46)
F_{MSY}	0.06 (0.05-0.06)
SSB_0(1000 t) (80% CI):	264 (226-302)
SSB_{2024} (1000 t) (80% CI):	152 (119-185)
SSB_{MSY}	58 (38-77)
SSB_{2024}/SSB_0 (80% CI):	0.58 (0.55-0.61)
SSB_{2024} / SSB_{MSY}	2.81 (1.97-3.64)
F_{2024} / F_{MSY}	0.34 (0.23-0.45)

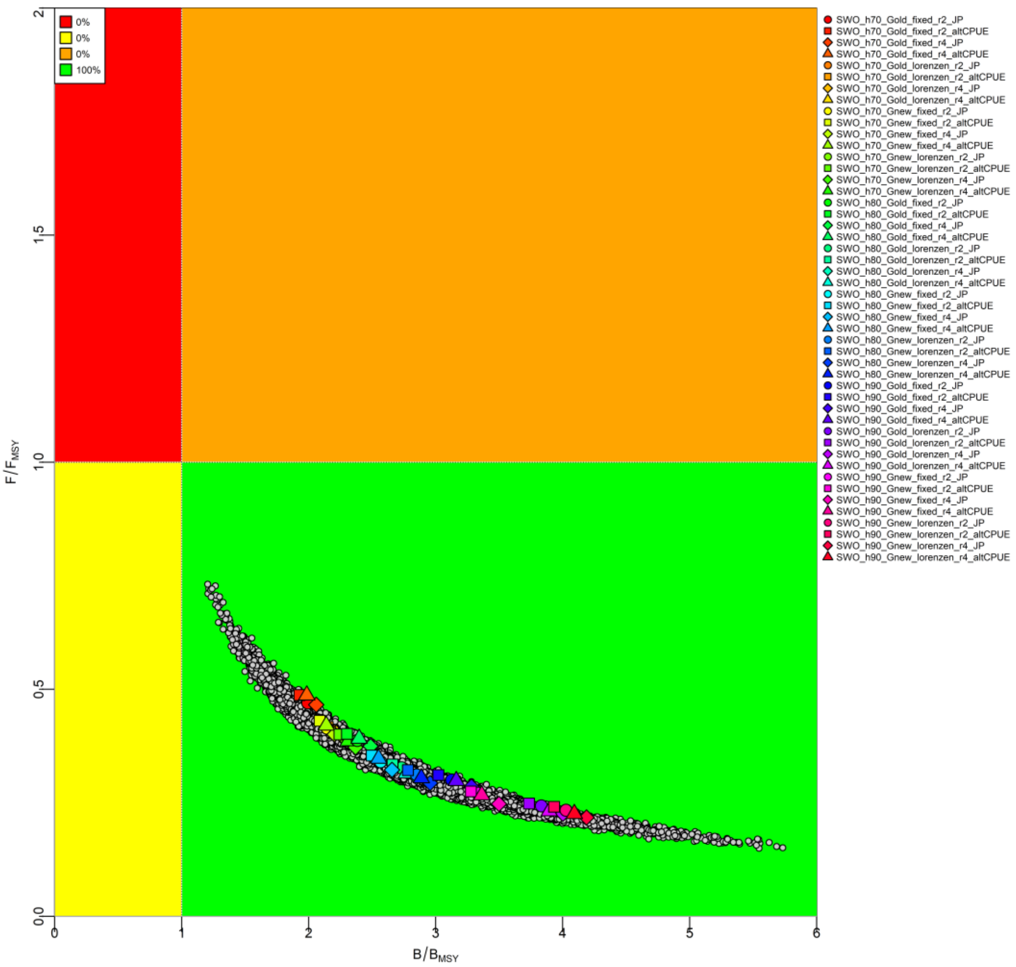

Figure i: Output from the KOBE plots from the ensemble of models in the grid.

In the 2023 assessment (using data up to 2022) the model ensemble estimated that the stock was **not overfished** and **not subject to overfishing**, and the 2020 assessment also estimated the stock to be **not overfished** and **not subject to overfishing**.

The estimated biomass trajectory shows a stock recovering from high exploitation in the mid-2010s to the present year. (Figure ii). Biomass levels appear to be increasing, while catch is below MSY, even with a small increase in the final year of the model. Fishing mortality has also been steadily decreasing from a peak around 2005.

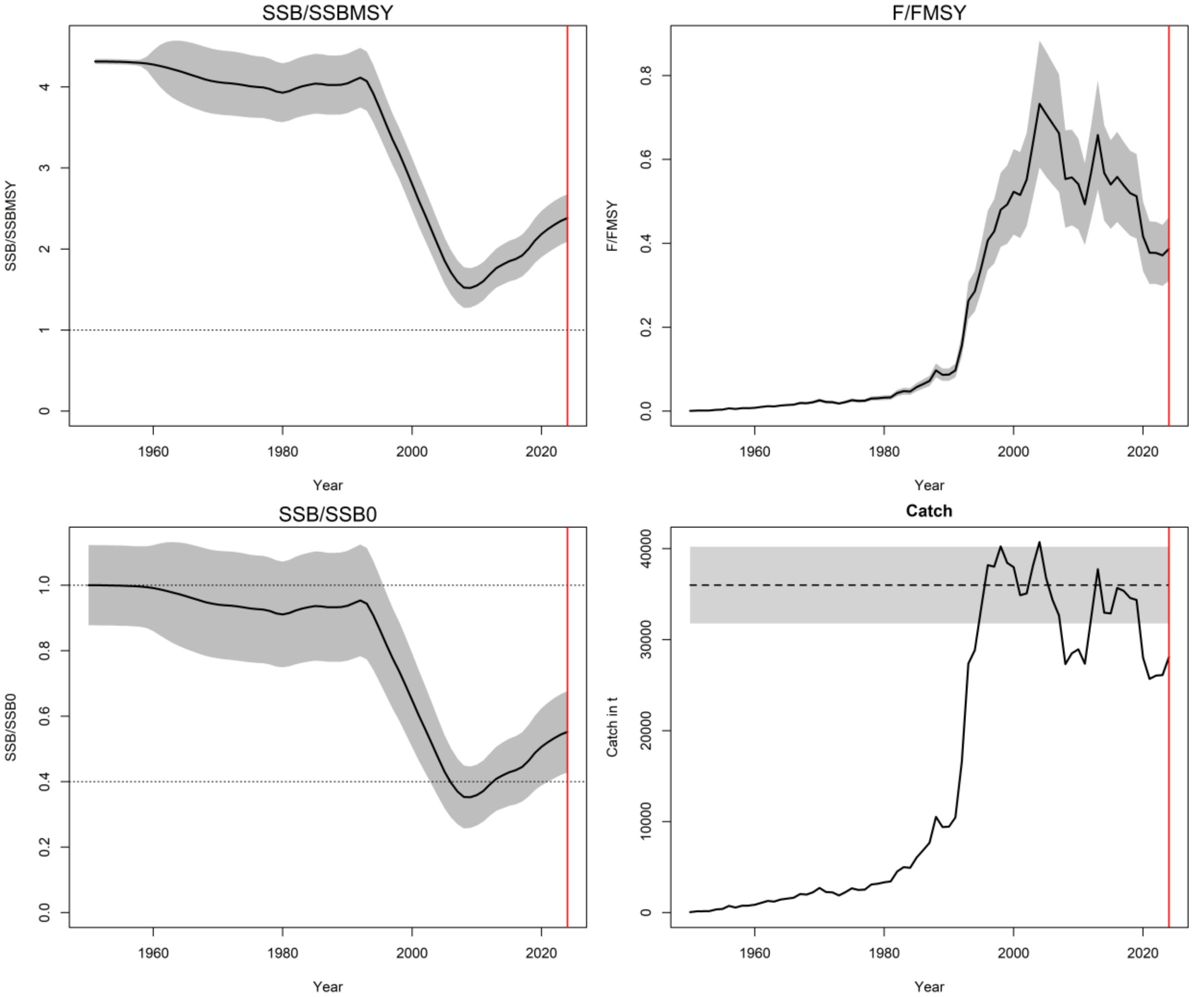

Figure ii: Management outputs from the ensemble of models (grid) used in 2026. Bounds around the main darker line represent the 80% confidence intervals. The grey band on the catch graph represents estimated optimal catch at MSY (80 % confidence interval). The horizontal lines indicate limit or reference points for SSB/SSB$_{MSY}$.

Catch

In the three years since the previous assessment (2022-2024), total catch has averaged 26,759 tonnes per year from all fleets within the fishery (Figure iii).

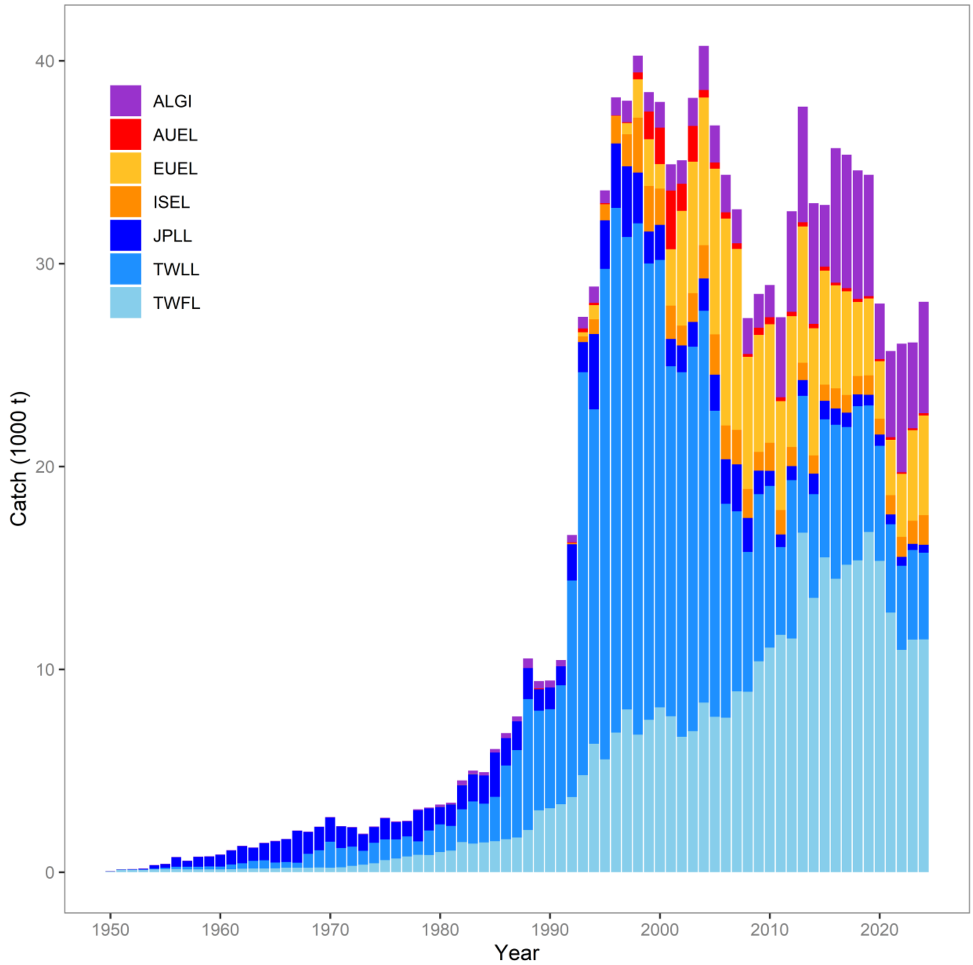

Figure iii: Estimated raised catches for the Indian Ocean swordfish fishery by model fleet from 1950-2024.

Catch rates

Standardised catch rates included in the base model are: (Figure iv). Detailed methods for these indices can be found in the documents provided at the 24th Working Party for Billfish (2026).

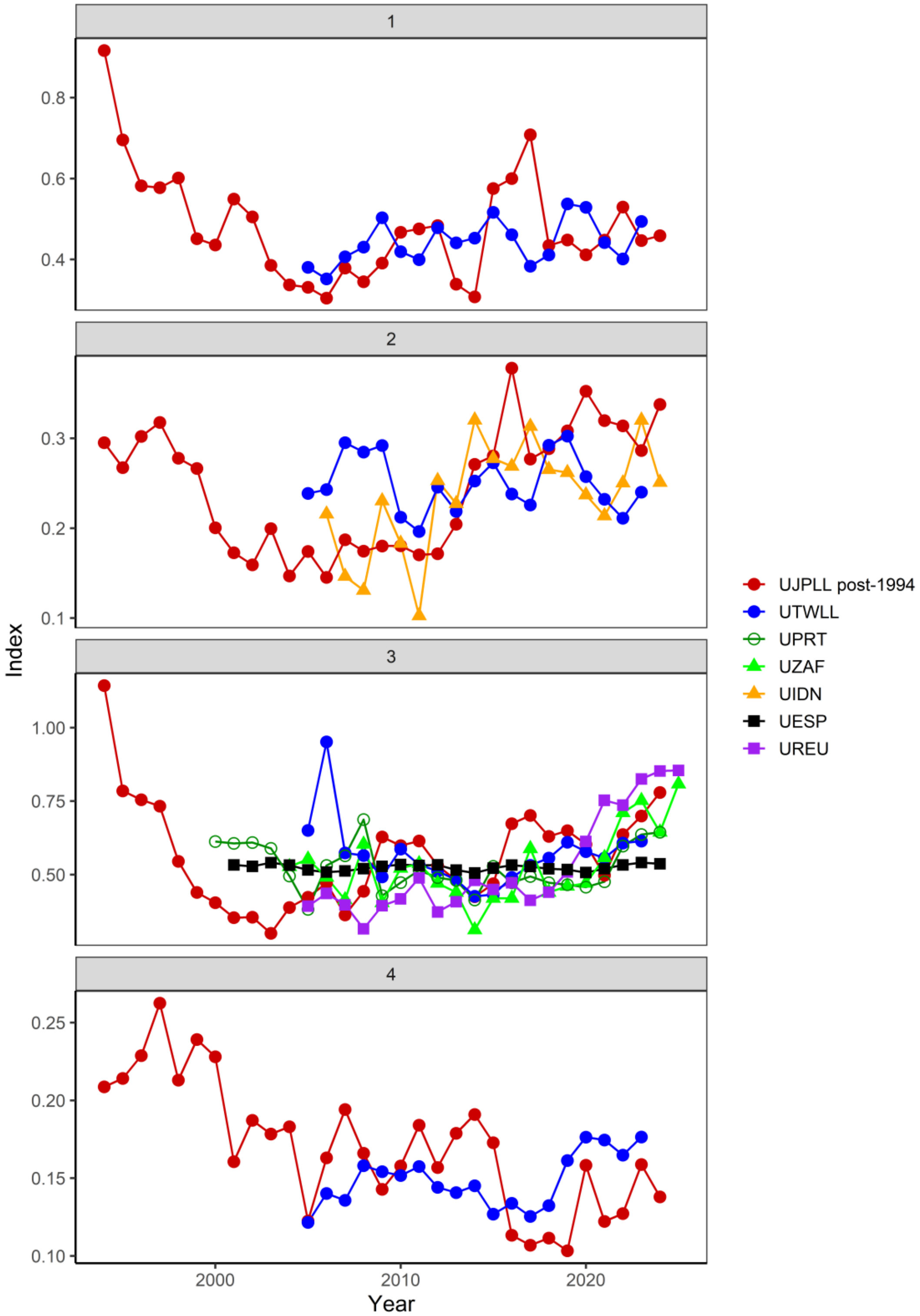

Figure iv: Annual standardised catch rates (CPUE) available for the 2026 model.

Key sensitivities

The model was sensitive to changes to the inclusion of specific CPUE indices, in particular, whether the "flatter" European Union (Spain) or Taiwan (China) indices were used as the main abundance indices. The estimates of biomass provided by model appear to be mostly driven by the recruitment deviates, and removing (fixing) these in the age-structured production models showed the major influence of this parameter. This is a key issue for the model, as these are estimated, based on the abundance indices, and catch data, thereby providing a circular logic within the modelling framework.

Future research should, therefore, focus on improving the sparse biological data available for this species (834 anal fin ray specimens and 181 otoliths have been analysed for age data for Indian Ocean swordfish, which is a start, however no new data have been collected since 2008 in the Indian Ocean). Improving the biological data inputs in the model would reduce the reliance on the CPUE indices as the main driver(s) of biomass estimates in the model.

Recommendations for future assessments

- **Improved quality and quantity of length composition data**: The model is relatively sensitive to the length-frequency data. It is recommended that improvements in both quantity and quality of length frequency data are provided to the Secretariat prior to the next assessment of swordfish in 2029, and that any length data omitted in this assessment are reassessed for suitability and inclusion in 2029. Of particular interest would be sex-specific measurements, considering the model is sex-specific with regards to growth, and currently the model does not assume different length frequencies for individual sexes.
- **Development of independent abundance indices**: as with other assessments in the IOTC, there are no fishery-independent abundance indices included in the stock assessment. Two of the CPC's CPUE indices (Spain (European Union), and Taiwan (China)) show very flat trajectories compared to the other indices – this could be a plausible representation of regional swordfish abundance, which would mean that biomass is extremely high. However, with no independent abundance indices, it is currently not possible to know which of the indices trajectories is biologically accurate. Additionally, as with other IOTC assessments, the CPUE indices are driving the assessment, and the model is estimating recruitment trends based on the estimates of biomass (that are being driven by the CPUE indices). The model is heavily influenced by the estimated recruitment.
- **Ageing data**: It is strongly recommended that more fish are aged, encompassing both male and female fish, from all length-bins across the spatial extent of the fishery, to build a reasonable timeseries of biologically informative data. Age data should be accompanied by detailed information on the source of the fish (e.g. time, date, location, sex, fishing gear, vessel flag etc.) if the data are to be used to either estimate age-at-length within the model (as data need to be allocated to appropriate timesteps, model areas, and model fleets) or to account for changes in age-at-length over time or space (due to population dynamics, environmental factors, such as climate change or high fishing effort). Estimating age within the model allows for more accurate diagnosis of the cause of potential model misspecification. Fish could be aged on a yearly basis, to provide additional information.
- **Transition to a biologically relevant population dynamics model**: Currently the SS3 stock assessment model for Indian Ocean swordfish is partitioned and structured based on fleet dynamics (e.g. data are aggregated into métiers) with an underlying assumption that similar fleets are targeting a similar biological portion of the stock. However, there are little, if any, biological data to support these assumptions, other than fishery-dependent size measurements. As with other IOTC stock assessments, the model would benefit from fishery-independent biological data to support a biologically plausible population dynamics model (e.g. structured based on the biological characteristics of the species, rather than fishery behaviours). This is particularly important if we want to avoid fishing sensitive portions of the stock(s) – e.g. spawning aggregations, or juvenile 'nursery' areas.
- **Incorporation of climate variables**: As stipulated under Resolution 25/01 the IOTC "Commission should support further research into the relationship between climate change, fisheries for IOTC fisheries…and the ecosystems…". Currently the assessment does not incorporate any information on potential changes in population distribution due to climate change. This part of the assessment could benefit from targeted research from CPCs or research organisations.

ACKNOWLEDGEMENTS

This stock assessment was informed by previous assessments of Indian Ocean swordfish (*Xiphias gladius*), and from reading reports of recent assessments undertaken by the International Commission for the Conservation of Atlantic Tunas (ICCAT), the Western and Central Pacific Fisheries Commission (WCPFC), and the Inter-American Tropical Tuna Commission (IATTC) in the Atlantic, Western Pacific, and Eastern Pacific Oceans respectively. The previous assessment provided the starting input parameters, and intersessional discussions provided scenarios to test for model sensitivities, alongside possibilities for the final grid of models presented in this report, that will be discussed and finalised at the 24th meeting of the Working Group for Billfish (Assessment meeting) in September 2026, in Réunion, Republic of France (European Union).

The assessment benefited greatly from updated abundance indices (CPUE) from the following CPCs: Indonesia, Japan, Taiwan (China), European Union (France (Réunion Island); Spain; Portugal), and South Africa.

We thank all the observers who collect and provide biological data for the assessment of swordfish stocks in the IOTC Area of Competence, the IOTC Data Team for providing data to allow for a complete assessment of the stock, and previous stock assessment scientists at the IOTC for their code, and previous models which form the basis of this assessment.

1. INTRODUCTION

This paper presents the preliminary 2026 stock assessment of swordfish (*Xiphias gladius*; SWO) in the Indian Ocean (IO). As in previous assessments, the objectives of the 2026 swordfish assessment are to estimate population level parameters which indicate the stock status and the impacts of fishing, such as time series of recruitment, spawning stock biomass, biomass depletion, and fishing mortality. The stock status is summarised using reference points that are adopted by the Indian Ocean Tuna Commission (IOTC).

The current assessment is carried out using the stock assessment framework Stock Synthesis 3.30 (Methot, 2013, Methot & Werner, 2013) using a length-based, age- and spatially structured population model.

The first formal stock assessments for Indian Ocean swordfish were carried out as surplus production models fitted to catch data and catch per unit effort data (CPUE) at the 5th Working Party on Billfish (WPB). These models provided plausible inferences about the impact of the swordfish fisheries on the Indian Ocean population.

Kolody (2009) conducted preliminary work towards an Indian Ocean swordfish stock assessment using Stock Synthesis. The prime motivation for developing this model was to increase the resolution of spatial processes, so that the differential and possibly elevated depletion in the southwest Indian Ocean could be more explicitly described. The model population was age-structured, sex-based, and spatially disaggregated into four regions. Kolody (2010) and Kolody et al., (2011) updated the assessment, with a separate southwest region model, due to assumptions that the southwest portion of the swordfish population constituted a separate swordfish stock.

In 2014, the Indian Ocean swordfish assessment model was updated (Sharma & Herrera (2014)). Based on newer evidence from Muths et al., (2009, 2013) there were hypothesised to be no distinguishable differences in genetic structure between the southwest region and the rest of the Indian Ocean. Therefore, one assessment was completed for the whole Indian Ocean. Subsequent assessments have also adopted the one-stock hypothesis.

Recent work by Chevrier et al., (2025) using single nucleotide polymorphisms (SNPs) which are more appropriate identifiers of genetic population structure suggest genetic differentiation between the north and south Indian Ocean, split approximately at the equator (pers. comms. Sylvain Bonhommeau). The genetic differentiation is likely caused by a chromosomal inversion, splitting the stock into two sub-populations, however the impact of the chromosomal inversion on reproductive isolation is currently unknown (Chevrier et al., 2025). Migration rates and or potential mixing rates between the northern and southern Indian Ocean are not known, but there is some evidence to suggest that adults may form two sub-populations. In this assessment we elected to continue to use the current stock assessment structure (four regions in the model, based on fishery dynamics rather than population dynamics). We suggest in the future that further biological data are necessary (e.g. growth, age, stronger genetic evidence) to partition the model into true population dynamics-based areas, rather than continuing to structure a model based on fleet dynamics. We therefore encourage CPCs to provide biological data from their regions of the Indian Ocean to support accurate stock assessment.

The assessment in 2017 (Fu 2017) adopted a revised fleet structure by partitioning the longline fishery among several major industrial fleets to better account for the variability in the length compositions. The assessment in 2022 (Fu 2022) continued on from the 2017 model, with the assumption that the Indian Ocean swordfish is one population stock, with spatial disaggregation into four areas (based on fleet dynamics). In the 2022 assessment, a single area model was tested, and the influence of length-frequency data was also tested, along with sensitivity runs using biological parameters.

This report provides an updated stock assessment for Indian Ocean swordfish using fishery data up to the end of 2024 (31st December 2024), building on the previous assessment in 2022, assuming a single

Indian Ocean stock, that is spatially disaggregated into four areas (Figure 1). The model incorporates the following updates:

- Three additional years of catch and length-frequency data (2022, 2023, 2024)
- Revised CPUE series from Japan (NW, NE, SW, SE), Taiwan,China (NW, NE, SW, SE), Portugal (EU) (SW), Spain (EU) (SE), Indonesia (NE), South Africa (SW), and Réunion (EU) (SW).

New information relating to growth of swordfish in the Indian Ocean were made available for this assessment (Wang et al., 2026). The study provided data on sex-specific growth parameters, updating an earlier study (Wang et al., 2010). The analysis used anal-fin ray specimens and cross-validated these data with otolith readings from swordfish collected by Taiwan,China observers based on Indian Ocean longliners between May 2007 and April 2008. These data were used in a sensitivity run of the model, for consideration by the group to replace the current reference growth data which are borrowed from the southwest Pacific Ocean (Farley et al., 2016).

The assessment provides estimates of stock status, and reference management quantities. Model uncertainties are characterised under combinations of model assumptions and parameter values using a grid approach.

Based on the management strategy evaluation developed over several years, the Commission adopted a management procedure (MP) for swordfish through Resolution 24/08. The adopted MP is data-based, relying on a CPUE index as an indicator of recent trends in stock biomass. During implementation of the MP in October 2025, a discrepancy was identified between the approach used to apply the MP for the first time in real-world conditions and the approach used in the MSE (IOTC-2024-WPM15-11). This discrepancy was found not to affect the performance of the MP or the resulting TAC output. Subsequently, in May 2025, a revised management procedure for swordfish was adopted by the IOTC Commission under Resolution 25/07, correcting the minor error identified. The revised MP was applied to determine a recommended TAC of 30,527 t for swordfish. In 2026, under Resolution 26/02, the Commission formally adopted this TAC of 30,527 t per year for the period 2027–2028. A review of evidence for exceptional circumstances was conducted in 2025. The review did not identify any exceptional circumstances impacting on the application of the MP

In summary, this report documents the 2026 iteration of the stock assessment of the Indian Ocean swordfish stock for consideration at the 24th WPB due to be held in Réunion, in September 2026. The stock assessment is based on the 2022 modelling framework and has incorporated revised and updated data up to the end of 2024, and newly available biological information. The assessment implements a length-based, age-structured and spatially explicit population model fitted to catch per unit effort (CPUE, abundance indices), and length composition data. The assessment is implemented in Stock Synthesis (v3.30.25.1). Code to prepare the data and run the models will be made available on Github once the assessment is finalised.

2. BACKGROUND

2.1. Stock structure

The stock structure of adult of adult Indian Ocean swordfish has been examined using several methods, including genetic analyses. The first such study, in 2006 (Lu et al., 2006) described three putative stock delineations based on mitochondrial DNA (mDNA) within the Indian Ocean. The results suggested that samples from the waters off northern Madagascar and the Bay of Bengal formed two distinct groups, separate from other stocks in the Indian Ocean and Western Pacific Ocean. Later, evidence gathered by the Indian Ocean Swordfish Stock Structure (IOSSS-ESPADON) project led by IFREMER, Réunion suggested that there is likely genetic distinction of stocks (Bradman et al., 2010; Bourjea et al., 2011), but results in 2013 (Muths et al., 2013) but the project did not identify clear differences in genetic structure, suggesting it was appropriate to consider Indian Ocean swordfish a single stock in the Indian Ocean.

The most recent genetic analyses, presented at the 23rd Working Party for Billfish in 2025, using newer genetic methods (assessing differences in single nucleotide polymorphisms, SNPs) suggests that there may be two genetic populations of swordfish in the Indian Ocean, split approximately at the equator (Chevrier et al., 2025). However, this study does not include estimates of movement between populations and does not elaborate on the functional importance of the hypothesised chromosomal inversion that causes the genetic differentiation between northern and southern sub-populations of Indian Ocean swordfish. Therefore, for the purposes of this assessment, we have assumed a single stock for the Indian Ocean. However, we recommend revisiting the stock structure within the three years prior to the next assessment, in 2029, as having a biologically appropriate stock structure is fundamental to effective stock assessment modelling.

The current model splits the Indian Ocean into four areas (Fig.1), similar to the areas used in the tropical tunas, however for swordfish there is no movement between these areas. The areas are based purely on fleet dynamics (e.g. aggregating fisheries, or fleets, that have similar gear types, and similar fishing strategies i.e. métiers), with catch per unit effort (CPUE) indices representing the differential “abundance” between the areas.

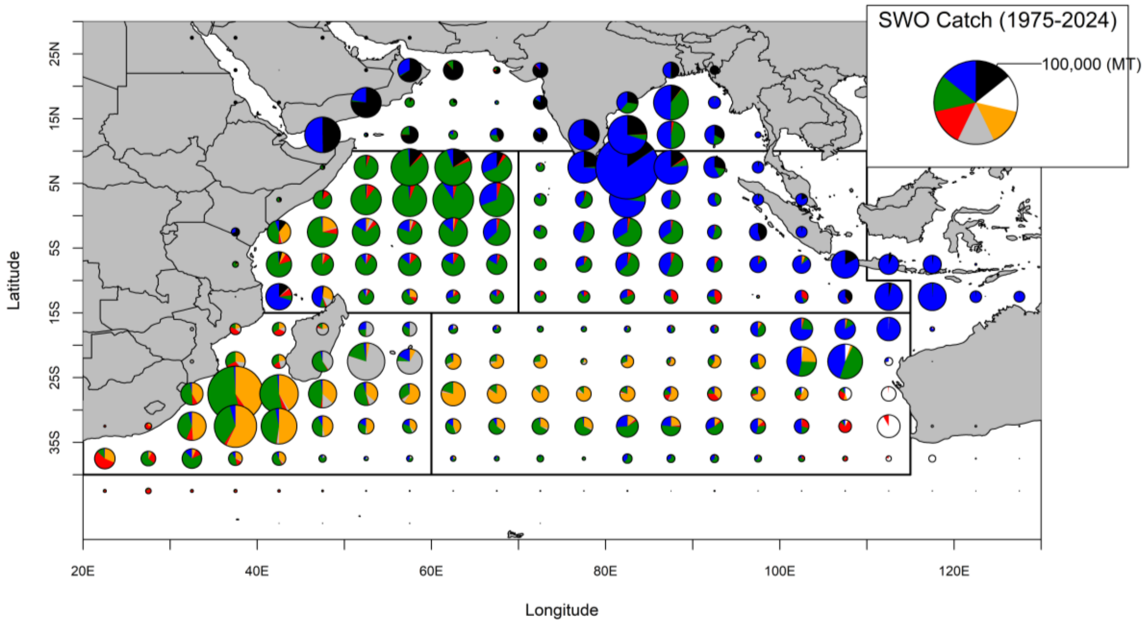

Figure 1: Spatial structure showing the 4 areas used in the assessment model, and distribution of SWO catches in the Indian Ocean by fleet aggregated for 1975-2024.

2.2. Biology

Indian Ocean swordfish (*Xiphias gladius*) are a large pelagic species, broadly distributed throughout the Indian Ocean to a southern limit of 50°south. Swordfish are highly fecund, migratory fish that grow quickly when young, and reach maximum size at approximately 15 yrs of age. Swordfish have a wider geographical distribution than other billfish, and routinely perform diel vertical migrations, remaining in shallow waters at night, and diving to depths of over 400 m during the day (Dewar et al, 2011; Evans et al, 2014; Braun et al., 2019; Bigelow et al, 1999; Abecassis et al., 2012; Abascal et al, 2015).

Swordfish diel vertical migrations are likely driven by both abiotic (temperature, salinity, currents), and biotic factors (physiology, prey availability), moving to cooler waters during the day, and / or chasing preferred prey items such as Teuthoidea (squids), Teleostei (ray-finned fishes), and Crustacea (e.g. crabs) (Preti et al, 2023; Potier et al., 2007, 2008). It is unclear whether swordfish are opportunistic predators, or have preferential feeding on certain taxa, as prey is varied, but also correlated with positioning within the water column during feeding hours.

Although daily movements of Indian Ocean swordfish are unclear, daily displacements of Atlantic Ocean swordfish are between 24 – 100 km / day, with some individuals travelling up to 10,000 km over the course of a study (Abascal et al., 2015). If similar in the Indian Ocean, it is likely that most swordfish perform daily movements in a similar order of magnitude, with some individuals making much longer movements. Indeed, they are fast swimmers and have evolved many physiological characteristics that require them to swim continuously, making it likely that they do swim substantial distances within the Indian Ocean.

There is some evidence for spatial heterogeneity in size and sex composition in other oceans (Ward and Elscot, 2000) - for example larger, predominantly female fish are observed in the more southern latitudes of the Pacific Ocean, while in the Atlantic Ocean, medium and large-sized swordfish tend to dominate longline catches in temperate waters, while smaller swordfish are more common in warmer waters. In the Indian Ocean, adult females move to temperate areas to feed in summer, moving to warmer tropical waters for spawning (Muths et al., 2009).

Age-at-length in swordfish (*X. gladius*) has been investigated using both anal fin ring counts, and counting opaque bands in sagittal otoliths (Wang et al., 2026; Wang et al., 2010; Farley et al., 2016). While there are documented differences between ages estimated from anal fins, and otoliths (Farley et al., 2022), a recent Indian Ocean study compared the readings from anal fin counts to those of otoliths of the same fish and the results were encouraging (Wang et al., 2026), leading to greater support for using anal fin counts as legitimate aging structures in swordfish. Additionally, recent aging of South Atlantic swordfish also used anal fin ray sections to count growth increments, and these have been used in the recent SS3 stock assessment for swordfish (Kikuchi et al., 2026). Estimates of size-at-age for Indian Ocean swordfish show distinct sexual dimorphism, with females reaching larger terminal size than males.

Farley et al. (2016) undertook a growth study for swordfish in the Southwest Pacific Ocean comparing the use of both fin-rays and otoliths samples. The study found that age estimates from fin rays and otoliths produce different growth curves in the SW Pacific, with discrepancies evident in age classes > 7 years for females and > 4 years for males. The otolith-based growth curves indicate slower growth and a higher maximum age for both males and females, compared to the ray-based growth curves of Young & Drake (2004) and DeMartini et al. (2007). Although direct validation of the ageing method was not carried out in the study, age estimates from otoliths are suggested to be more reliable than fin-rays, especially in larger/older fish, as fin-rays are subject to resorption and vascularisation of the core (Farley et al. 2016). Consequently, the WPB15 agreed that the stock assessment for swordfish should use the new otolith-based estimates from Farley et al. (2016) (Figure –left).

In the 2022 assessment, estimates from Taiwan,China taken from observers onboard vessels in the Indian Ocean (Wang et al. 2010) were also included in final model options. In 2026, there was an update to this study, where otolith readings were compared to the original anal fin-ray readings. As stated above, the recent ICCAT assessment of South Atlantic swordfish also incorporated anal fin-ray readings as suitable estimates for swordfish age. Therefore in this iteration of the assessment, the Taiwan,China estimates have been included as a sensitivity run, and are recommended for inclusion in the model grid.

There are several studies that have estimated the size at maturity for Indian Ocean swordfish, however, the considerable uncertainty that still exists between size and age undermines the current maturity at age relationship. This assessment uses the previous assessment's approach that an age-based logistic relationship should be used (from data from South Pacific swordfish), assuming a 50 % maturity at between 4-5 years old (4.34 years).

Swordfish are considered batch spawners (Arocha et al, 2002; Poisson & Fauvel 2009a). One estimate suggested that female swordfish in equatorial waters may spawn as frequently as once every three days over a period of seven months (Ward & Elscot, 2000). Swordfish larvae are likely rare in the western Indian Ocean, however there are some records of swordfish larvae reported in from the Mozambique Channel and east of Madagascar. By contrast, high concentrations of larvae occur in the north-east Indian Ocean (from north-western Australia to south-west Java), and in equatorial waters to approximately 80° East (Ward & Elscot, 2000). Continuous larval distribution in the eastern Indian Ocean is described in Nishikawa et al., (1985), however other regions have not been as heavily sampled so it is unclear whether larval distribution is only limited to the eastern Indian Ocean, or the result is simply a result of sampling bias.

The estimates for the instantaneous rate of natural mortality for swordfish are highly uncertain given the current methods of age estimation are poorly validated. There are a broad range of M values assumed in other swordfish assessments worldwide, ranging from at least 0.2 – 0.5 (Davies et al. 2013). This assessment used the previously used constant M (constant over all ages) of 0.25 in the base or reference model.

2.3. Indian Ocean swordfish fishery overview

The Indian Ocean swordfish fishery has a distinct two-phase history: the fishery was predominantly a bycatch fishery from the early 1950s until the late 1980s when a fresh longline target fishery for swordfish developed (Figure 2). This has produced a distinct change in both fishing practice, and in reported catches, with catches from the mid-1980s to today being around 10 x that of the early bycatch fishery. Initially, the bycatch fishery was dominated by the Japanese longline fleets, whereas the first target fishery was initiated by the Taiwan,China fleets in the late 1980s. At this point, annual catches rose rapidly to around 35,000 tonnes. At this point, the European longline fleet (dominated by Spain) also started targeting Indian Ocean swordfish in the early 1990s. Other fishing methods such as driftnet, and purse seine are rare. Since the mid-2000s, catches declined substantially, presumably due to piracy off the coast of Somalia. There was an increase in total catches from 2010 to 2020, most notably an increase in gillnet fishery catches, and a steady increase from the Taiwan,China fresh longline fleets (Figure 2). Since 2020, catches have been notably reduced, mainly driven by a reduction in catch from the Taiwan,China fresh longline fleets. Swordfish are a high value catch that represent an increasingly important source to many coastal nations in Indian Ocean.

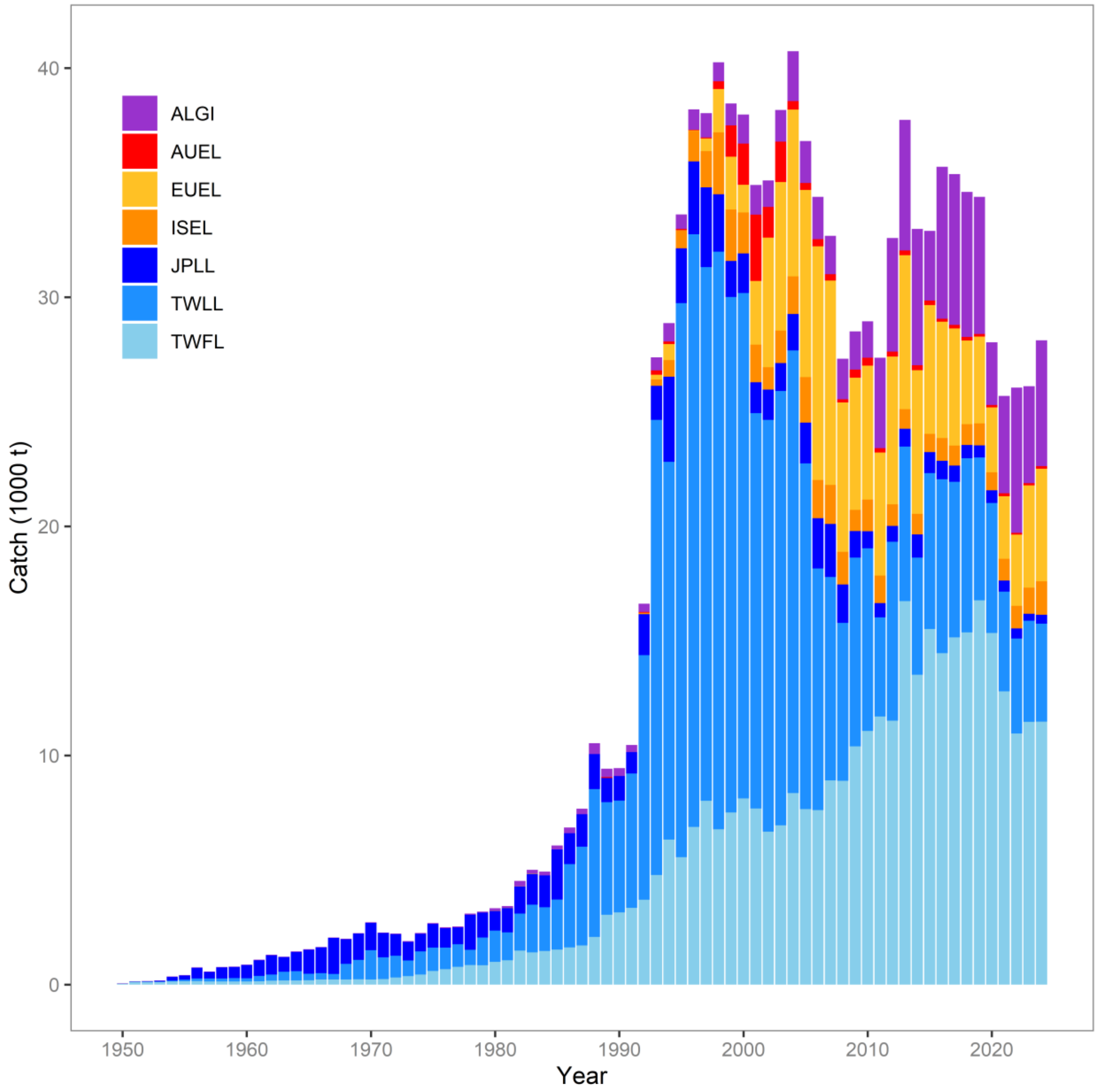

Figure 2: Total swordfish catch in tonnes by model fleet 1950 – 2024 for the whole Indian Ocean.

3. DATA INPUTS

3.1. General notes

Data used in this stock assessment consist of catch, length composition data, and longline CPUE indices, alongside biological parameters such as growth (length at age), natural mortality, and maturity information. Data are continually being improved and as such catch and length composition data may not be identical to those in previous assessments. Where data inputs have substantially changed, it is noted in the sections below, and links to relevant methods papers are provided for further detail.

Model input files along with reproducible code to run the assessment, and all sensitivities are stored by the Secretariat and are available on request.

3.2. Spatial stratification

The appropriate spatial structure for the assessment remains uncertain. Different hypotheses have been proposed, various options have been explored for IO swordfish to date, including (1) one or more discrete stocks (2) two or more populations that are produced from a common spawning ground, but have foraging grounds site fidelity (i.e. while this is a single population genetically, depletion can differ in different regions at different rates) 3) discrete spawning populations with mixing in common foraging grounds.

Some evidence suggests that there may be genetic distinction within the IO (Bradman et al. 2010, Bourjea et al 2011). Based on results obtained in 2013 (Muths 2013), there are no differences in genetic structure obtained from the SW Region and the entire IO Region. As such, the assessment is based on the single stock IO model (Shared spawning with foraging grounds site fidelity). However, the model is disaggregated into 4 areas corresponding to those used in the Japan and Taiwan (China) catch rate standardisation analyses in recent years. Given the vast size of the Indian Ocean, and the migration rate inferences that have been made from tagging studies to date, it seems unlikely that there would be rapid mixing processes across the whole basin, even if the population was genetically homogeneous. As such, localised overfishing could result in negative local consequences even if the population is genetically homogenous. The 4-area structure is a pragmatic disaggregation that conveniently partitions most of the national fleets.

SS3 can estimate movement rates among areas, however, these estimates are generally of little value in the absence of tagging data. In all models, migration rates were fixed at very low levels (<< 1% per year), which essentially creates 4 populations except for the shared spawning and recruitment dynamics (foraging grounds site-fidelity).

The previous assessment also developed sub-regional models in which each region was assumed to be a single stock, and each model was fitted only to the region-specific data. However, the sub-regional models were mainly to derive weighing factors for determining biomass distributions in a spatially disaggregated IO model.

3.3. Temporal stratification

The model covers the period 1950 – 2024, and assumes an exploited, equilibrium initial state in 1950. The model is temporally structured as annual data.

3.4. Definition of model fleets

In SS3, data are required to be aggregated or defined in "fleets" within the overall fishery. Individual fleets represent relatively homogenous fishing units, with similar selectivity and catchability characteristics that do not vary significantly over time (métiers). Fifteen (15) fleets were defined in the model (Table 1), with an additional five "survey" fleets, for which only CPUE indices were assigned. The use of "survey" fleets for the CPUE indices was chosen as these indices are based on aggregated datasets and allow for separate estimation of selectivity and catchability within the model framework.

Fishing fleets were defined based on the fishing gear type, fishery type (e.g. fresh *vs.* frozen longline), and fleet dynamics (e.g. spatial and temporal extent of the fishery).

The definitions of model fleets were the same as those used in the previous two iterations of the SS3 stock assessment. Earlier assessments which aggregated the longline fleets as one homogeneous fishery group in each region except for SW (Fu 2017). However, there are somewhat differences in the size compositions of samples taken by different longline fleets (e.g. the JPLL fleet catches larger fish than other longline fleets) which potentially indicate differential selectivity patterns amongst the fisheries. Therefore, the current assessment maintained the disaggregation of the fleet structure for the longline fisheries as in the 2020 assessment.

- ALGI – Gillnet, trolling and other minor artisanal fisheries
- AUEL – Longline fishery of Australia (target is SWO)
- EUEL – European Union longliners targeting SWO plus other longliners assimilated to EU longliners
- ISEL – Semi-industrial longline fleets operating in Réunion (EU,France), Mayotte (EU.France), Madagascar, Mauritius and Seychelles
- JPLL – Longline fishery of Japan plus other fleets assimilated to the Japanese fleet
- TWLL – Large scale frozen longline fleet of Taiwan,China, plus other longline fleets assimilated to the Taiwanese fleet
- TWFL – Fresh longline fleets of Taiwan and Indonesia, plus other fresh longline fleets assimilated to those

Table 1: Fleet definitions (numbers 1–15) used within the SS3 assessment. Suffixes denote regions within the Indian Ocean as indicated in Figure 1: NW – North-West; NE – North-East; SW – South-West; SE – South-East.

Name	Fleet Number	Area	Description
ALGI_NW	1	NW	Northwest Gillnet and other non-longline/-handline gears
JPLL_NW	2	NW	Northwest Japan and assimilated longliners (target tunas)
TWLL_NW	3	NW	Northwest Taiwan,China and assimilated longliners and handlines (mixed target)
ALGI_NE	4	NE	Northeast Gillnet and other non-longline/-handline gears
JPLL_NE	5	NE	Northeast Japan and assimilated longliners (target tunas)
TWLL_NE	6	NE	Northeast Taiwan,China and assimilated longliners and handlines (mixed target)
TWFL_NE	7	NE	Northeast fresh-tuna longliners (target tunas)
EUEL_SW	8	SW	Southwest European and assimilated longliners (target SWO)
ISEL_SW	9	SW	Southwest semi-industrial longliners (target SWO)
JPLL_SW	10	SW	Southwest Japan and assimilated longliners (target tunas)
TWLL_SW	11	SW	Southwest Taiwan,China and assimilated longliners and handlines (mixed target)
AUEL_SE	12	SE	Southeast Australia Longline fishery of Australia
EUEL_SE	13	SE	Southeast Southeast west European and assimilated longliners (target SWO)

JPLL_SE	14	SE	Southeast Japan and assimilated longliners (target tunas)
TWLL_SE	15	SE	Southeast Taiwan,China and assimilated longliners and handlines (mixed target)

3.5. Catch data

Catch data were compiled based on the fleet definitions in Table 1. An update of annual catches by fleet was provided by the IOTC Secretariat, including catches since the last assessment (2022–2024 "iotc_swordfish_raised_catch_dataset_base_case.csv").

The time series of catches are similar to those included in the 2023 assessment. A revision to the the Indonesia's fresh longline catches was conducted in 2018 (Geehan 2018). The revision incorporated changes to IOTC Secretariat's catch estimation methodology that led to Indonesia's fresh longline catches of swordfish being revised down from over 50,000 t to less than 35,000 t after that revision (Geehan & Setyadji 2018). There were also some revisions to the swordfish catches from I.R. Iran and Pakistan's gillnet fishery (**Error! Reference source not found.**). From the previous assessment to this one, there have been some increases in reported catches for the TWFL (NE) fleet as a result of Indonesia's 2025 revision to historical catch data.

Overall, the TWFL (NE) longline catches currently comprise 40.8 % total swordfish catches in the Indian Ocean.

Total annual catches for 2022, 2023 and 2024 included in the updated catch history are 26,056, 26,110, and 28,112 t respectively (Table 2). The total catch in 2024 is the highest amongst the last five years, although catches have remained relatively stable through this period (Figure 2, Table 2).

Table 2: Recent swordfish catches (metric tonnes, t) aggregated by model fleet that have been included in the stock assessment model. The annual catches are presented for 2020- 2024.

Fleet	2020	2021	2022	2023	2024
ALGI_NW	1648	2301	3768	2200	2529
JPLL_NW	24	11	5	20	57
WLL_NW	3958	2843	2559	2838	2264
ALGI_NE	1090	1953	2573	2030	2960
JPLL_NE	250	326	268	169	191
TWLL_NE	15340	12795	10959	11467	11477
TWFL_NE	273	346	363	301	569
EUEL_SW	2535	2329	2615	3262	3340
ISEL_SW	787	946	981	1141	1454
JPLL_SW	120	47	32	45	104
TWLL_SW	888	592	779	646	537
AUEL_SE	96	131	83	98	116
EUEL_SE	298	397	493	1197	1573
JPLL_SE	160	102	132	70	37
TWLL_SE	558	572	446	627	905
Total (t)	**28026**	**25691**	**26056**	**26110**	**28112**

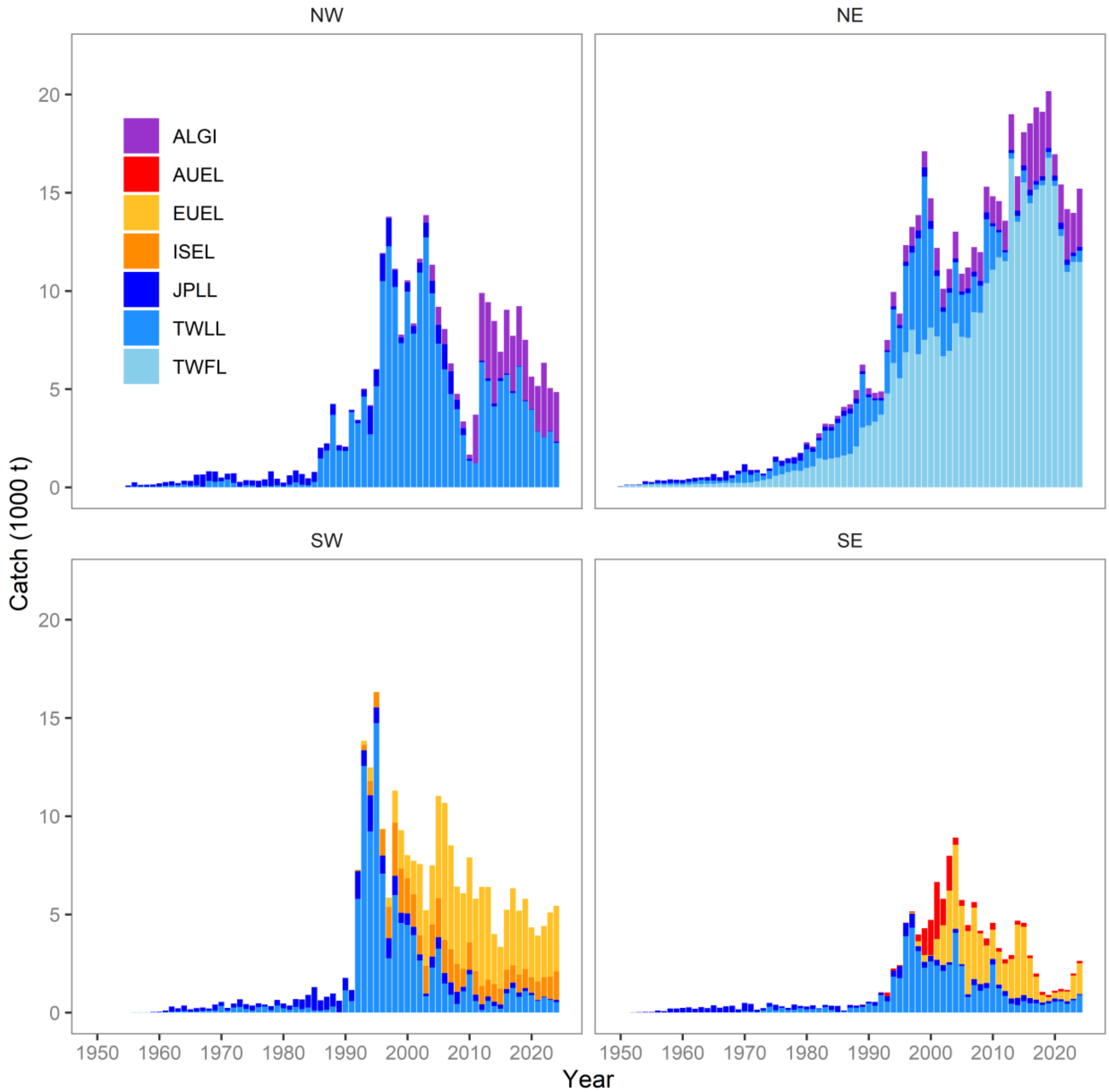

Figure 2: Model fleet catches (x 1000 metric tonnes) aggregated by model region and coloured according to fishing fleet in the model.

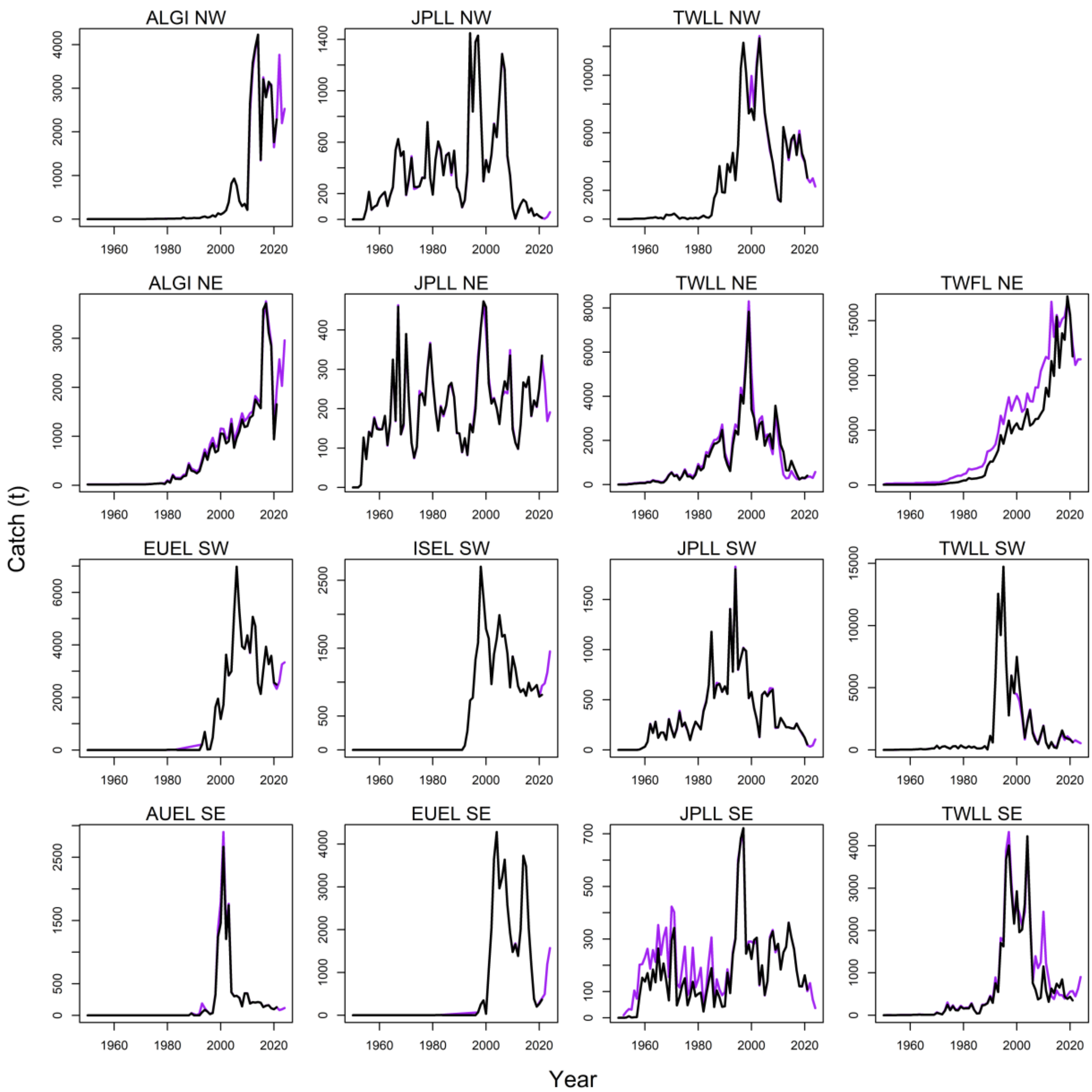

Figure 3: Fishery catches (metric tonnes) aggregated by year. Note the y-axes differ between plots. Purple lines are catches used in the 2023 assessment. The differences in catch are mainly due to general improvements in the data quality over time.

3.6. Abundance indices

Thirteen standardised CPUE series (Table 3, Figure) were available at the time of the assessment, from the following CPCs:

- Indonesia (Setyadji et al., 2026; IOTC-2026-WPB-17)
- European Union (Portugal) (Coelho et al., 2026; IOTC-2026-WPB-18)
- European Union (Spain) (Fernández-Costa and Ramos-Cartelle, 2026; IOTC-2026-WPB-19)
- South Africa (West and da Silva, 2026; IOTC-2026-WPB-20)
- Japan (Takahashi and Kai, 2026; IOTC-2026-WPB-22)
- Taiwan (China) (Lin et al., 2026 ; IOTC-2026-WPB-23)
- European Union (Réunion Island) (Bonhommeau, 2026)

The CPUE series are included in the assessment as relative abundance indices.

In the previous assessment, each region had two Japanese CPUE series that were standardised as separate series (1979-1993 and 1994-2022) as there were significant differences between the two periods in terms of gear configuration, and presumably targeting practices (Matusmoto et al., 2023). In this iteration of the stock assessment model, only the later time period was supplied by Japan (1994-2024. In the 2020 model, it was shown that the 1979 – 1993 index was uninformative of the stock depletion and did not have any appreciable impact on model estimates (Fu 2020), so not including them in this assessment is unlikely to have an impact on final biomass estimates.

In each region, the Taiwan (China) indices were standardised for 2004 to 2023. In the NE region, the CPUE index fluctuates around the mean, with higher variability than in the NW, SE or SW, possibly reflecting less consistent fishing effort in this region. In the NW region, the index is very flat, with little change in CPUE after an initial high at the start of the series. In the SE, the CPUE index decreases over time, in conflict or contrast to the Japanese longline index in this region. In the SW, the index increases over time, similarly to other indices in this region (Japan, Réunion, Portugal), but in contrast to the South African and Spanish indices (which remain flat).

The Portuguese pelagic longline fishery in the Indian Ocean started in the late 1990's, targeting mainly swordfish in the southwest, but also catches relatively high quantities of sharks as bycatch in certain areas and seasons (Coelho et al. 2023). The Portuguese series showed a declining trend between 2000 and 2021 but since the last assessment there has been a marked increase in CPUE, corresponding to that of the Réunion index in the same region. The index is assigned to the SW region in the assessment model.

The Spanish series from 2000 to 2023 is also assigned to the SW region although the fleet has fished a much larger area. Shifting targeting (i.e. shark vs swordfish) is very important in this fishery. Earlier analysis demonstrated that the inclusion or exclusion of the species ratio factor makes very little difference to the annual time series in this case, suggesting that the seasonal targeting shifts are probably not introducing any consistent bias to the time series. The index is relatively "flat" in terms of overall trend, but with some variation around the mean.

The South African series is based on a swordfish target fishery within the pelagic longline fleet operating along the west and east coast of South Africa. The index (West and da Silva, 2026) shows a declining trend between 1994 and 2014. From 2015 to 2017 the index increases, followed by a lower, stable CPUE from 2018 to 2024. The index is assigned to the SW region in the assessment model.

The Indonesian CPUE series derived from observer data covering 2006 to 2024 is assigned to the NE region. The index shows a stable start from 2006 to 2020, and in the final years, the index increases markedly, similarly to the Taiwan (China) index in the same region.

In the NW, Japanese and Taiwan (China) indices are very stable, and both have shown an upward trend from 2004 to 2012 followed by a relatively flat trend from 2012 to 2024 for Taiwan (China), and a declining trend for the Japanese fleet. In the NE the Japanese index increased in 2012 to a plateau of high CPUE to 2024. In the SW, there is a noticeable consistency between Portuguese, South African, Japan, and Taiwan (China) indices. In the SE, the Japanese and Taiwan (China) indices were relatively comparable from 2005 to 2015, but from 2016, they diverge, with the Taiwan (China) index decreasing and the Japanese index increasing.

For a full comparative analysis of the CPUE indices, see Appendix 1.

There has been a large reduction of effort by the Japanese longline fleet since 2005, coinciding with the onset of the piracy activity in the western Indian Ocean. The reduction of fishing mostly occurred in the north-west Indian Ocean as the Japanese fleet pulled out of the region but is also evident in other regions. Although the piracy activity has abated after 2012, the effort has not returned to the previous levels. As such, the spatial overage of the Japanese CPUE may have been poor in recent years, particularly in the NW and NE regions.

All available CPUE are included in the assessment model. However, depending on the model option, some of these CPUE series may have been downweighted to the point that they were uninformative, as in the previous assessment).

Table 3: CPUE series available for the SS3 Assessment. Suffixes denote regions within the Indian Ocean as indicated in Figure 1: NW – North-West; NE – North-East; SW – South-West; SE – South-East. Number is the SS3 index number

Name	Number	Area	Description
UJPLL	16	NW	JPN CPUE series (1994–2024)
UJPLL	17	NE	JPN CPUE series (1994–2024)
UJPLL	18	SW	JPN CPUE series (1994–2024)
UJPLL	19	SE	JPN CPUE series (1994–2024)
UTWLL	20	NW	TWN CPUE series (2004–2023)
UTWLL	21	NE	TWN CPUE series (2004–2023)
UTWLL	22	SW	TWN CPUE series (2004–2023)
UTWLL	23	SE	TWN CPUE series (2004–2023)
UIDN	24	NE	IDN CPUE series (2006-2025)
UZAF	25	SW	ZAF CPUE series (2004-2024)
UPRT	26	SW	PRT CPUE series (2000-2024)
UREU	27	SW	REU CPUE series (2005-2025)
UESP	28	SW	ESP CPUE series (2005-2023)

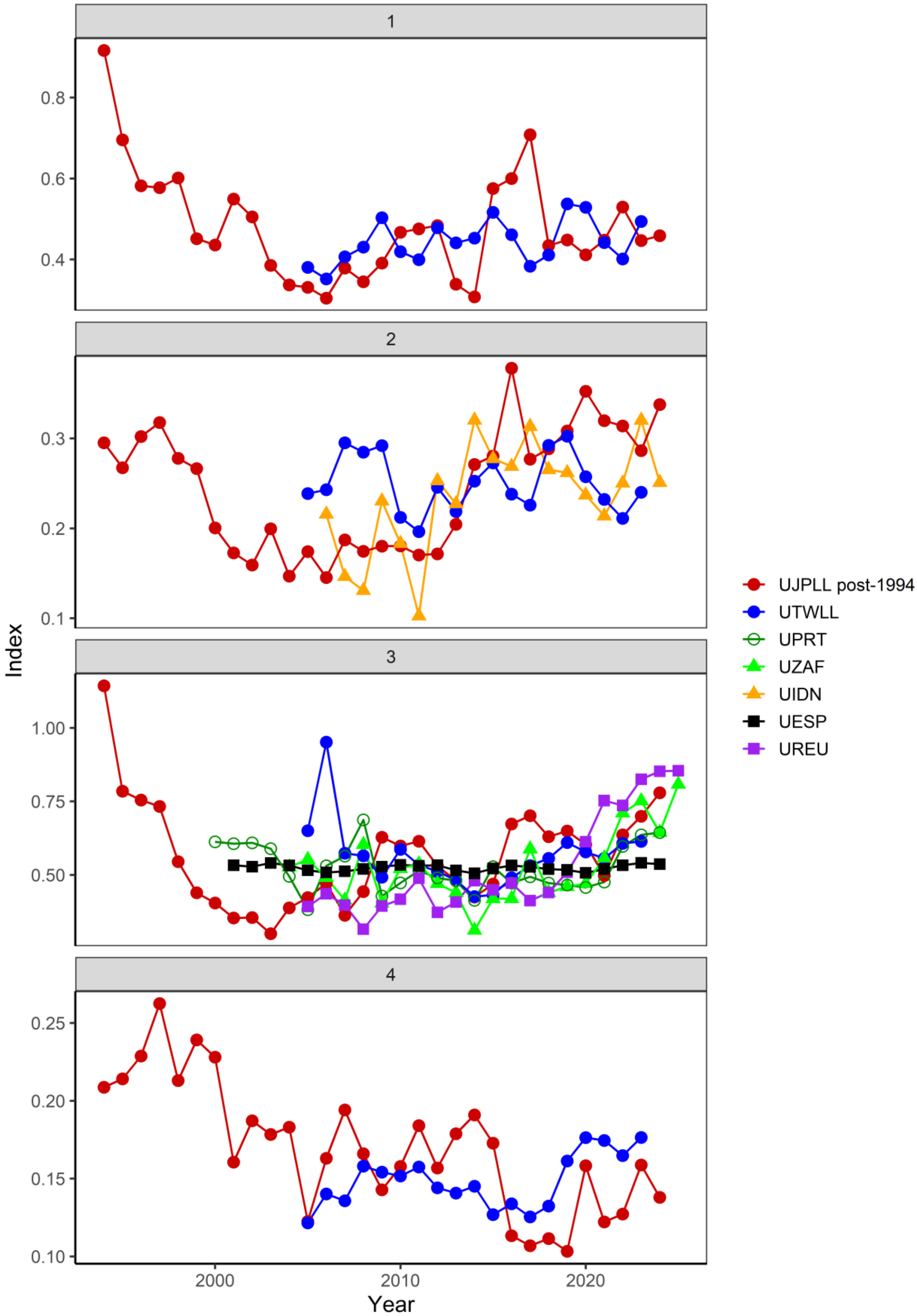
1
2
3
4
0.8
0.6
0.4
0.3
0.2
0.1
1.00
0.75
0.50
0.25
0.20
0.15
0.10
Index
2000
2010
2020
Year
UJPLL post-1994
UTWLL
UPRT
UZAF
UIDN
UESP
UREU

Figure 4: Standardized CPUE by area for Japanese, Taiwanese (China), Portuguese (EU), South African, Indonesian, Spanish (EU), and Réunionese (EU) fleets by model region. All series have been rescaled so that they are visually comparable for relevant periods of overlap. Note that this re-scaling does not reflect the relative weighting that is applied to the Japanese fleet.

3.7. Length frequency data

Length-frequency observations are available for 14 of the 15 defined fisheries (not for the gillnet fishery in the NW). Size composition was partitioned into 25 bins of width 9 cm (except the first and last), from <45cm to >270 cm). The length frequency observation for each fishery represents the actual number of swordfish measured. In the assessment, all length composition strata from all fleets were down weighted by dividing the number of fish included in the aggregated sample by a factor of 10, with a maximum sample size of 20, to account for sampling is probably not truly random. Explorations from the previous assessment suggested that this weighting option is consistent with the effective sample sizes determined using the Francis (2012) method. The time series of length frequencies for each model fishery are shown in Figure 5 (Length samples with less than 20 fish measured per year and fishery are excluded from the assessment). (Figure 5).

The length compositions of the fleets are relatively similar, all showing dome-shaped distributions. However, the TWLL fleet in all areas appears to be more selective than other fleets, with a narrower peak of length distribution. The JPLL fleet appears to have taken larger fish in all areas except the NW (Figure 6). The TWFL fleet has a wider range of lengths within the catch compared to the TWLL fleet. Length distributions in the AUEL fleet (SE) appear to also select for larger fish, compared to the ALGI (NE) fishery where smaller fish have been reported. The previous assessment noted that according to Herrera and Pierre (2014), most samples available from the longline fishery of Japan come from training vessels in recent years. The representativeness of the samples collected on training vessels is uncertain, as these vessels do not necessarily operate in the same areas or use the same fishing techniques as the commercial vessels from Japan.

Within the SW region, there appears to be a decreasing trend in the size of fish being reported (Figure 7), compared to the SE where fish size appears to be increasing in recent years. Most fleets in the model have relatively long timescales of length frequency data (Figure 5) that were available for inclusion in the model.

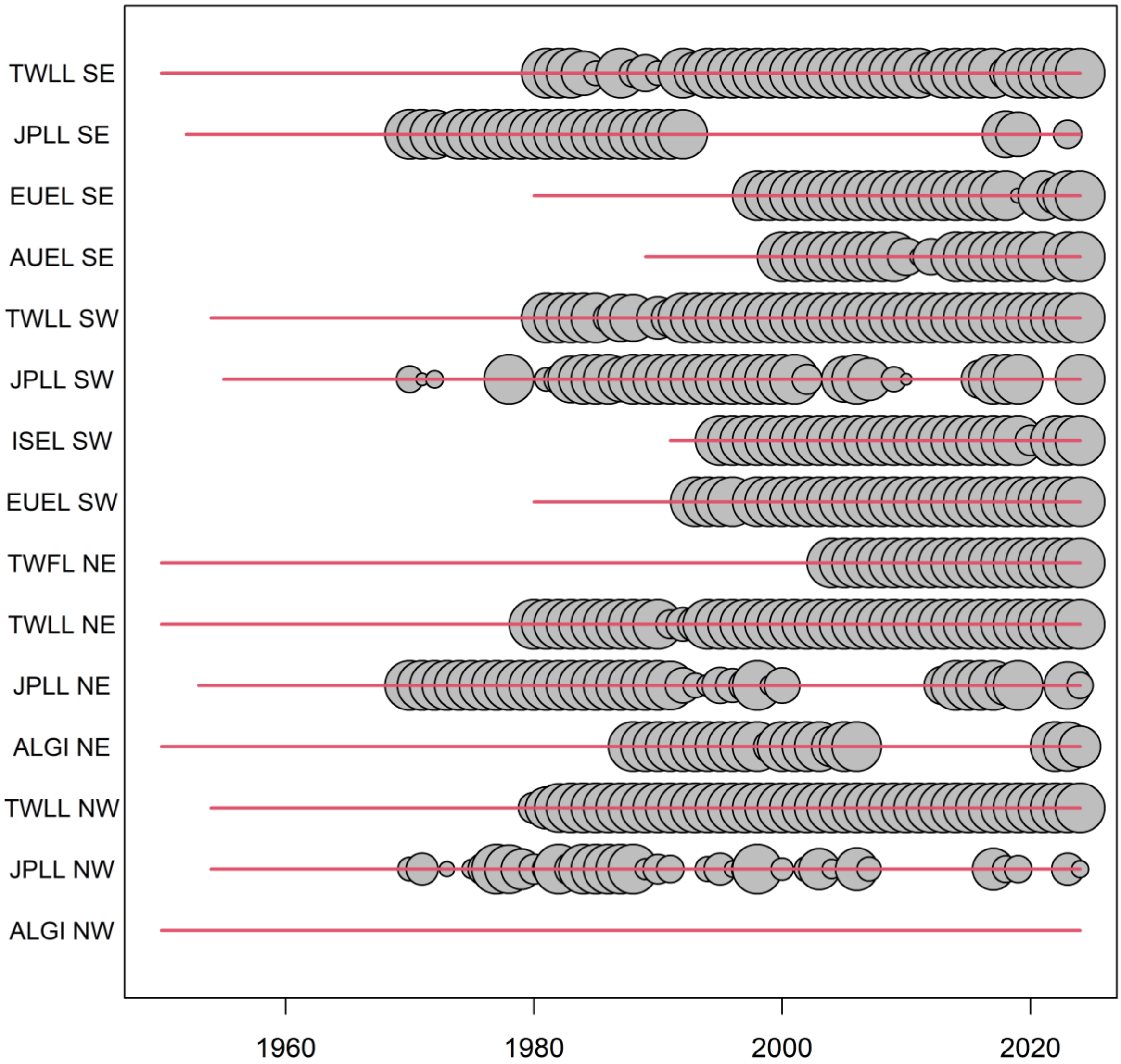

Figure 5: The availability of length sampling data from each fishery by year. The grey circles denote the presence of samples in a specific year (the size indicate number of quarters being sampled). The red horizontal lines indicate the time period over which each fishery operated.

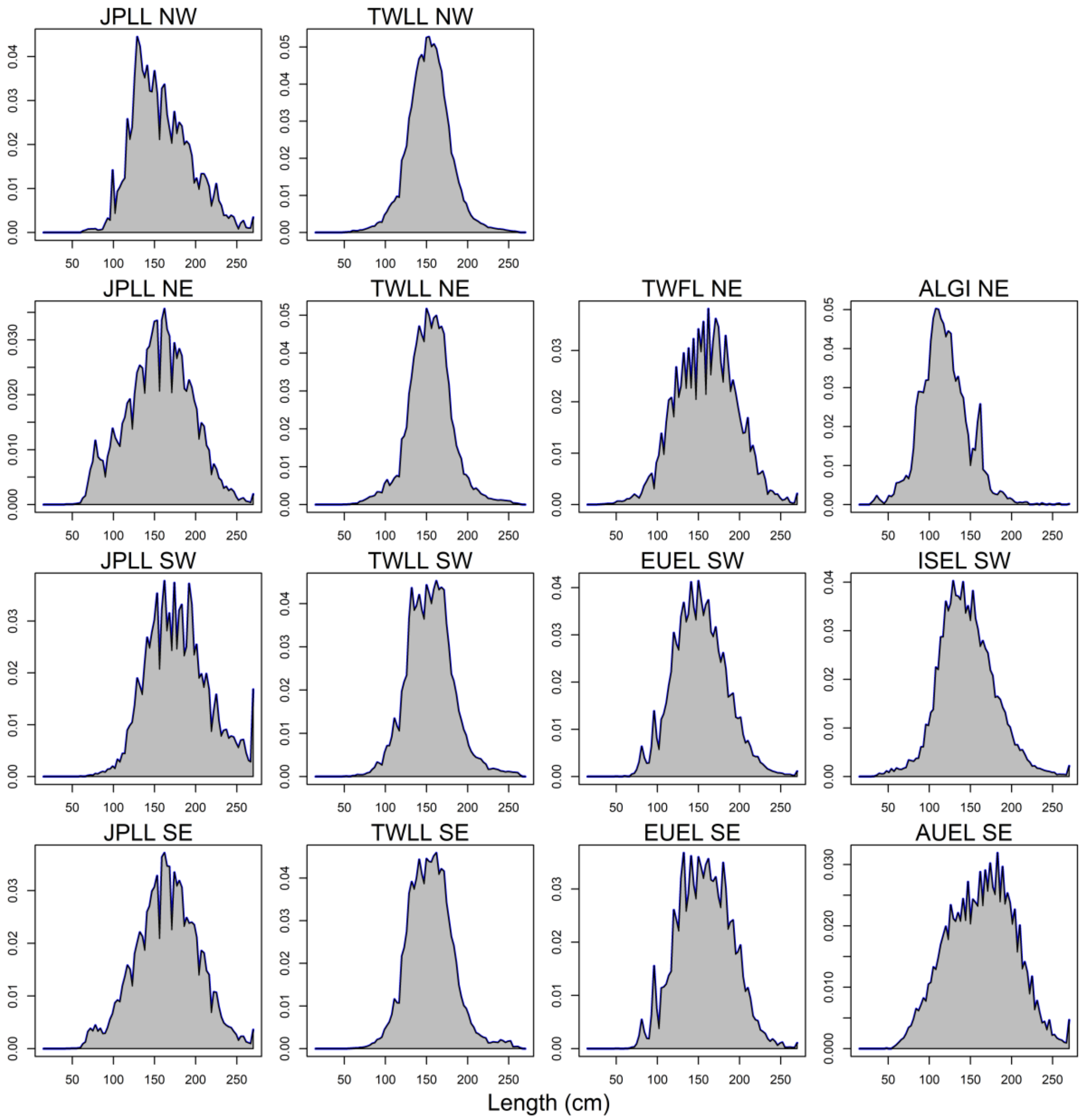

Figure 6: Length compositions of swordfish samples aggregated by model fishery.

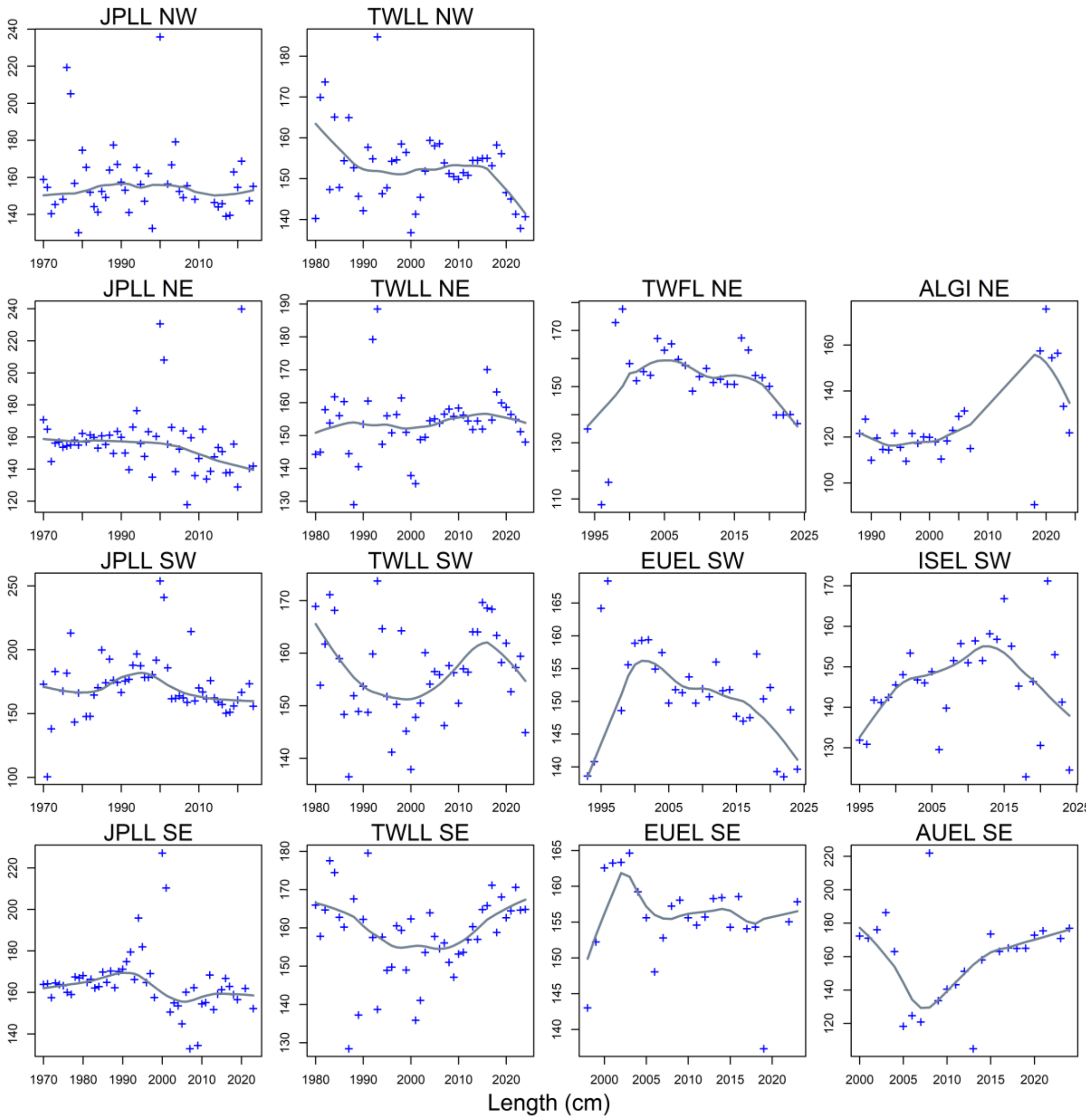

Figure 7: Mean length (fork length, cm) of swordfish sampled from the principal fisheries by year quarter. The grey line represents the fit of a loess smoother to the dataset.

4. MODEL DESCRIPTION

The model was implemented in Stock Synthesis 3.30.25.1 (August 2026). A detailed description of the model and the general assumptions, alongside detailed technical descriptions of various components can be found in the SS3 User Guide, and associated webpage, and publications. Most of the structure of the model has remained the same since the 2023 model, and as such the sections are the same as in the previous stock assessment report. There have been updates in 2026 to both the growth and natural mortality.

4.1. Population dynamics

The stock assessment model partitioned the Indian Ocean swordfish population into four areas, two sex groups, and age groups 1–30 years with the last age a plus group (in unfished equilibrium, <0.25% of the population survives to reach the plus-group with the M value considered).

The swordfish population is sex-structured to (potentially) account for a number of sex-specific population features that may be worth describing. Notably, growth curves differ by sex, and it is useful to be able to represent the two distributions (or aggregated of the two distributions) in the catch-at-length likelihoods (or it would be useful in principle, if we were confident about the growth curves, size composition data, mortality estimates and stationary selectivity assumptions). Spatial distributions often differ by sex (e.g. large females are disproportionately found in cooler temperate waters in the south Pacific). Selectivity may differ by sex due to the differing spatial distributions, and there also may be direct size biases in some fisheries (e.g. commercial fishers report that large swordfish may be less vulnerable to circle hooks). Natural mortality may also be sex-specific, but no distinction was made in these models. However, there is no evidence that the sex structure is contributing much to the behaviour of the model in its current form.

The population was assumed to be in unfished equilibrium in 1950, the start of the catch data series. The model was iterated from 1950-2024 using an annual time-step. The nominal unit of time in the model is one year during which population processes (e.g., recruitment, spawning, and ageing) were applied in sequence according to the dynamics implemented within the Stock Synthesis model (Methot 2020). Observations were fitted to model predictions within the year. The main population dynamics processes are as follows:

4.1.1. Recruitment

Recruitment was assumed to occur annually at the start of the year. New recruits enter the population as age-class 1 fish (averaging approximately 70 cm). Annual recruitment deviates from the recruitment relationship were estimated in the model for 1950–2023 (73 deviates). The recruitment deviates were estimated for the period that may be informative regarding the variation in recruitment. Recruitment in the final year was deterministic from the stock recruitment relationship (because these cohorts are only weakly observed by the data). The final model options included three (fixed) values of steepness of the BH SRR (*h* 0.7, 0.8 and 0.9).

Recruitment deviates were assumed to have a standard deviation (σ_R) of 0.2, with an alternative value of 0.4 also included in the final model options. There is anecdotal evidence to suggest that spawning (and recruitment) may be out of phase in the southern and northern hemispheres, however, the growth, size sampling and selectivity assumptions are such that the quarterly model explored in 2010 could not provide much insight into recruitment processes. Swordfish are often assumed to have lower recruitment variability than tuna populations, and the recent summary of tuna populations suggest that the estimated (annual) variability is often lower than has been a priori assumed in the tuna assessments (ISSF 2011 reports values of 0.2 – 0.5).

Area-specific parameters were estimated to distribute the mean recruitment among regions. Recruitment anomalies by region were estimated with a very high CV, such that the spatial distribution of recruits was only indirectly constrained by the overall recruitment CV.

4.1.2. Growth

Swordfish exhibit phenomenal growth in the first year of life and there is a marked difference in growth rate between male and female. The strong evidence for sex dimorphism in swordfish can be potentially important in the right-hand tail of the size distribution, which is often estimated to consist predominantly of large, mature females. The 2020 assessment considered four alternative sets of growth curves to allow for uncertainty due to potential area-specific growth rates, and ongoing concerns about age estimation from fin spines.

- CSIRO estimated very slow growth based on South-East Indian Ocean fin ray samples (Young and Drake 2004).
- NMFS estimated higher growth from Hawaiian samples (DeMartini et al. 2007).
- Wang et al. (2010) described an intermediate growth curve (pooled western and eastern samples from the Indian Ocean equatorial region).
- New CSIRO estimates based on SW pacific fin ray samples (Farley el al. 2016).
- New CSIRO estimates based on SW pacific otolith samples (Farley el al. 2016).

Farley et al. (2016) undertook a growth study for swordfish in the Southwest Pacific Ocean comparing the use of both fin-rays and otoliths samples. The study found that age estimates from fin rays and otoliths produce different growth curves in the SW Pacific, with discrepancies evident in age classes > 7 years for females and > 4 years for males. The otolith-based growth curves indicate slower growth and a higher maximum age for both males and females, compared to the ray-based growth curves of Young & Drake (2004) and DeMartini et al. (2007). Although direct validation of the ageing method was not carried out in the study, age estimates from otoliths are suggested to be more reliable than fin-rays, especially in larger/older fish, as fin-rays are subject to resorption and vascularisation of the core (Farley et al. 2016). Consequently, the 2023 model used the new otolith-based estimates from Farley et al. (2016) (Figure –left), despite these estimates coming from the Pacific Ocean, and not the Indian Ocean.

In the 2023 assessment, estimates from Taiwan,China taken from observers onboard vessels in the Indian Ocean (Wang et al. 2010) were also included in final model options. In 2026, there was an update to this study, where otolith readings were compared to the original anal fin-ray readings. As stated above, the recent ICCAT assessment of South Atlantic swordfish also incorporated anal fin-ray readings as suitable estimates for swordfish age. Therefore, in this iteration of the assessment, the Taiwan,China estimates have been included as a sensitivity run, and are recommended for inclusion in the model grid, particularly as these estimates come from individuals in the Indian Ocean.

The growth curves included in the assessment are shown in Figure 8 (left hand side).

Length-at-age was assumed to be normally distributed around the mean length-at-age relationship with a CV of 15% at age 0, decreasing linearly (in proportion to length) to 10% at age 30+.

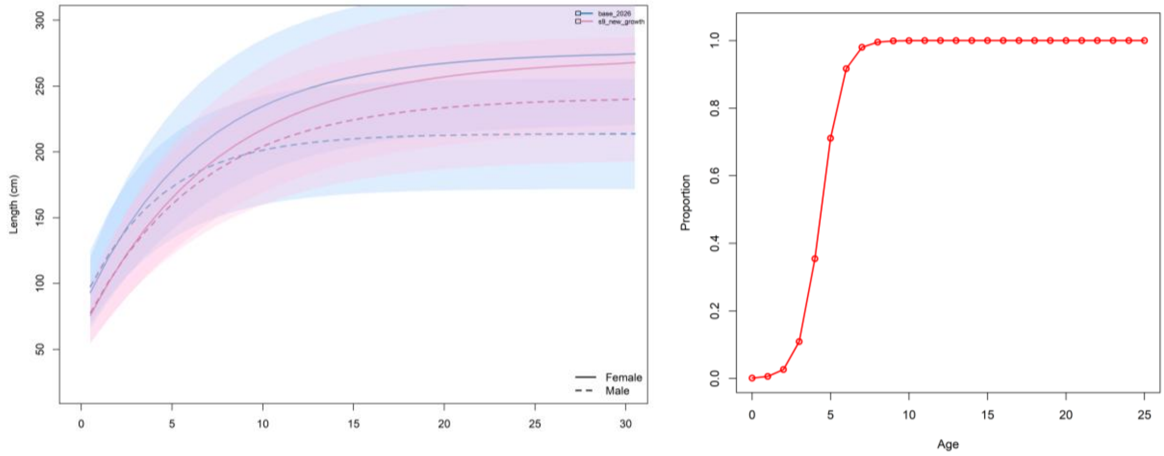

Figure 8: Growth (left) and age-based maturity (right) for swordfish. Two growth options are considered in the assessment: CSIRO SW Pacific otolith (Gold) and Taiwan Indian Ocean (Gnew).

4.1.3. Maturity

While a number of studies quantify the relationship between size and maturity, the uncertainty of age estimation that undermines the growth relationships also undermines the maturity/fecundity by age relationship. Following recommendations from WPB15, the assessment used the age-based logistic ogive from Farley et al. (2016) (as applied from the new otolith-based growth from SW pacific), which suggested a 50% maturity at about age 4.34 (Figure –right).

4.1.4. Natural mortality

The instantaneous rate of natural mortality (*M*) varies with age and consists of an average over age classes and age-specific deviations from the overall average *M*. In many fish stock assessments, *M* is fixed at a pre-specified value for all ages or sizes and is often not based on data related to the species or fishery being assessed. Incorrectly specifying *M* within stock assessments (and therefore having a mis-specified model) has been shown to have significant impacts on the relevant estimations of management-relevant indicators (Punt et al., 2021; Maunder et al., 2015).

Natural mortality estimates for swordfish are highly uncertain given the current methods of age estimation are poorly validated. There are a broad range of M values assumed in other swordfish assessments worldwide, ranging from at least 0.2 – 0.5 (Davies et al. 2013). The value of M of 0.25 (constant over ages) was adopted for the current assessment (Figure 9).

Additionally, using the Lorenzen curve to have age-varying M (across an age-range, Option 6 in SS3) was included in a sensitivity run. Adult swordfish ages were specified (5-12 years, based on the length at 50% maturity, and the oldest fish potentially caught in the fishery), and a median M of 0.25 set to preserve continuity with the fixed M estimate. The subsequent curve follows a Lorenzen functional form. See Figure 9 for all values of M used in the assessment.

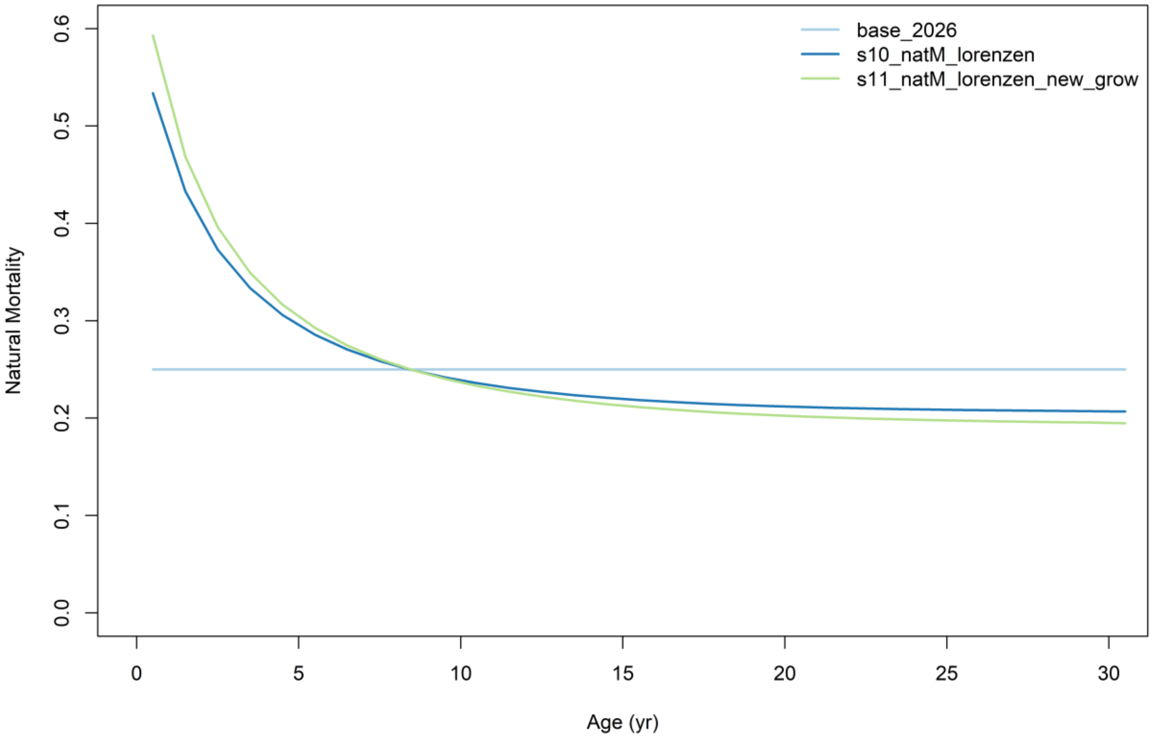

Figure 9: The different instantaneous rates of natural mortality (M) used in the base model (fixed at 0.25) and a sensitivity run of the 2026 assessment model. The base model used fixed M (0.25). The two models using the Lorenzen M are shown, as one uses the new growth provided by Wang et al., (2026).

4.2. Fleet dynamics

4.2.1. Selectivity

In the 2017 assessment, only two different size-based "double normal" selectivity curves were estimated, one for longline fleets, and one for the gillnet (and other associated) fleets. This assumption was revisited in the 2020 assessment, and separate selectivity was estimated for a number of longline fleets, i.e., JPLL, TWLL, TWFL, and EUEL. A monotonically increasing logistic selectivity was estimated for the JPLL fishery, and a double normal selectivity for the TWLL and EUEL fisheries. The selectivity for the ISEL and AUEL fleets were assumed to be same as the EUEL. The assumption of an asymptotic selectivity for at least one of the fisheries (i.e. JPLL) should prevent the model from producing cryptic biomass. The selectivity for each fleet was shared by region (e.g. a common TWLL selectivity in the IO). A cubic spline selectivity (5 nodes) was assumed for the gillnet fishery in the NW and NE. The cubic spline selectivity has considerable freedom to represent a dome-shape, or an approximately logistic curve that either reaches a plateau or is monotonically increasing.

The selectivity assumption was revised in the previous (2023) assessment: For the JPLL fishery, separate selectivity estimated for each region (the logistic selectivity in the NW fishery was replaced by a double normal selectivity); for the EUEL (shared amongst ISEL and AUEL), a logistic selectivity was used instead of the double-normal. The former is to account for regional differences in the length compositions of Japanese longline fleets, which may have reflected spatial heterogeneity in swordfish size distribution. The regional heterogeneity, however, is not evident in length samples from other fleets. The latter is to account for there are comparatively more larger fish in the samples from the EUEL (and ISEL and AUEL) fleet than in the TWLL fleet. As in the last assessment, the selectivity for each fleet (except for JPLL) is shared across regions to improve the model's stability. The 2026 model used the same selectivity assumptions as in the 2023 iteration.

Selectivity was parameterized as a pseudo-length-based function, i.e. the length-based curve is internally converted to an age-based function based on the length-at-age relationship. In this application, the potential benefit of this arises as a result of the sex dimorphism (i.e. two sex-specific age-based selectivity functions are derived from a single length-based selectivity function because of the difference in length-at-age). While the length-based selectivity function often exhibits a very steep ('knife-edge') slope, this is deceptive because there is considerable overlap in length-at-age.

4.2.2. Catchability

Catchability was assumed to be constant over time for all CPUE series. An area-specific scaling was applied to the Japanese CPUE series to convert the indices to relative abundance indices that are comparable among areas (i.e. CPUE = 1 in the NW region and CPUE =1 in the SW region implies that the two regions have identical abundance, not simply identical density). This allows catchability to be shared among areas for regional CPUE index. The shared catchability constraint is often useful for preventing localised behaviour in spatial models.

In the 2017 assessment, two alternative sets of regional scaling factor were used: one is based on the area of the region (Nishida 2008), and the other on biomass estimates from region-specific models (Fu 2017). The area-based scaling factor implies that the Japanese CPUE are essentially density estimates. However, the validity of the assumption that density is uniform within each large sub-region is questionable (it may be unrealistic to expect that swordfish catchability in a northern swordfish fishery has much relation to swordfish catchability in a southern SBT fishery). Further, changes in the CPUE standardisation methodologies have resulted in very different regional weighting being applied between assessments (see Figure 17 of Sharma (2014) and Figure 13 of Kolody et al. (2011)). The biomass-based estimates were derived by fitting region-specific models which included only regional fishery catches and observations, and the resulting stock biomass in each region were used to provide prior information on regional abundance distribution in the spatially disaggregated IO model. Estimated scaling factors for the NE, NW, SE, and SW regions are 1.06, 1.11, 0.67, and 1.17, respectively. To incorporate in the assessment model, the standardised JPLL CPUE index in each region was normalised to its mean and was then scaled by the respective regional scaling factor.

4.3. Modelling methods, parameters, and likelihood

The model is conditioned on catch (weight), such that it is assumed to be known without error and extracted perfectly. The SS3 "hybrid" fishing mortality parameterisation was used, where SS3 starts with Pope's approximation and then conducts a fixed number (4) of iterations to approximate instantaneous F from the Baranov catch equation.

Parameters were estimated by minimising the objective function consisting of the following terms:

4.3.1. Likelihoods

- Relative abundance indices with lognormal observation errors.
- Length frequencies – multinomial sampling assumptions (with assumed sample sizes << reported sample sizes depending on the option)

4.3.2. Prior distributions and Penalties:

- Annual recruitment deviates (lognormal) from the stock-recruitment relationship.
- Every estimated parameter for selectivity, catchability, and R0, requires a prior probability distribution. For these parameters, the prior adopted was very diffuse, such that a bound was likely to be hit before the prior would exert an appreciable influence (e.g. SD = 99).
- Weak penalty (e.g. SD = 99) on the spatial distribution of the recruitment deviates in the 4 area model.
- Smooth penalties for parameters approaching bounds were adopted, however, bounds were not approached for any of the models discussed here (i.e. presumably because the parameters that are most difficult to estimate were generally fixed (i.e. growth, M, steepness).

The informative parameters estimated by the model include:

- Catchability for the informative CPUE series
- Selectivity parameters
- Virgin recruitment
- Annual recruitment deviations from the stock recruitment relationship
- Annual area-specific recruitment deviations
- Recruitment distribution by area

The Hessian matrix computed at the mode of the posterior distribution was used to obtain estimates of the covariance matrix, which was used in combination with the Delta method to compute approximate confidence intervals for parameters of interest.

5. ASSESSMENT MODEL RUNS

A base model was configured that represents a continuity run from the 2023 assessment with updated data and several revisions of the model. A range of sensitivity or exploratory models were later conducted explore alternative assumptions and parameter configurations. On basis of the analyses, final model options were tentatively proposed that include an ensemble of models running over permutations of plausible parameters and/or model settings, from which the stock status was estimated, and uncertainty was quantified (the Grid). The assessment was conducted using the 3.30.25.1 version of the Stock Synthesis software using R. Most diagnostic plots, and model updates were coded in R and generated using the *r4ss* and *ss3diags* packages. Stock status is reported for the terminal year of the model (2024).

5.1. Updates to the base model for 2026

In the 2023 assessment, final model options selected to quantify stock status by the WPB included 48 models with alternative CPUE configurations (two options); alternative growth parameters (two options); different length-frequency effective sample sizes (two options); alternative recruitment variability (two options); and three values of steepness (three options). The final reference model included Japanese, Portuguese, and South African CPUE indices

The 2023 reference model was re-run to ensure continuity, and some revisions were incorporated based on preliminary analyses. These revisions are to improve the assessment model, but they do not represent any major structural changes to the model. The revisions included:

- Updating the SS3 executable to the latest version
- Updating the catch, length-frequency, and CPUE data inputs.
- Updating the recruitment deviations to the appropriate timeframe
- Updating the bias adjustment to the recruitment deviations to recommended values in SS3

A sequential, stepwise approach was taken for the model updates (Table 4). The configuration of the resulting base model is summarised in Table 5. The base model in 2026 only included the Japanese longline CPUE indices, without the ZAF and PRT indices. This was chosen as when all three indices were included in the model, the model failed to converge without allowing for further runs. It was also to allow for sufficient sensitivity testing to identify the most appropriate model as a reference model.

Table 4: Description of the sequence of model runs to update the 2026 base model.

Model	**Description**
0_base_2023	2023 reference model
0_base_2023_exe	Updated R and SS3 executable (version – 3.30.25.1)
1-update-catch	Updated and revised catch series, extended the model to 2024
2-update-lf	Updated and revised length-frequency data (no filtering of data)
2_update_lf_algi_nw	As above, with removal of data from ALGI_NW (low levels of data)
2_update_lf3	Updated and revised length-frequency data, with same filtering as 2023, plus additional filtering where necessary
3-update-cpue	Updated and revised CPUE data as 2023
3_update_cpue2	Updated and revised CPUE data – just Japanese LL indices (all years)
4-update-rec	Update rec-devs to appropriate time frame, and change bias adjustment values to those recommended by SS3.

Table 5: Main structural assumptions of the swordfish *base* model and details of estimated parameters. Changes to the 2023 reference model are highlighted in red.

Parameter	**Assumptions**	**Values**
Recruitment	Recruitment is a function of Beverton-Holt stock-recruitment relationship (SRR). Regional apportionment of recruitment to NW, NE, SW, and SE. Temporal recruitment deviates from SRR, 1955–2023. Temporal deviates in the proportion of recruitment allocated to NW, NE, SW, and SE from 1955–2023.	R_0 Norm(10,10); h = 0.80 *PropR2* Norm(0,1.0) σ_R = 0.2. 48 deviates.
Initial population	A function of the equilibrium recruitment in each region assuming population in an initial, unexploited state in 1950.	
Age and growth	32 age-classes, with the last representing a plus group. VonBert Growth based on otolith estimates by Farley *et al* (2016). Mean weights (W_j) from the weight-length relationship $W = aL^b$.	$L_\infty^f = 275$ $L_\infty^m = 213.8$ $K^f = 0.157$ $K^m = 0.235$ a = 3.815 e-06, b = 3.188
Instantaneous rate of natural mortality (*M*)	Constant at 0.25	
Maturity	Age specific logistic function from Farley *et al* (2016). Spawning population includes female fish only.	α = -6.6, β = 1.50 ($a_{50} = 4.42$)
Movement	Movement rates were fixed at very low levels (<< 1% per year)	
Selectivity	Length specific, constant over time. **Japanese longline fisheries**: Double normal selectivity in NW, Logistic in other regions **Taiwan,China longline fisheries**: Double normal selectivity, common among regions **EUEL, ISEL, and AUEL longline fisheries**: Logistic selectivity, common among regions	Logistic Double Normal Five node cubic spline

	Gillnet fisheries: Cubic spline (5 nodes) selectivity **CPUE indices** mirror to principal LL selectivity.	
Fishing mortality	Hybrid approach (method 3, see SS3 User Guide (Methot & Wetzel 2013).	
CPUE indices	UJPLL: 1994-2024 (NW,NE,SW,SE). CV of 0.1	Unconstrained parameter *q*
Length composition	Length composition for 14 out of the 15 fisheries (no ALGI_NW). Multinomial error structure: Length samples assigned maximum ESS of 20.	

5.2. Model sensitivity testing

The base model ("**4_update_rec**") was the starting point for further analyses and exploration of potential sensitivities within the model. Within this phase, variations of key data inputs, biological parameters, and model structures were explored. In 2023, several structural components of the model were explored. In this year's assessment, no major structural changes were tested, and instead the model sensitivity to data inputs, and biological parameters was tested. The aim of doing these runs was to identify any major sources of uncertainty that would impact assessment outputs. If specific data inputs or biological parameters were found to impact the assessment output, the plausible variations in these values were kept in the final ensemble of models used in the 'grid' from which stock status is derived.

Sensitivity testing was discussed via email with WPB participants, and some initial explorations agreed on. Further runs were included as model development continued. Table 6 below provides a brief description of the range of alternative model options explored in sensitivity testing.

Table 6: Description of various data inputs and biological parameters that were varied to test model sensitivity to them.

Sensitivity	Description of test
Time period of model	
s1_update_rec_short	Change time period of estimated recruitment to only the 'target' fishery time period (1985-2023) while still allowing catch from 'bycatch' fishery (1950 onwards)
s2_update_mod_time	Change time period of model to just the 'target' fishery time period (1985-2023)
CPUE indices	
s3_cpue_tw	Inclusion of Taiwan,China CPUE indices only (all others downweighted) for each area of the model
s4_altCPUE	Inclusion of Japanese (NW, NE, SW, SE; weight = 1.0); Indonesian (NE; weight 0.5); South African (SW; weight = 0.1); EU (Réunion; SW; weight = 0.5) indices. Based on CPUE comparison analyses.
s5_altCPUE_esp	Inclusion of Japanese (NW, NE, SW, SE; weight = 1.0); Indonesian (NE; weight 0.5); South African (SW; weight = 0.1); EU (Réunion; SW; weight = 0.5); EU (Spain; weight = 0.1) indices.
s6_altCPUE_esp_noreu	Inclusion of Japanese (NW, NE, SW, SE; weight = 1.0); Indonesian (NE; weight 0.5); South African (SW; weight = 0.1); EU (Spain; weight = 0.1) indices.
s7_altCPUE_prt_reu	Inclusion of Japanese (NW, NE, SW, SE; weight = 1.0); Indonesian (NE; weight 0.5); EU (Portugal; SW; weight = 0.5); EU (Réunion; weight = 0.5) indices.
s8_altCPUE_prt	Inclusion of Japanese (NW, NE, SW, SE; weight = 1.0); Indonesian (NE; weight 0.5); EU (Portugal; SW; weight = 0.5) indices.
Growth	
s9_new_growth	Use of new, revised growth parameters from Wang et al. (2026) using Indian Ocean swordfish age data from anal fin rays and otoliths.
Instantaneous rate of natural mortality (*M*)	
s10_natM_lorenzen	External estimation of age-based *M*, based on the Lorenzen functional form. Reference ages were 5 and 12 years old. M was not estimated internally. Initial M was set at 0.25 (to provide continuity from the reference model where M is fixed at 0.25).
s11_natM_lorenzen_new_grow	As above for M, with the new growth from Wang et al., (2026)
Recruitment variability	
s12_sigma_R4	$\sigma_r = 0.40$
s13_sigma_R6	$\sigma_r = 0.60$
Steepness (*h*)	
s14a_h70	h = 0.70
s14b_h90	h = 0.90

5.3. Proposed ensemble models (Grid)

On basis of the sensitivity analyses, further model options were configured to capture the main uncertainties in the model. From the results of the sensitivity analyses, the model was most sensitive to changes in the inclusion or not of the Tawian,China CPUE index (relatively "flat" compared to the other indices), and changes to recruitment variability. Indeed, the model is mainly driven by the estimated recruitment (which in turn is driven by the CPUE indices). However, the biomass estimates from the model that only used the TWLL CPUE indices were significantly higher than any of the other models. Whether this should be included within the grid, as a completely alternative solution could be debated (e.g. with no independent abundance indices, the current abundance could feasibly be either represented by the TWLL CPUE indices, or the other, more variable CPUE indices). In the context of catches, the TWFL fleet represents over 40 % of the total catch in the Indian Ocean.

The grid was run using the TWLL CPUE index as an additional variable, however the results below do not include these runs, due to the uncertainty surrounding initial biomass estimates from these models. Depending on the assessment group's decision, these runs could be included in the final uncertainty grid, or continue to be omitted.

Therefore, the grid incorporates an alternative CPUE option (where Indonesian, South African, and Réunion indices are included), new growth, Lorenzen instantaneous rate of natural mortality (*M*), and variation in recruitment, along with uncertainty in the steepness (*h*) parameter, and growth. The final models proposed for inclusion in the ensemble of models are:

- two options for growth;
- two options for *M*;
- two options for recruitment variability;
- two options for CPUE;
- three options for *h*.

Table 7: Description of the proposed final model options for the grid for the 2026 assessment. The final models consist of a full combination of options below, making a total of 48 models. The options adopted within the reference (base) model ('') are highlighted.

Model options	Description
Steepness (*h*) in SRR	• h70: $h = 0.70$
	• **h80: $h = 0.80$**
	• h90: $h = 0.90$
Growth	• Gnew: VB growth parameters estimated by Wang et al. (2026) • **Gold**: VB growth parameters estimated by Farley et al., (2016)
Natural Mortality	• Lorenzen: – Lorenzen functional form *M* with reference ages 5-12 yrs, and fixed M of 0.25
	• **Fixed M of 0.25 for all ages**
Recruitment variability	• **$\sigma_r = 0.20$**
	• $\sigma_r = 0.40$
CPUE	• **Only Japanese longline indices (NW, NE, SW, SE)**
	• altCPUE: Inclusion of Japanese (NW, NE, SW, SE; weight = 1.0); Indonesian (NE; weight 0.5); South African (SW; weight = 0.1); EU (Réunion; SW; weight = 0.5) indices. Based on CPUE comparison analyses.

6. MODELLING RESULTS

6.1. Continuity runs from 2023 model

Updating the SS3 executable ("**0_base_2023_exe**") had no impact on the model estimates. Updating the 2023 base model with catch had some impact to historical estimates of spawning stock biomass (hereafter referred to as biomass), between 1950 to ~ 1995, presumably due to re-estimation of catches over time. Biomass estimates in more recent years (1995-2024) were very similar to those of the 2023 model.

Updating the length frequency composition (all data, no filtering "**2_update_lf**") increased the overall estimate of biomass, but not the trajectory. Removal of the "ALGI_NW" fishery length frequency data did not affect estimates much at all, but using the filtering from the previous assessment ("**2_update_lf3**") reduced the overall estimate of biomass closer to that of the 2023 model. The addition of the length frequency data had limited impact on the biomass estimates from the model (compare the overall biomass estimate from "**1_update_catch**" and "**2_update_lf3**", Figure 10).

Updating the CPUE indices (first iteration = same indices included in the '***revised***' 2023 model – "**3_update_cpue**") mainly impacted the final 10 years of the model biomass estimates, with a sharper increase in biomass in the final years compared to the previous model. Down weighting all CPUE indices except the Japanese longline indices ("**3_update_cpue_2**") had almost no impact on the model biomass estimates (Figure 10), however the depletion (% SSB_0) showed a greater rate of recovery compared to when the ZAF, and PRT indices were included (as in 2023; Figure 11).

The recruitment bias correction ("**4_update_rec**") increased the overall scale of biomass slightly and showed a reduction in biomass trend in the earlier years of the model (1960-1980) during the bycatch portion of the fishery. In the final years of the model, the recruitment bias correction shows the depletion (% SSB_0) and estimated biomass increasing more than the previous model (where the bias correction was not applied).

The full output of management quantities is found in Table 8. There is ~ 5 % increase in C_{MSY} estimates from the 2023 base model to the 2026 base model.

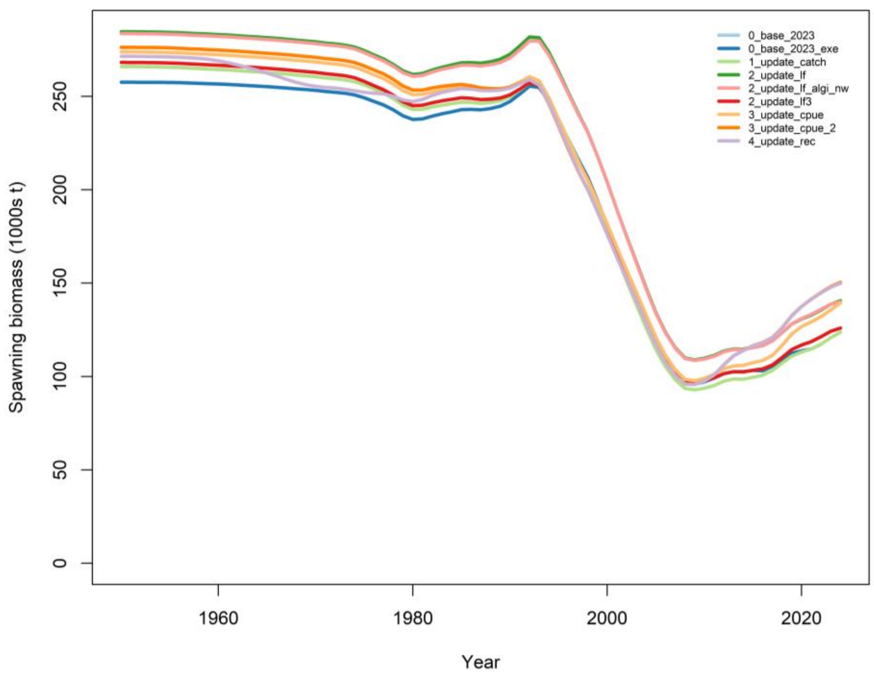

Figure 10: Spawning biomass trajectories for IO swordfish from the stepwise model updates. (from the 2023 assessment reference model '0_base_2023').

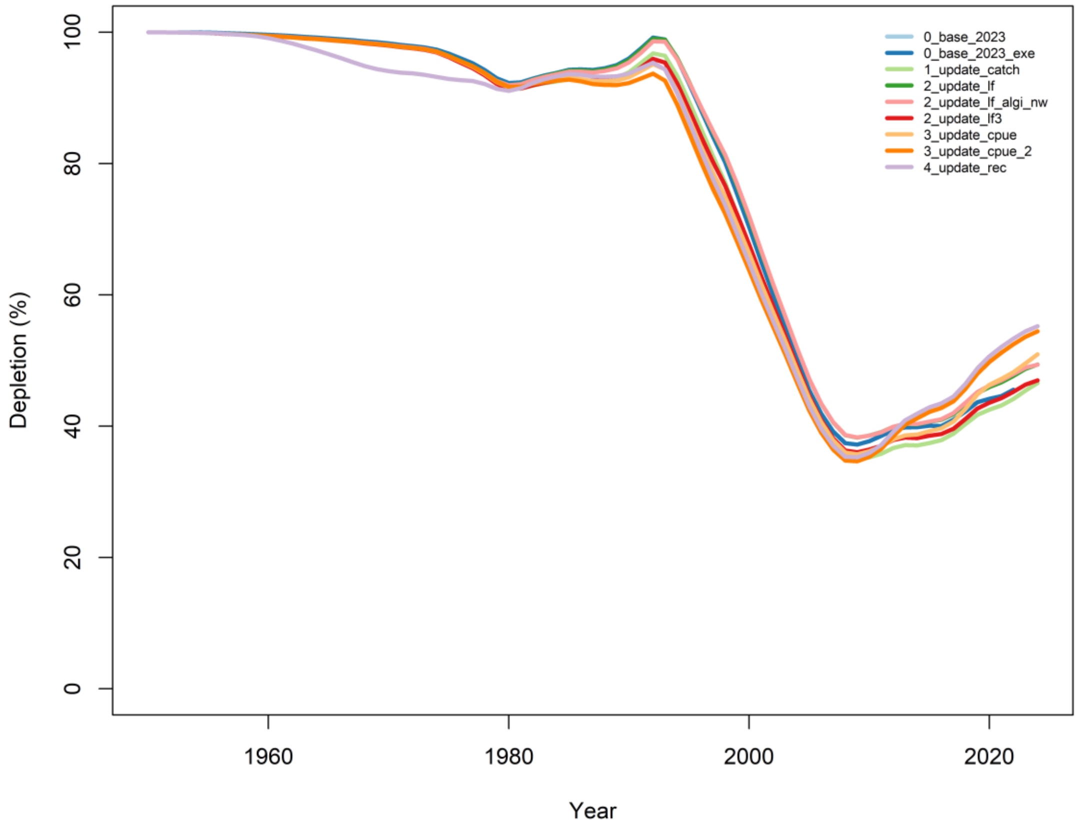

Figure 11: Spawning biomass trajectories (depletion (%)) for IO swordfish from the stepwise model updates. (from the 2023 assessment reference model '0_base_2023').

Table 8: Estimates of management quantities for the step-wise updates of the 2023 stock assessment reference model ('0_base_2023') to the 2026 reference model ('4_update_rec')

	SSB_{1950} (t)	SSB_{MSY} (t)	SSB_{2024} (t)	$SSB_{2024}SSB_{1950}$	$SSB_{1950}SSB_{MSY}$	F_{MSY}	F_{2024}	$F_{1950}F_{MSY}$	C_{MSY} (t)
0_base_2023	257567	60753.4	114838	0.4458568	1.890232	0.165637	0.071022	0.428781	34236
0_base_2023_exe	257567	60753.4	114838	0.4458568	1.890232	0.165637	0.071022	0.428781	34236
1_update_catch	265908	62196.4	123802	0.4655821	1.990501	0.165205	0.07754838	0.469407	34799.6
2_update_lf	284588	66517	140585	0.4939948	2.11352	0.165661	0.07124682	0.430076	37427.7
2_update_lf_algi_nw	283636	66273.7	140016	0.4936468	2.112693	0.166169	0.07194254	0.432948	37522.1
2_update_lf3	268188	62682.4	125993	0.4697936	2.010022	0.165875	0.07845025	0.472948	35422.1
3_update_cpue	273811	63747	139539	0.5096179	2.18895	0.166225	0.06891938	0.414615	36129.7
3_update_cpue_2	276286	64168.8	150443	0.5445191	2.344488	0.166447	0.06505248	0.39083	36415.4
4_update_rec	271449	62914	149921	0.552299	2.382951	0.167094	0.0646851	0.387118	35995.3

6.2. Model fits

6.2.1. Base model (4_update_rec)

The base model fits the new CPUE indices for each regional JPLL index well enough (Figure 12). Fits were best to the NE and SW indices, although for all regions, the predicted indices lacked the variation seen in the observations. The residuals did suggest an upward trend in recent years in the NE and SE regions. However, this trend was not that strong in the SE. An initial downward trend in the residuals in the SW region is quite severe, before flattening in the trend from around 2005. This corresponds to a decrease in overall catch of swordfish after high catches prior to 2005. (Figure 13 and Figure 2 (catches)). Although the trend lines suggest potentially worrying trends, the overall distribution of the residuals, if the lines were not estimated, do not produce obvious trends.

Overall, there were relatively good fits to the aggregated length frequency data for the main fisheries that have comprehensive sampling (Figure 14). The fisheries with the greatest catch by volume (TWLL in all regions) show relatively good fits to the length frequency data, with the exception of the TWLL in the NW where the predicted values underestimate the number of smaller fish in this region. In the EUEL SW and EUEL SE fisheries, the predicted length frequency distributions over estimated the number of small fish in these fisheries. For almost all fisheries, the model overestimated the number of very large fish in the final length bin, which were not observed in the data.

The recent trends in the predicted average fish size for all fisheries are well captured by the model. There was some underestimation of average fish size in the ISEL_SW and AUEL_SE fisheries, in the later years of the model. (Figure 15).

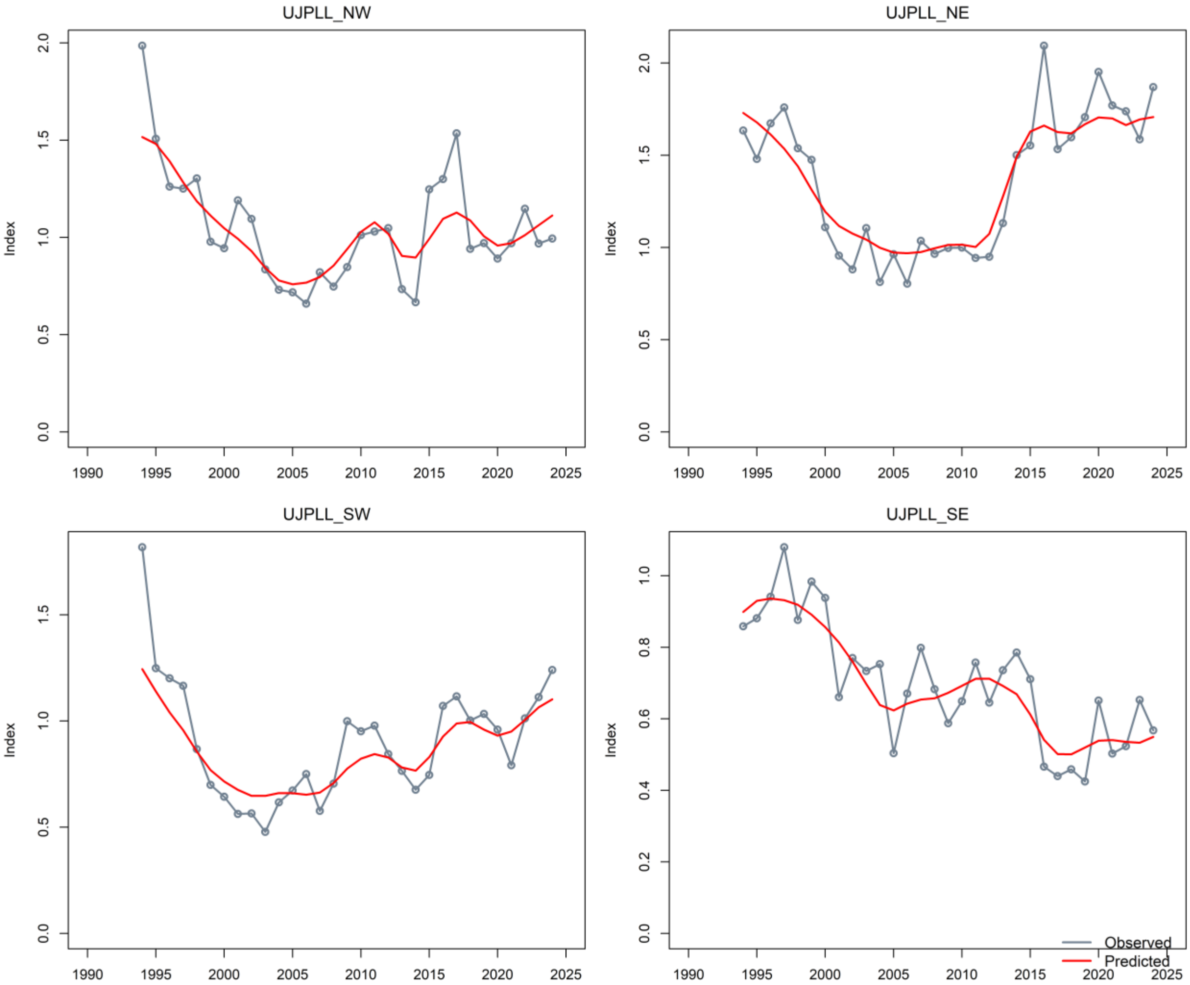

Figure 16: Fits to the CPUE indices 1994-2024 in the base model ''.

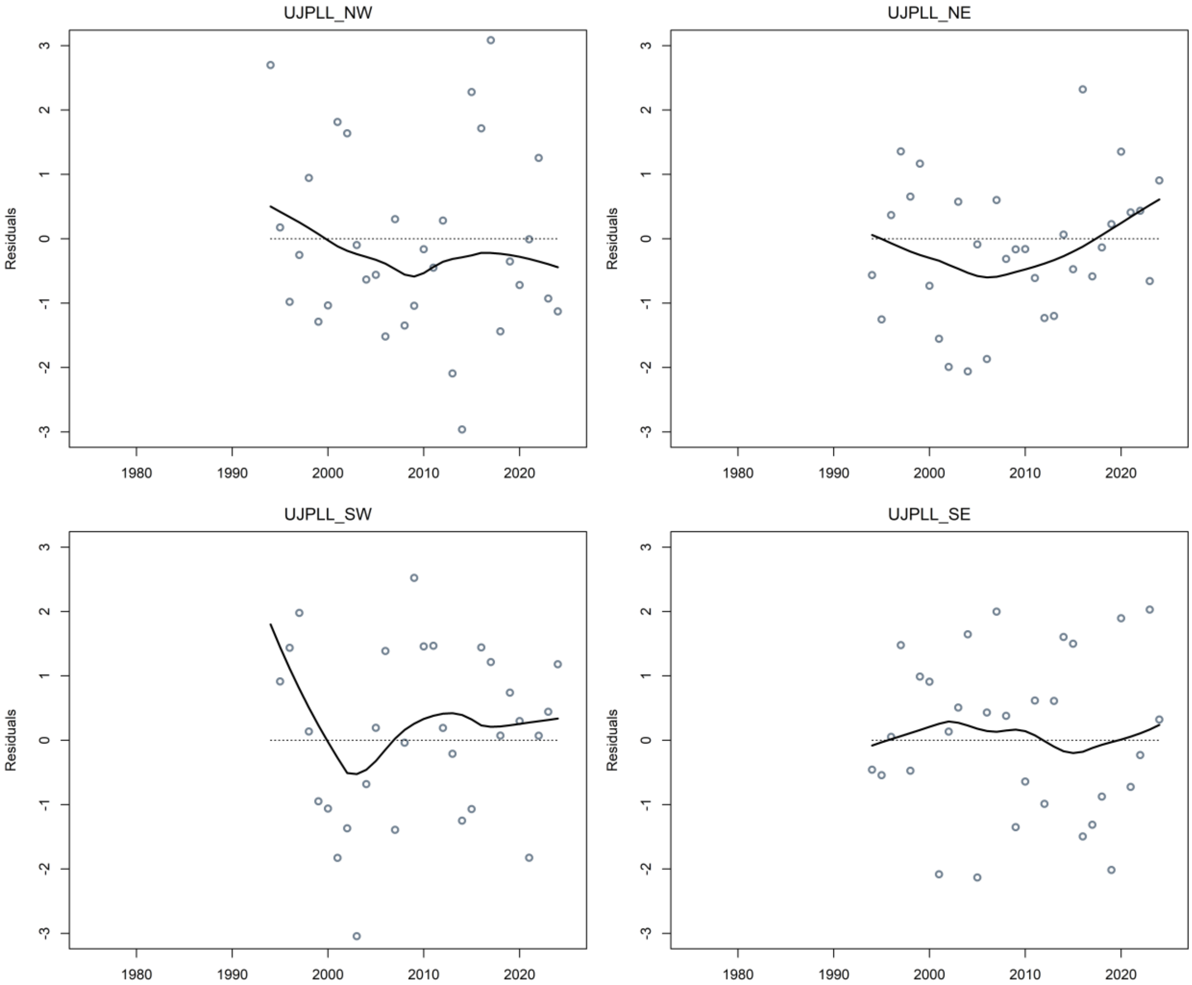

Figure 13: Standardised residuals from the fits to the CPUE indices from the base model '4_update_rec'.

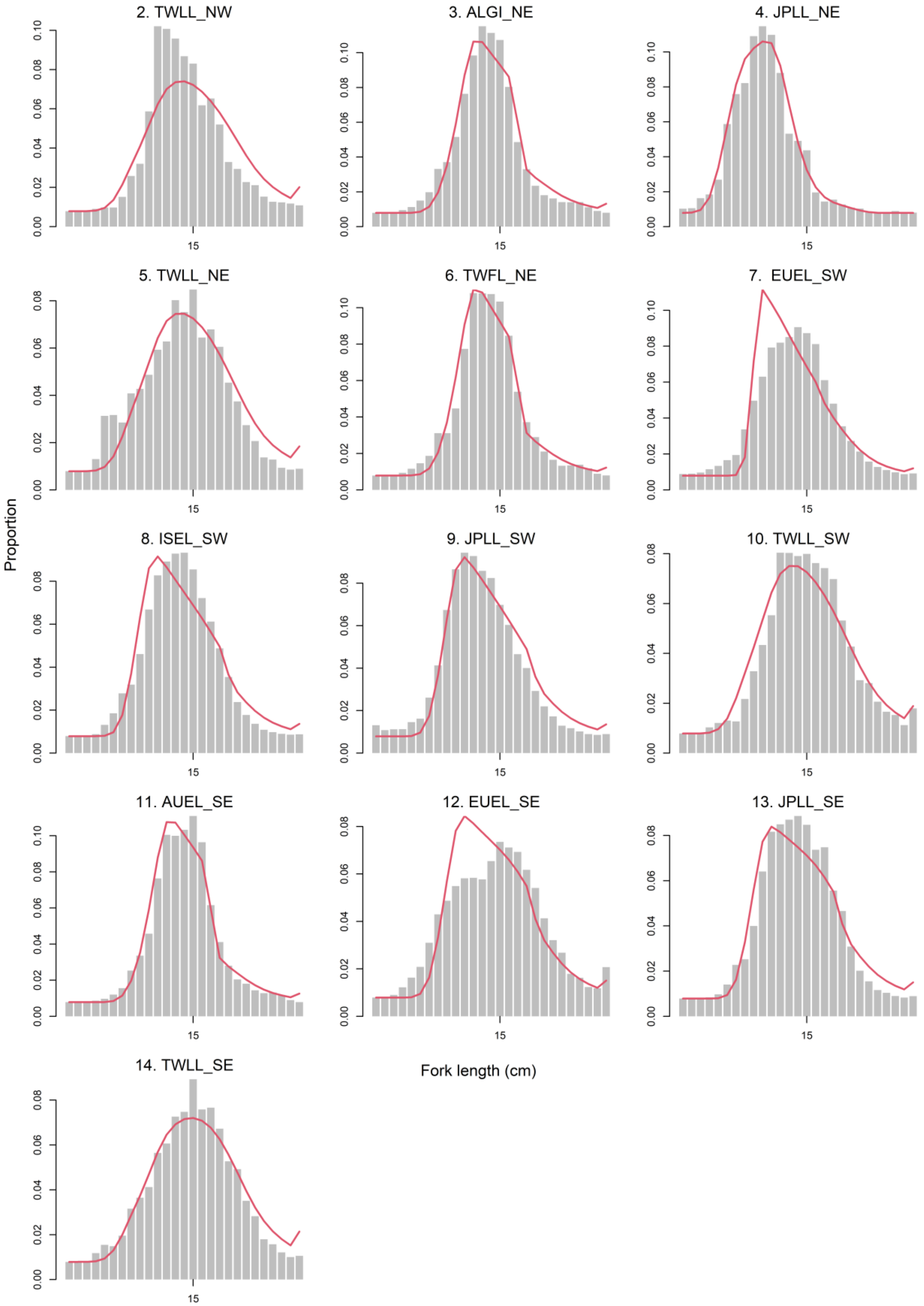
2. TWLL_NW
3. ALGI_NE
4. JPLL_NE
5. TWLL_NE
6. TWFL_NE
7. EUEL_SW
8. ISEL_SW
9. JPLL_SW
10. TWLL_SW
11. AUEL_SE
12. EUEL_SE
13. JPLL_SE
14. TWLL_SE
Proportion
Fork length (cm)
15

Figure 14: Observed (grey bars) and predicted (red line) length compositions (in 9 cm intervals) for each fishery of swordfish aggregated over time for the base model '4_update_rec'.

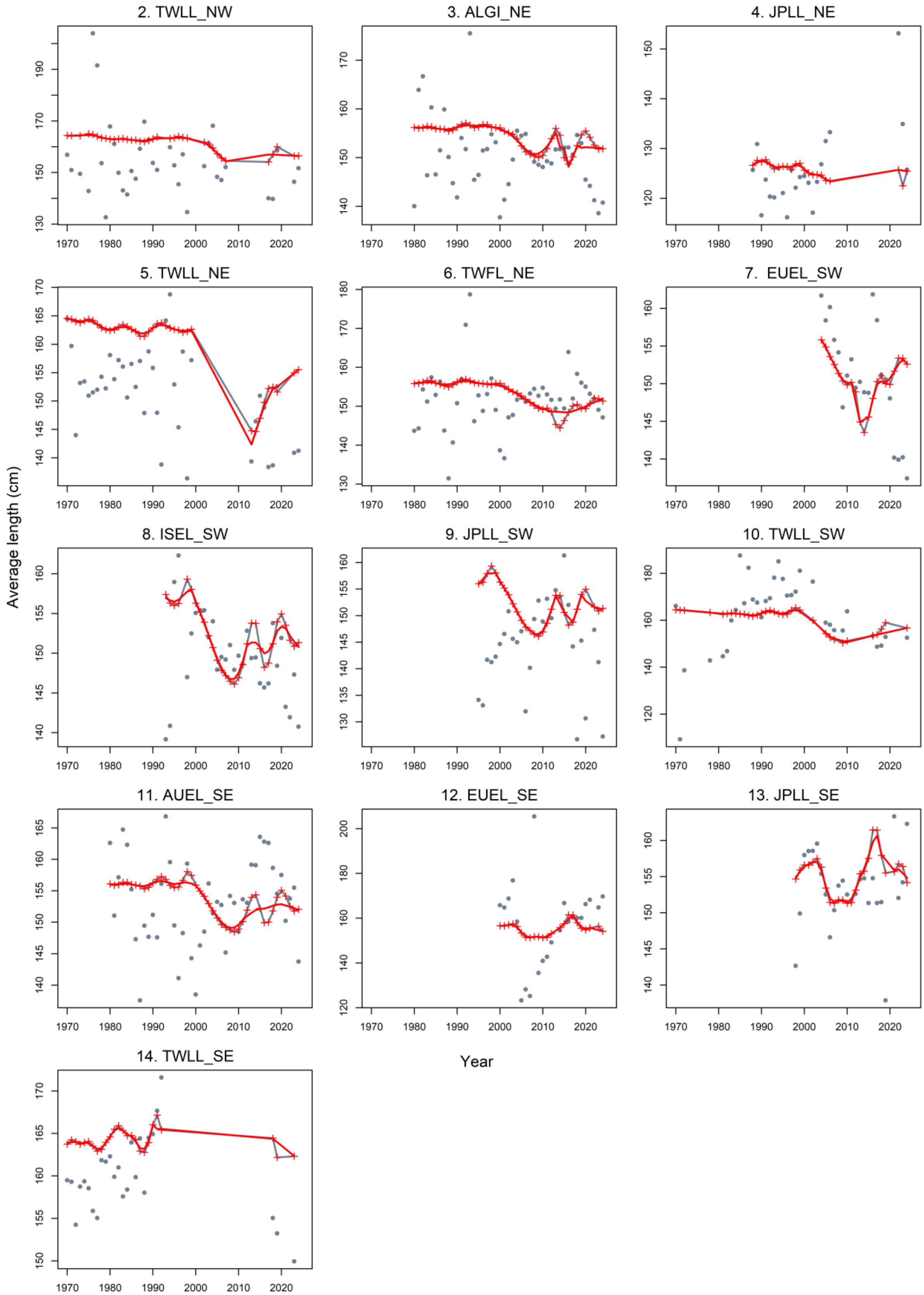
2. TWLL_NW
3. ALGI_NE
4. JPLL_NE
5. TWLL_NE
6. TWFL_NE
7. EUEL_SW
8. ISEL_SW
9. JPLL_SW
10. TWLL_SW
11. AUEL_SE
12. EUEL_SE
13. JPLL_SE
14. TWLL_SE
Average length (cm)
Year

Figure 15: A comparison of the observed (grey points) and predicted (red points and line) average fish length (FL, cm) of swordfish by fishery for the main fisheries with length data for the base model '4_update_rec'.

6.3. Model estimates

6.3.1. *Selectivity*

As in the 2023 model, the estimated parameters in the basic model include: the overall population scale parameter *R0*, the time series of recruitment deviates, the distribution of recruitment among regions, fishery selectivity parameters, and the catchability parameters for the CPUE indices.

The size-specific selectivity functions are presented in Figure 16. Full selectivity is reached for the JPLL fleets around 150 cm. For all other fisheries, there is a drop off from full selectivity to partial around 200 cm. Some fleets retain high selectivity of very large fish e.g. TWFL_NE, EUEL_SW, EUEL_SE, AUEL_SE, and ISEL_SW, while the ALGI_NW and ALGI_NE fisheries display a bimodal dome-shaped selectivity. This possibly represents two separate fishing métiers (e.g. different gillnet mesh sizes, or spatial and/or temporal heterogeneity in fleet dynamics).

Selectivity estimates are broadly similar to the 2023 model, with the exception of the EUEL_SW, EUEL_SE, AUEL_SE, and ISEL_SW fleets which were logistic curves with full selectivity around 150 cm (as the JPLL fleets).

6.3.2. *Recruitment*

Recruitment deviates were estimated from 1955 – 2023 (Figure 17). As in the 2023 model, there is a strong increase in recruitment from 2000 to 2015, followed by a decrease in estimated recruitment. From 2021 to 2023, the estimated recruitment increases again. As in the previous model, an interpretation of these estimates is that there was potentially high recruitment prior to the start of the targeted fishery in the 1990s, followed by anomalously low recruitment. As the previous stock assessment report stated, this trend is suspicious, but without the recruitment anomalies, the model could not provide an adequate fit to the CPUE series. As in the previous assessment, it could be expected that the recruitment signal might be corroborated by the size data, but there is no strong signal in mean sizes, except that the observed mean size for most fleets showed some decline through the 2000s in the SW (see Figure). The distribution of recruits among areas showed very similar patterns among regions (Figure 19) with the exception of a large pulse in the NE preceding the anomalously large increase of the Japanese longline CPUE towards the end of the time series.

6.3.3. *Spawning stock biomass*

This revised model suggests that the carrying capacity of the population in the southern regions (area 3 and area 4; SW and SE respectively) is lower than the northern regions (Figure 20). In the previous assessment, there was an increase in the population at the start of the targeted fishery (early 1990s). This is absent in the NW (area 2) and SE (area 4) regions of the 2026 model, but still exists in the other two regions (NE and SW). All regions (except the SE) have experienced a sharp decline in estimated biomass from the start of the targeted fishery to 2015, followed by overall increases in biomass (particularly in area 2, NW). The SE region has experienced a relatively slow reduction in biomass over the whole time period of the model. These differing estimates of biomass trends are driven by the CPUE indices.

The SW region was estimated to be depleted the most, however current biomass is stimated to be around 60 % of the initial level for all areas, in contrast with the previous model where the SW region was estimated to have a current depletion of 20 % of the initial levels (Figure 21).

6.3.4. *Trends in fishing mortality*

In most regions, estimates of fishing mortality for TWLL and TWFLL fleets were estimated to peak between the 1990s and early 2000, followed by an increase in the ALGI (northern areas) and EUEL fleets (southern areas) fishing mortality from 2010 onwards. In all areas, fishing mortality is estimated to have decreased from 2010 to 2024 (Figure 22).

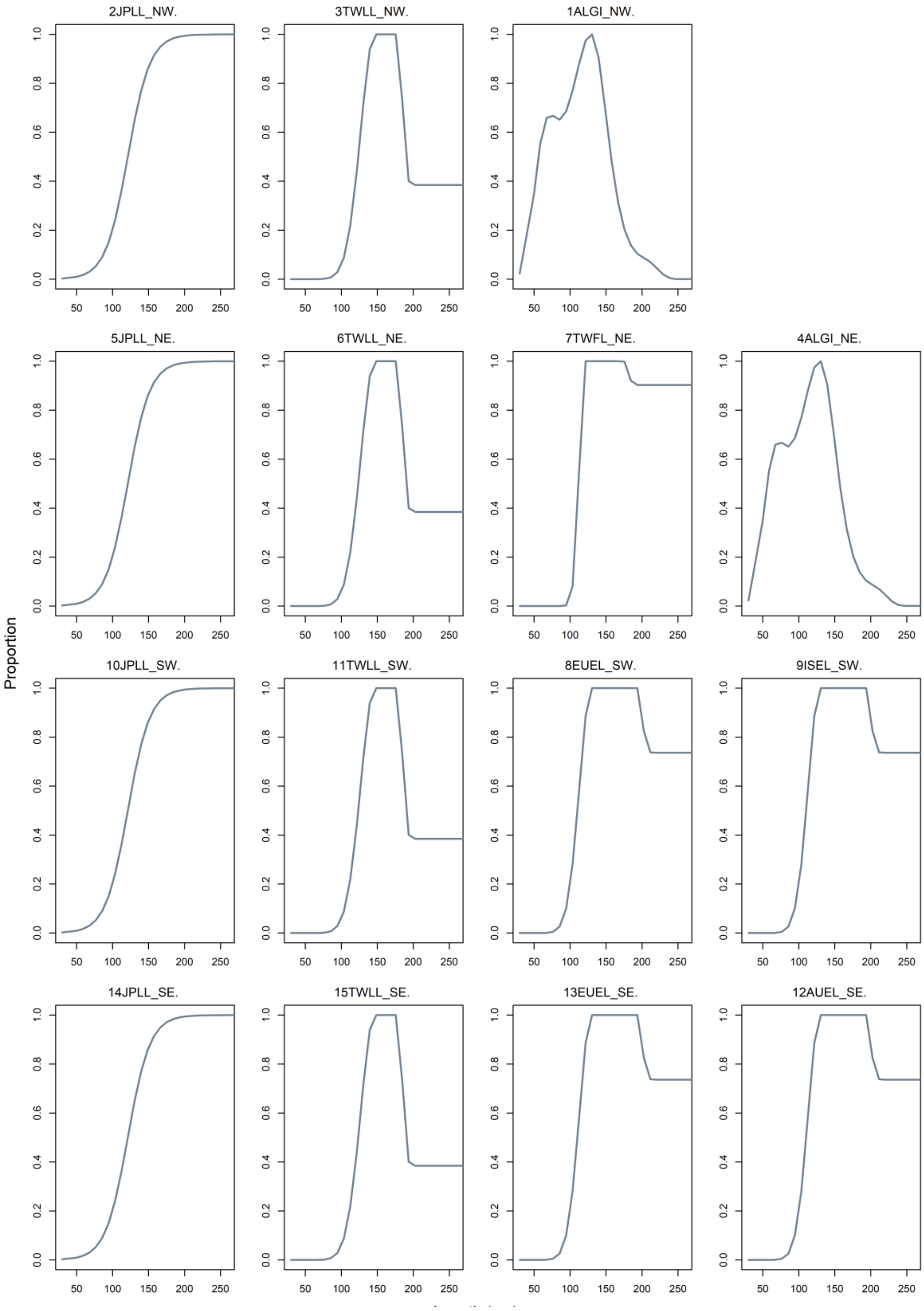

Figure 16: Estimated age-based (quarters) selectivity for model fleets within the base model '4_update_rec'.

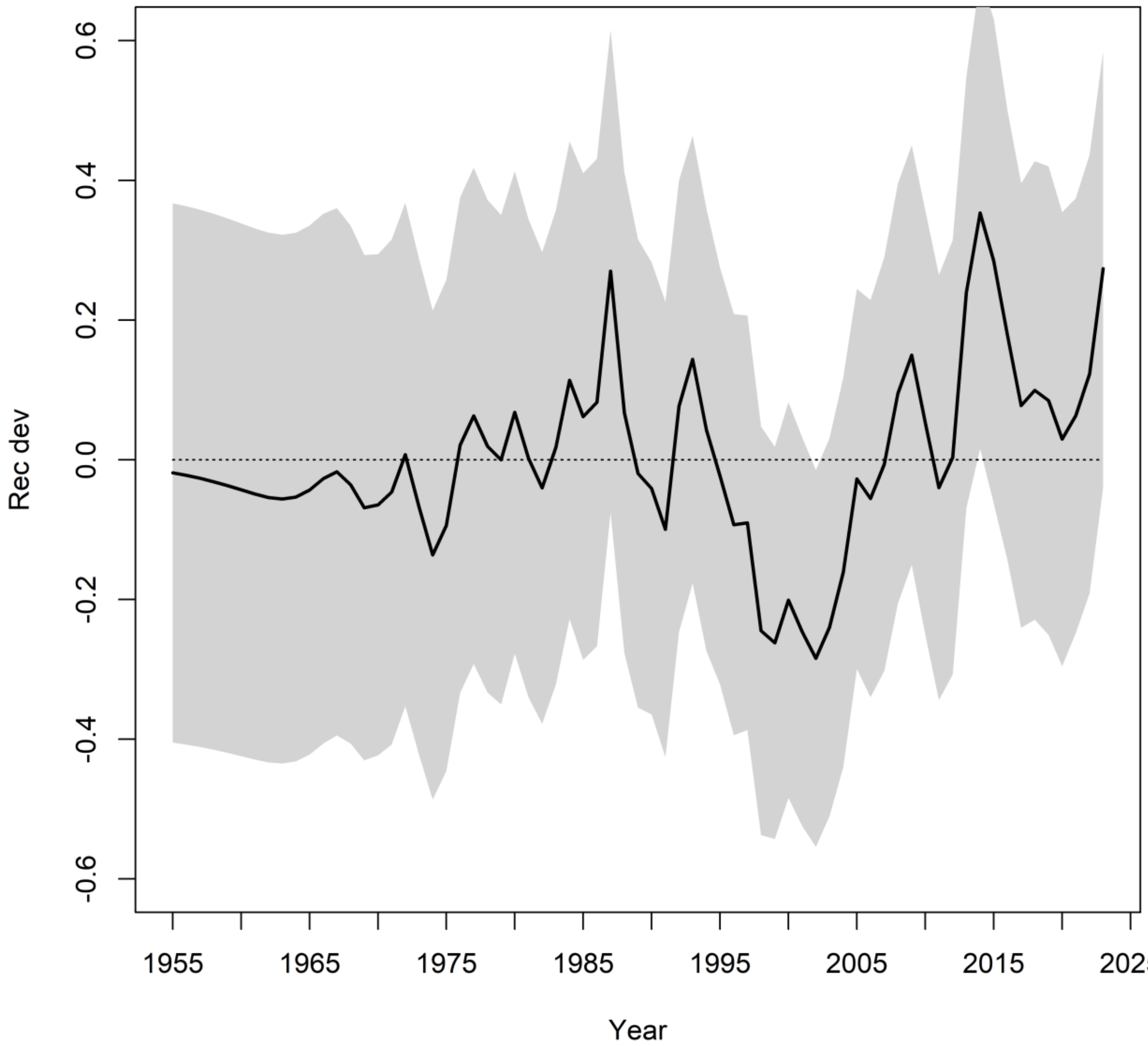

Figure 17: Recruitment deviates from the SRR with 95% confidence interval from the reference model '4_update_rec'.

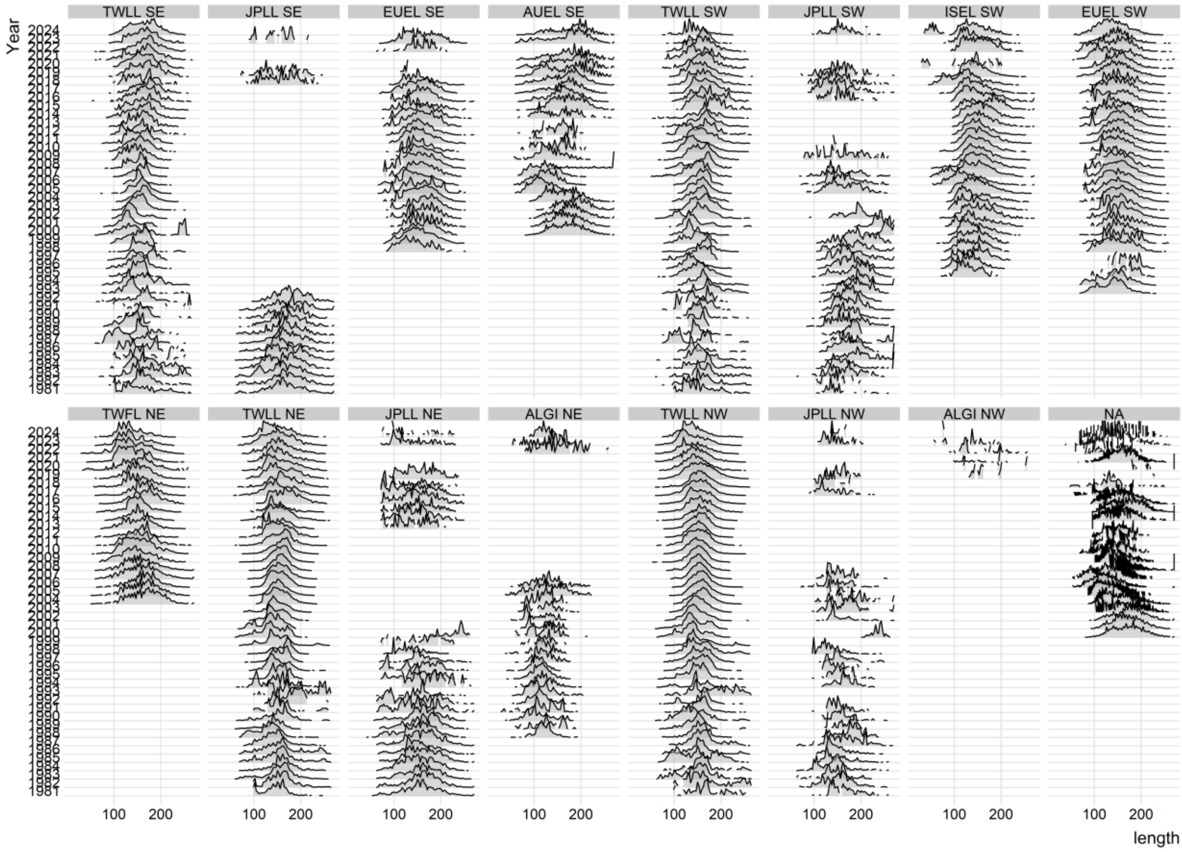

Figure 18: Length distributions within the model fleets (and some measurements that were excluded as they did not correspond to a fleet (NA). There are no obvious recruitment signals that line up with the estimates of recruitment from the model outputs (e.g. an increase in smaller fish around ~ 1995 that would then be recruited to the fishery around 2000).

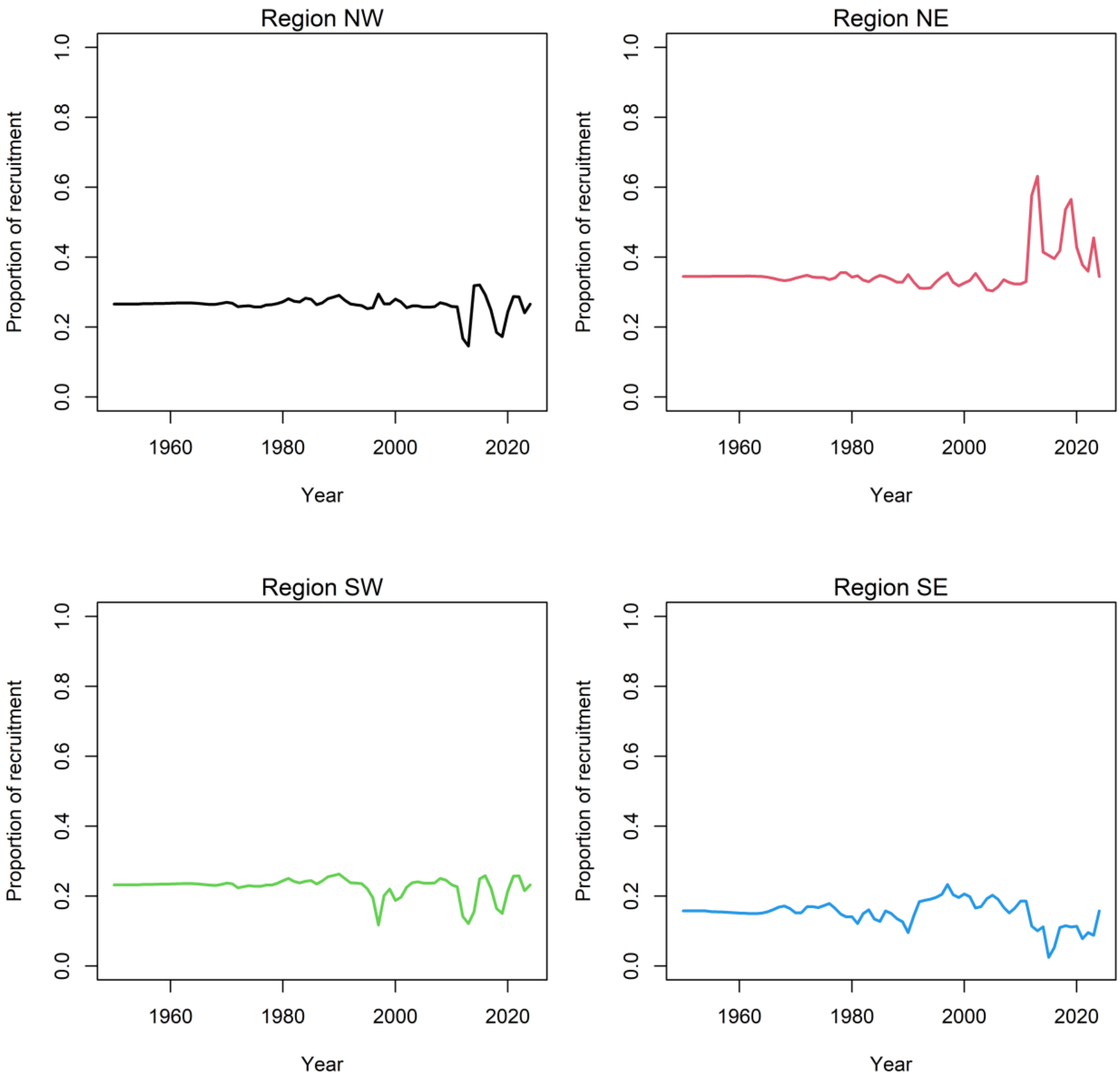

Figure 19: Recruitment proportions for the four areas of the model..

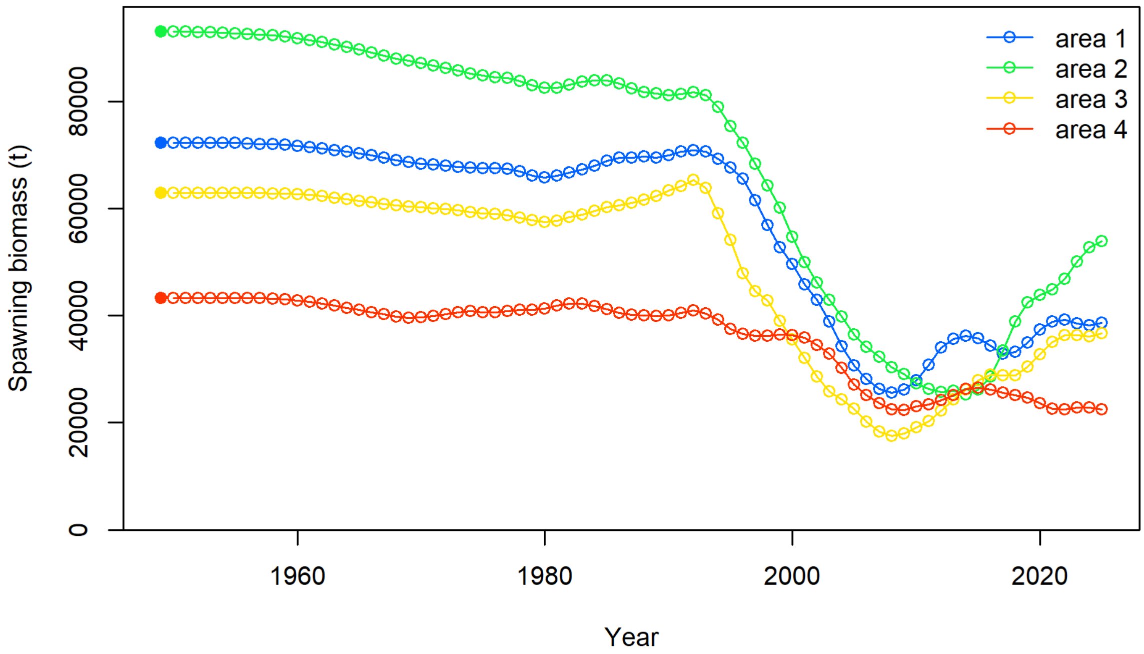

Figure 20: Estimated spawning biomass trajectories for the individual model regions from the base model '4_update_rec'.

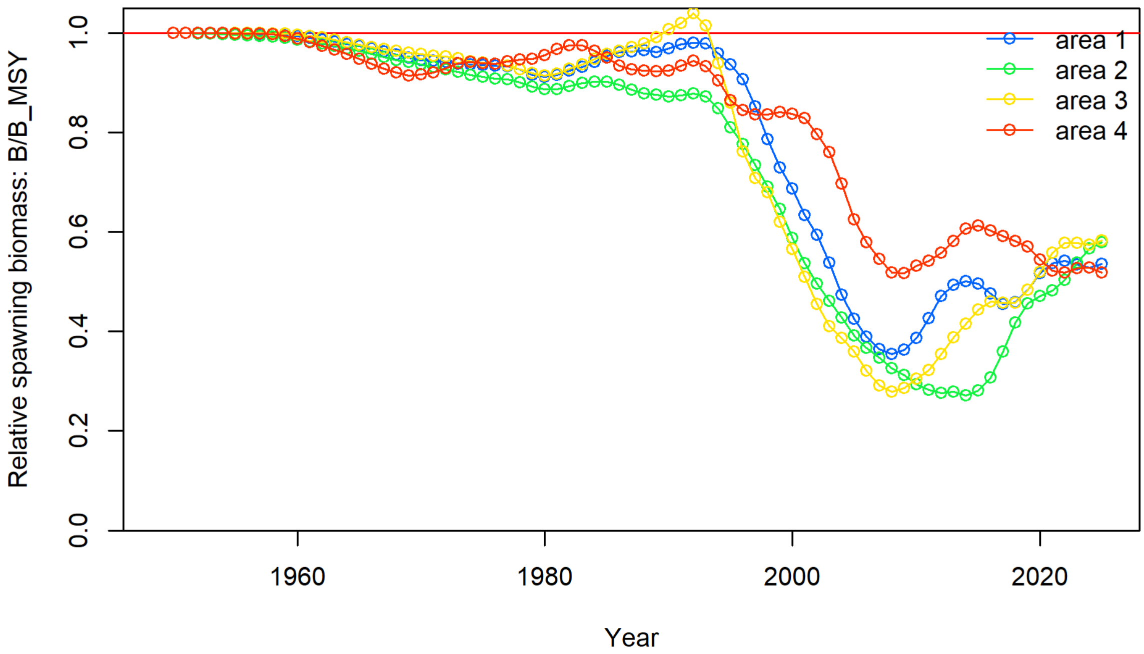

Figure 21: Estimated relative spawning biomass trajectories for the individual model regions from the base model '4_update_rec'.

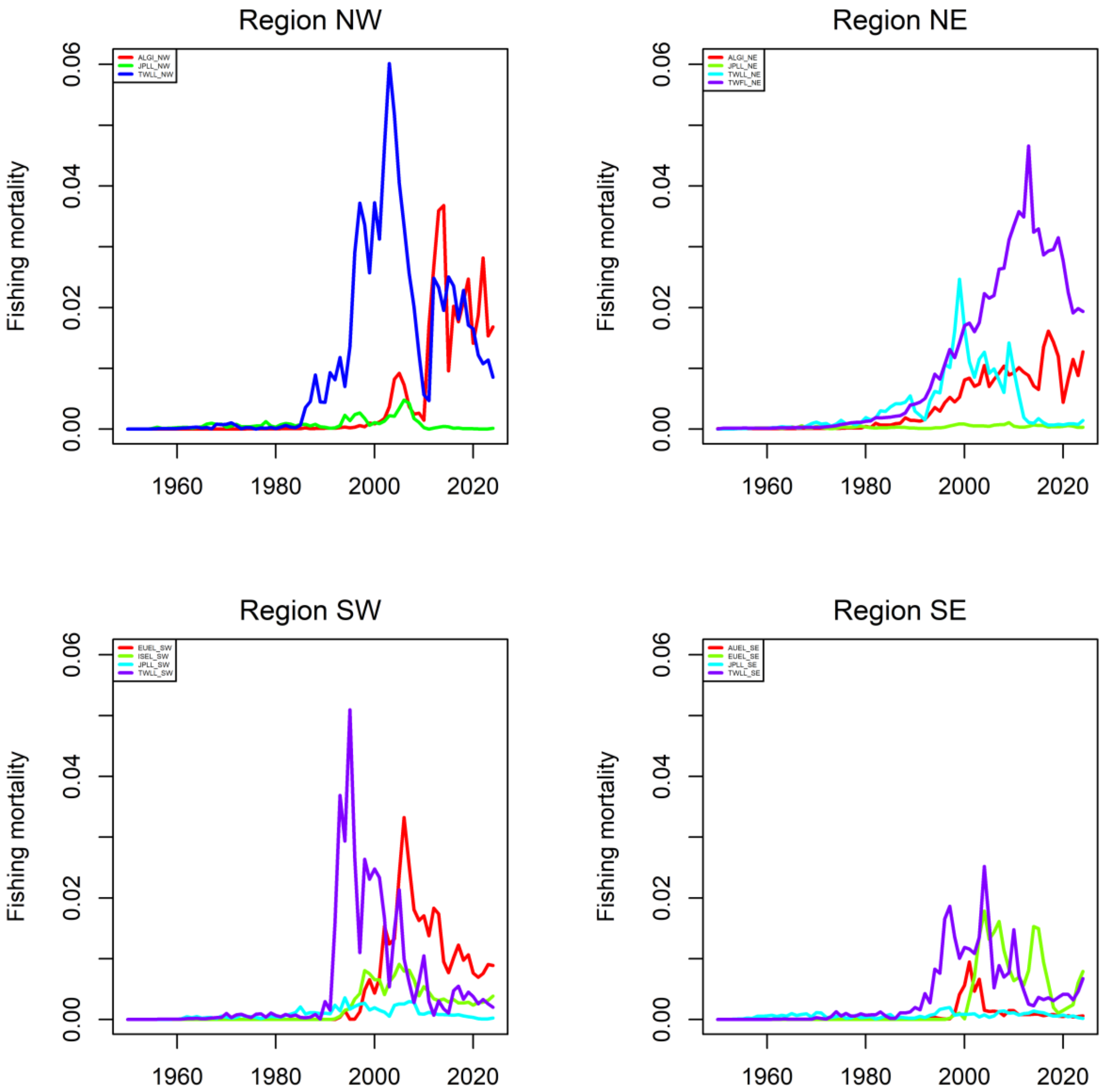

Figure 22: Trends in fishing mortality (yearly) by fleet for the base model '4_update_rec'.

6.4. Diagnostics

Some diagnostic tools were run for the base model, including running an age structured production model (ASPM), likelihood profiling, and a retrospective analysis.

6.4.1. ASPM analysis

The Age Structured Production Model (ASPM) analysis (Maunder & Piner, 2015) was used to illustrate the main drivers of the population trend, and to understand whether the length composition data has an undue influence on the estimates of abundance. The ASPM analysis involved running two variations of the reference models: *ASPMfixed* where length composition data were removed from the model (by fixing selectivity parameters) and recruitment deviates were fixed at zero; and *ASPMrec* where fixed recruitment deviates (estimates from the reference model) were added back into the model (and selectivity remained fixed).

The estimated absolute spawning stock biomass from both ASPM model runs for the base model is shown in Figure 23. All three configurations track closely from the start of the series through the late 1980s, describing a slow, gradual decline. A sharp, shared decline occurs across all three models between approximately 1990 and 2005, indicating this signal is robust to the removal of length composition data and to constraining recruitment to the stock–recruit relationship.

The absolute biomass trajectory reproduces the same pattern seen in relative terms: a shared decline to a minimum around 2003–2008 (approximately 85,000–165,000 t depending on configuration), followed by partial and configuration-dependent recovery. *ASPM_rec* estimates the lowest biomass throughout almost the entire time series, including the initial (1950) biomass, while *ASPM* estimates the highest.

Exploitation rate estimates are consistent with the biomass patterns. All configurations show negligible exploitation prior to 1990, followed by a rapid increase through the 1990s–early 2000s. From that point, *ASPM_rec* estimates substantially higher and more variable F/FMSY than the other two configurations, exceeding 1.0 (i.e., nominal overfishing) around 2003 and again in 2012. The *Base* model and *ASPM* remain below approximately 0.75 throughout the series (Figure 24).

All three configurations broadly track the shape of the observed indices in each region (Figure 25, Figure 26, Figure 27, Figure 28). The estimated catchability coefficients differ substantially between configurations though, summarised in each plot. This is to be expected with estimated biomass differing between the three models.

To summarise, the core depletion signal for the swordfish assessment is driven by catch and index data, not by the composition data. However, a significant share of the base model's fit depends on estimated recruitment deviations. This raises the question of whether recruitment deviations are compensating for misspecification elsewhere (e.g., steepness, natural mortality, index standardisation) rather than reflecting genuine recruitment variability, as stated previously.

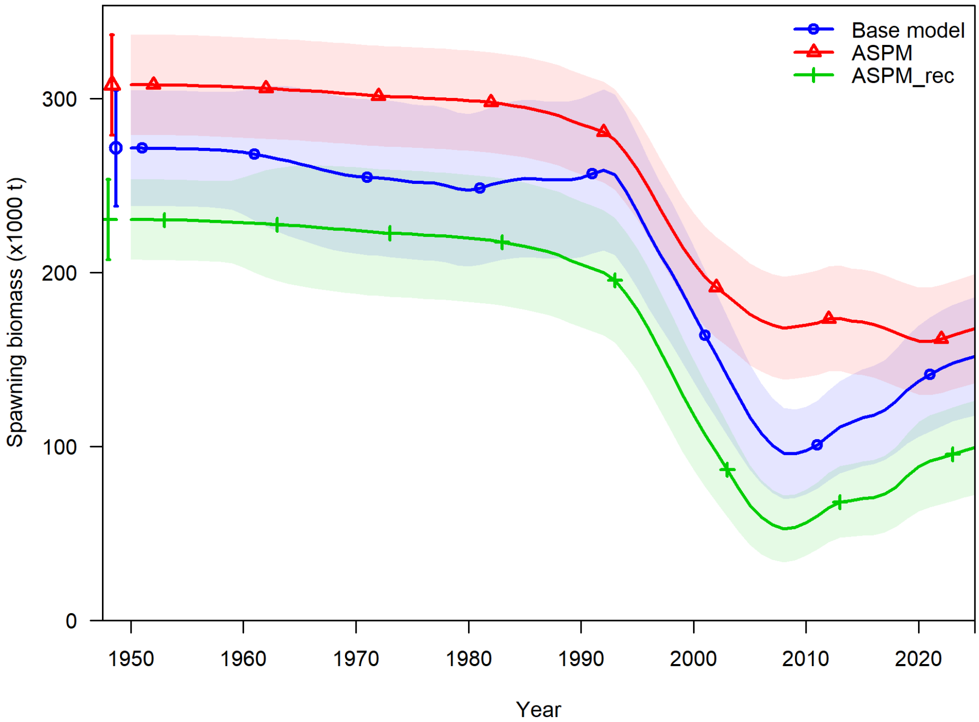

Figure 23: Estimated absolute spawning biomass (1000 t) for each model configuration.

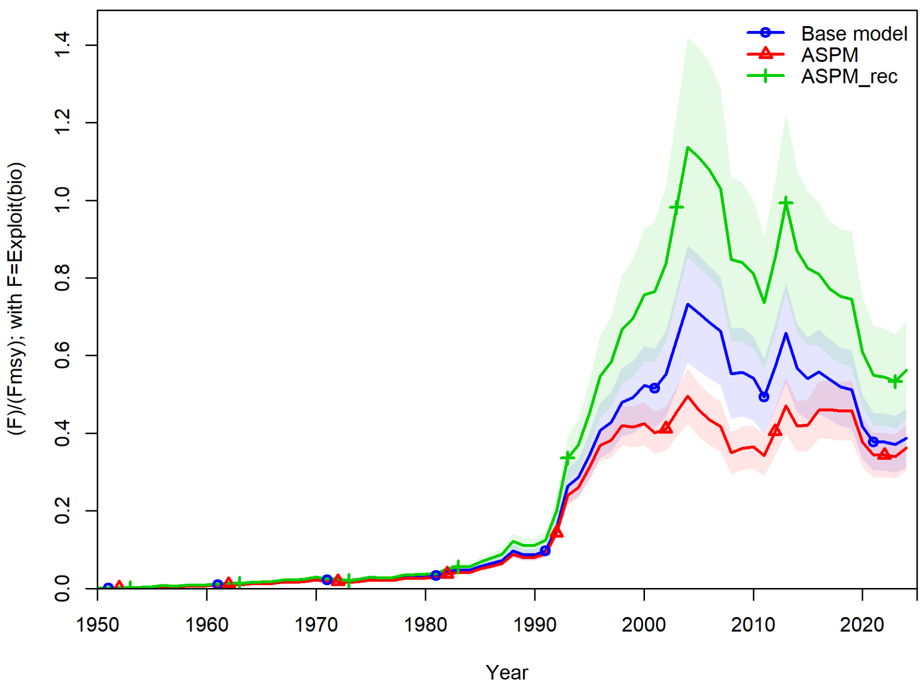

Figure 24: Estimated fishing mortality relative to FMSY, 1950–2024, by model configuration.

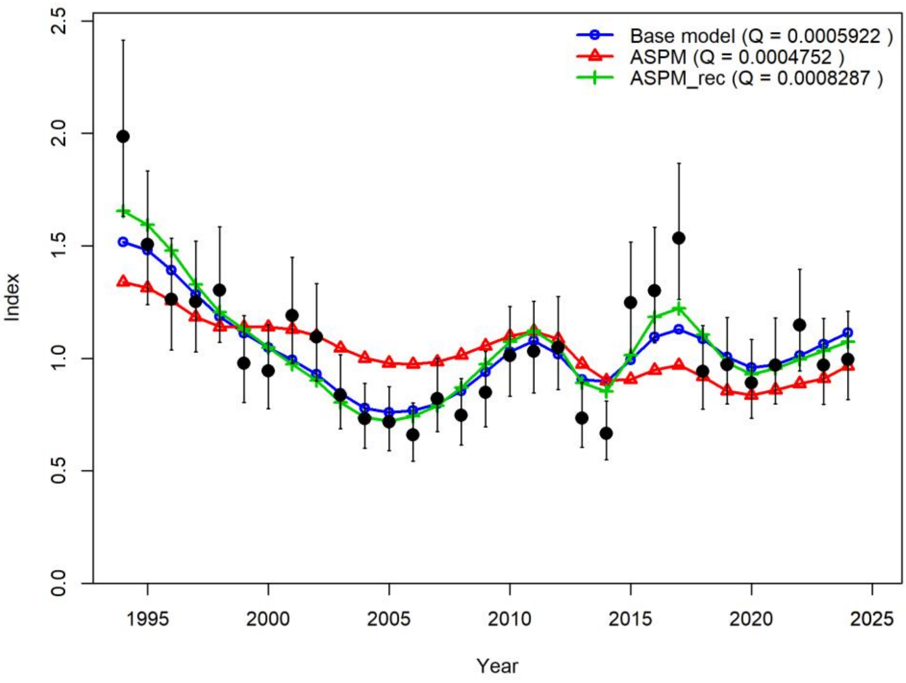

Figure 25: Observed (points) and predicted (lines) for the JPLL NE abundance index, 1994–2024, with estimated catchability (Q) by model configuration.

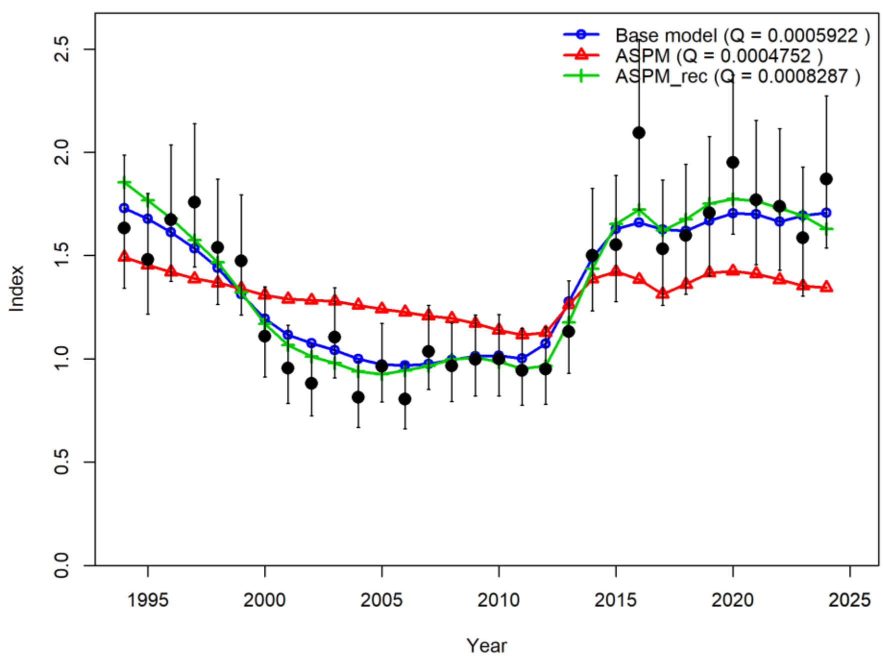

Figure 26: Observed (points) and predicted (lines) for the JPLL NW abundance index, 1994–2024, with estimated catchability (Q) by model configuration.

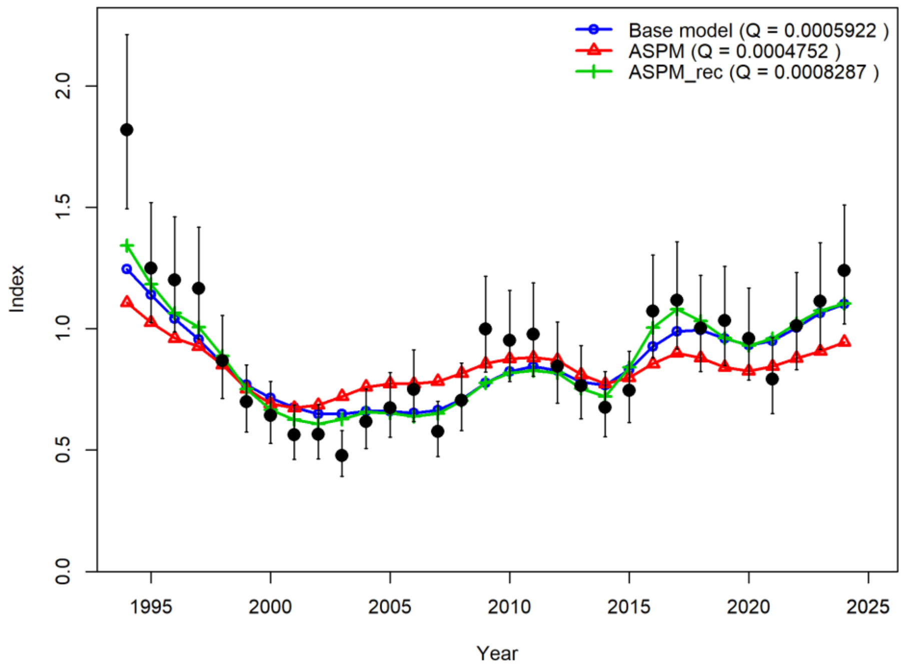

Figure 27: Observed (points) and predicted (lines) for the JPLL SW abundance index, 1994–2024, with estimated catchability (Q) by model configuration.

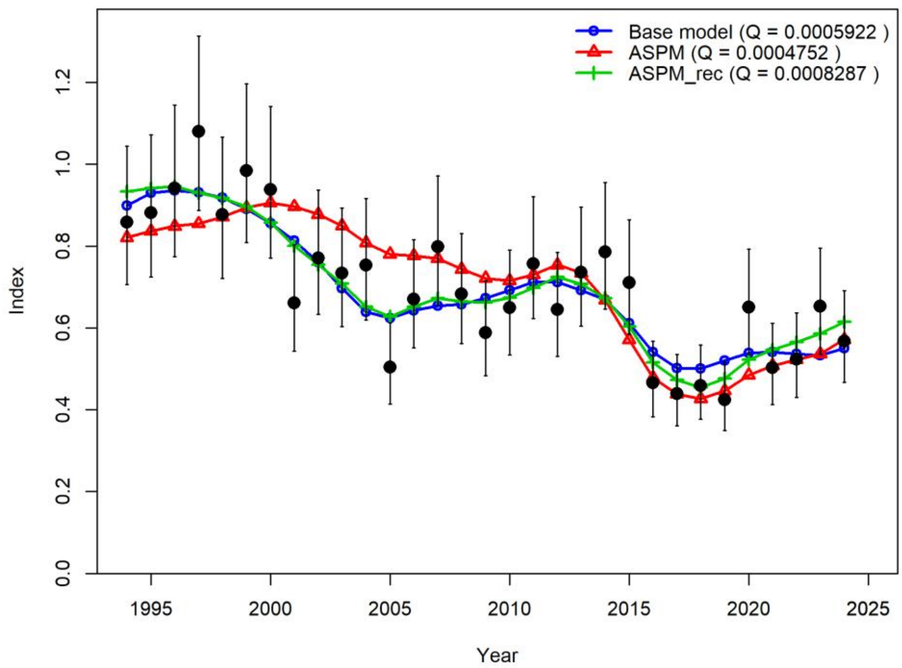

Figure 28: Observed (points) and predicted (lines) for the JPLL SE abundance index, 1994–2024, with estimated catchability (Q) by model configuration.

6.4.2. Retrospective analysis

Retrospective analysis is a diagnostic approach to evaluate the reliability of parameter and reference point estimates and will allow the revelation of systematic bias in the model estimation. It involves fitting a stock assessment model to the full dataset, and then sequentially removing data from the inputs from the most recent years. The analysis was conducted using the base model, and the last 5 years of data were removed in 1-year increments to evaluate whether there were any notable changes to the model results. The selected period mirrors that of previous assessments. The analysis of the impact of data removal was conducted on the outputs of estimated spawning stock biomass (SSB) and the ratio of $SSB_{current}$ to SSB_0.

There were no apparent retrospective patterns in the estimates for SSB or SSB_{2024}/SSB_0 (Figure 29), and this provides significant confidence in the robustness of the model with respect to inclusion of recent observational data.

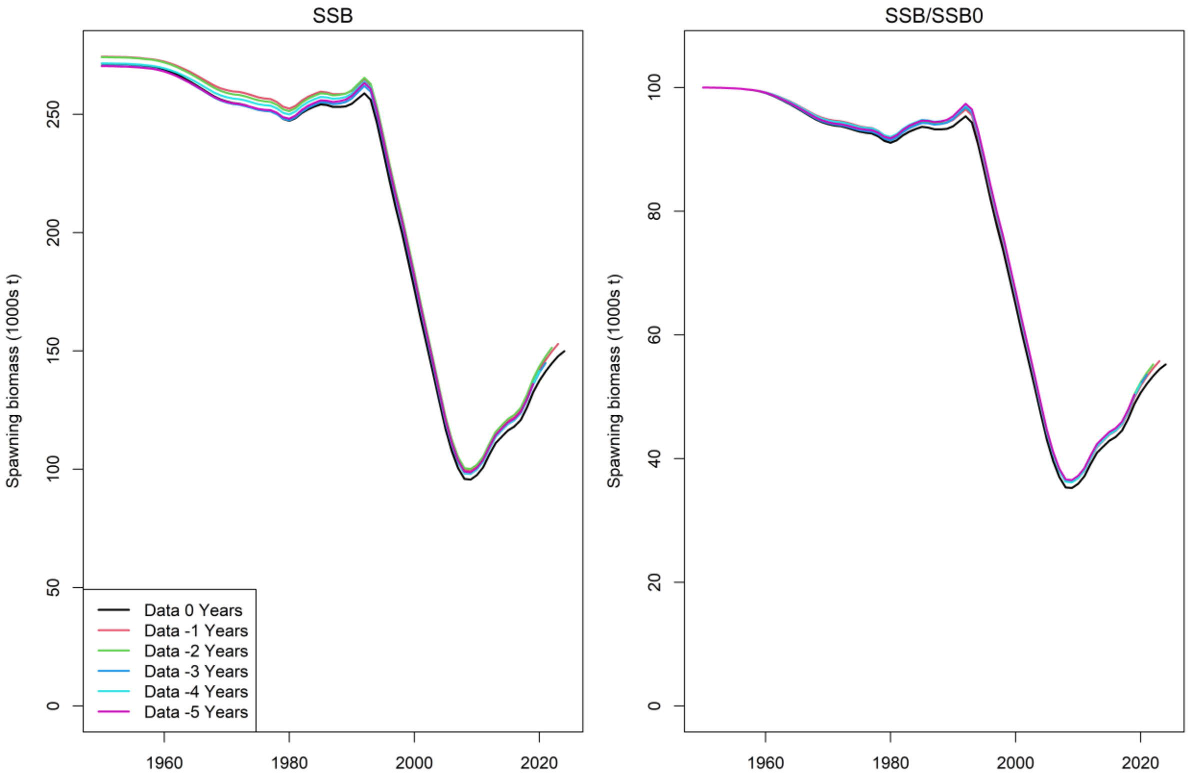

Figure 29: Retrospective analysis summary for the base model '4_update_rec'.

6.4.3. Likelihood profiling

A likelihood profile over log(R0) – the log of unfished recruitment – is a standard diagnostic used to evaluate how precisely the model estimates this key scaling parameter, and which data sources or model components are driving that estimate. As this was a parameter that appears to be influenced by the inclusion or not of recruitment deviates, and the length composition data, this profile was chosen to be investigated. R0 was fixed at a sequence of values spanning the range around its maximum likelihood estimate (MLE), and the model was re-optimised conditional on each fixed value, and the resulting total negative log-likelihood (NLL), together with its components (recruitment, length composition data, index data, priors, F ballpark, and parameter deviations), was estimated. The change in NLL relative to the minimum was plotted for the total and for each contributing component (Figure 30).

The likelihood profile shows a single, well-defined minimum with no evidence of secondary modes, suggesting LN(R0) is approximately 8.2. The left hand side is driven by the recruitment-likelihood component suggesting the data strongly reject low values of R0, whereas the shallower right hand size is driven primarily by the index data, suggesting high R0 values are restricted by fits to the CPUE indices. Therefore, the R0 estimates are being driven to a middle ground by the tension between the recruitment data, and the index data.

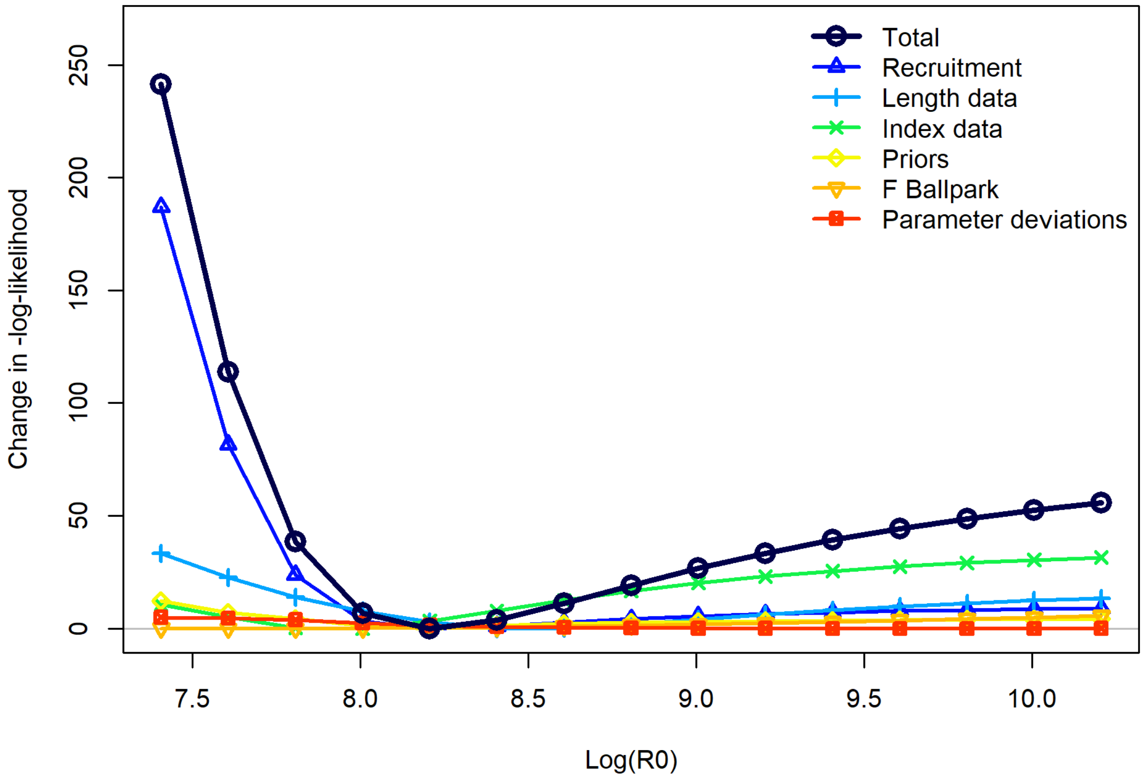

Figure 30: Profile likelihood of log(R0): change in total and component negative log-likelihood relative to the minimum, across a range of fixed log(R0) values.

7. SENSITIVITY RUNS

The exploration of the model's sensitivity to input parameters aimed to identify potential revisions to the base models, and to guide the assessment group in choosing the most appropriate values for running the grid or ensemble of models that encapsulates the uncertainty within the model. Key results for the sensitivity runs are summarised below.

7.1. Non-biological parameters

7.1.1. CPUE indices

Several alternative CPUE models were investigated. These are as follows:

1. **s3_cpue_tw**: TWLL (NE,NW,SW,SE, weighting 1)
2. **s4_altCPUE**: JPLL (NE,NW,SW,SE, weighting 1); IDN (NE, weighting 0.5); ZAF (SW, weighting 0.1); REU (SW, weighting 0.5).
3. **s5_altCPUE_esp**: JPLL (NE,NW,SW,SE, weighting 1); IDN (NE, weighting 0.5); ZAF (SW, weighting 0.1); REU (SW, weighting 0.5); ESP (SW, weighting 0.1).
4. **s6_altCPUE_esp_no_reu:** JPLL (NE,NW,SW,SE, weighting 1); IDN (NE, weighting 0.5); ZAF (SW, weighting 0.1); ESP (SW, weighting 0.1)
5. **s7_altCPUE_prt_reu:** JPLL (NE,NW,SW,SE, weighting 1); IDN (NE, weighting 0.5); PRT (SW, weighting 0.5); REU (SW, weighting 0.5).
6. **s8_alt_CPUE_prt:** JPLL (NE,NW,SW,SE, weighting 1); IDN (NE, weighting 0.5); PRT (SW, weighting 0.5)

These models investigated the effects of various CPUE configurations upweighting or downweighting individual indices. It was suggested by the WPB to test the inclusion of both the PRT(EU) and REU(EU) indices in the SW as these are hypothesised to track different components of the stock. One model was also run using just the TWLL indices, as these show quite different abundance trends over time (relatively flat), but also represent the fleets that have taken the vast majority of catch within the Indian Ocean. When the model was run using just these indices, the estimates of biomass were considerably higher than any other sensitivity (Figure 31), although the trend in stock depletion was similar (not in terms of absolute values though) (Figure 32).

Fits to the upweighted CPUE series, and length frequency data are provided in Appendix B for some sensitivity analyses. If any other outputs are required, these can be requested.

7.1.2. Time period of model

Two models were run to investigate the impact of running the assessment from the start of the "target" fishery (1985) as opposed to including data from the "bycatch" fishery (1950-1985). **s1_update_rec_short** kept the time series of the model the same as the base model, and restricted estimated recruitment deviations to 1985-2023. **s2_update_mod_time** went one step further and reduced the complete model time series to 1985-2023. The results of these updates suggest that the informative period for the model, is indeed the "target fishery" period, and the information prior to 1985 is unlikely contributing meaningfully to the model outputs. In saying that, estimates for spawning biomass (Figure 31, Table 9), and stock status (% depletion; Figure 32, Table 9) were not very different between these three models.

7.2. Biological parameters

7.2.1. Growth

The mean size of the new growth (Wang et al., 2026) is smaller across all age groups (Figure 4) for female fish, and male fish grow quicker and larger than male fish using the older growth data. This produced higher estimates of biomass across the entire model period, with a greater increase in biomass in the years from 2005 to 2024 (Figure 31).

7.2.2. *Natural mortality*

Changing the instantaneous rate of natural mortality (M) in the model had a significant impact on the estimates of biomass, and the scale of the biomass estimates (Figure 31, Figure 32, Table 9). The Lorenzen M lowered the overall estimates of biomass, while incorporating the Lorenzen M and the new growth brought estimates of biomass up to similar levels of that of the base model (Figure 31). These results highlight once more the sensitivity of these models to M.

7.2.3. *Recruitment deviations*

Allowing recruitment deviations to vary more around the mean (changing sigma r to 0.4 or 0.6) changed both the trend and absolute values in biomass estimates (Figure 31, Table 9). For both models, there was a significant deviation and reduction in estimated recruitment from 1960, rising to a peak in 1995. These changes are during the "bycatch" portion of the fishery. Once the fishery enters the "target" period, the trend and magnitude of biomass estimates returns to levels comparable to the base model, and other models in the sensitivity runs (Figure 31, Figure 32).

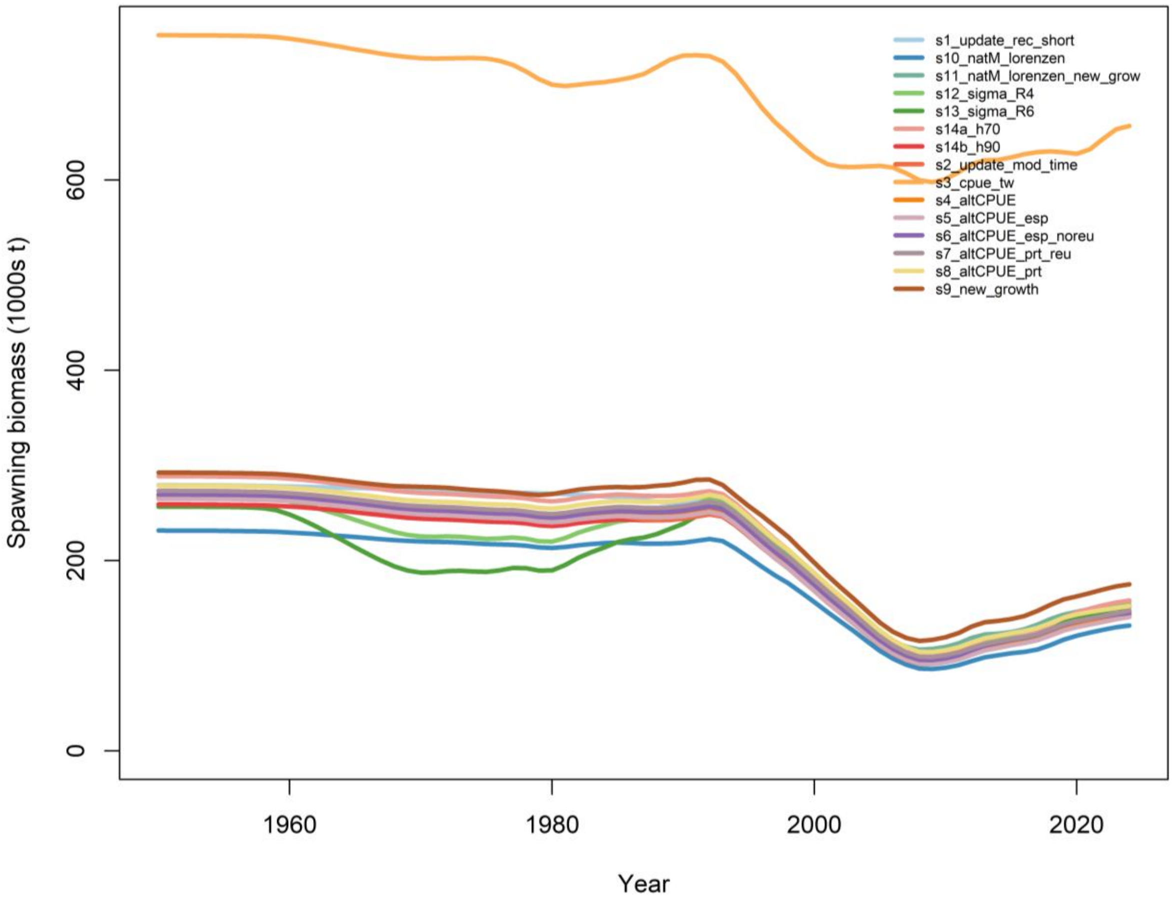

Figure 31: Biomass estimates from sensitivity runs

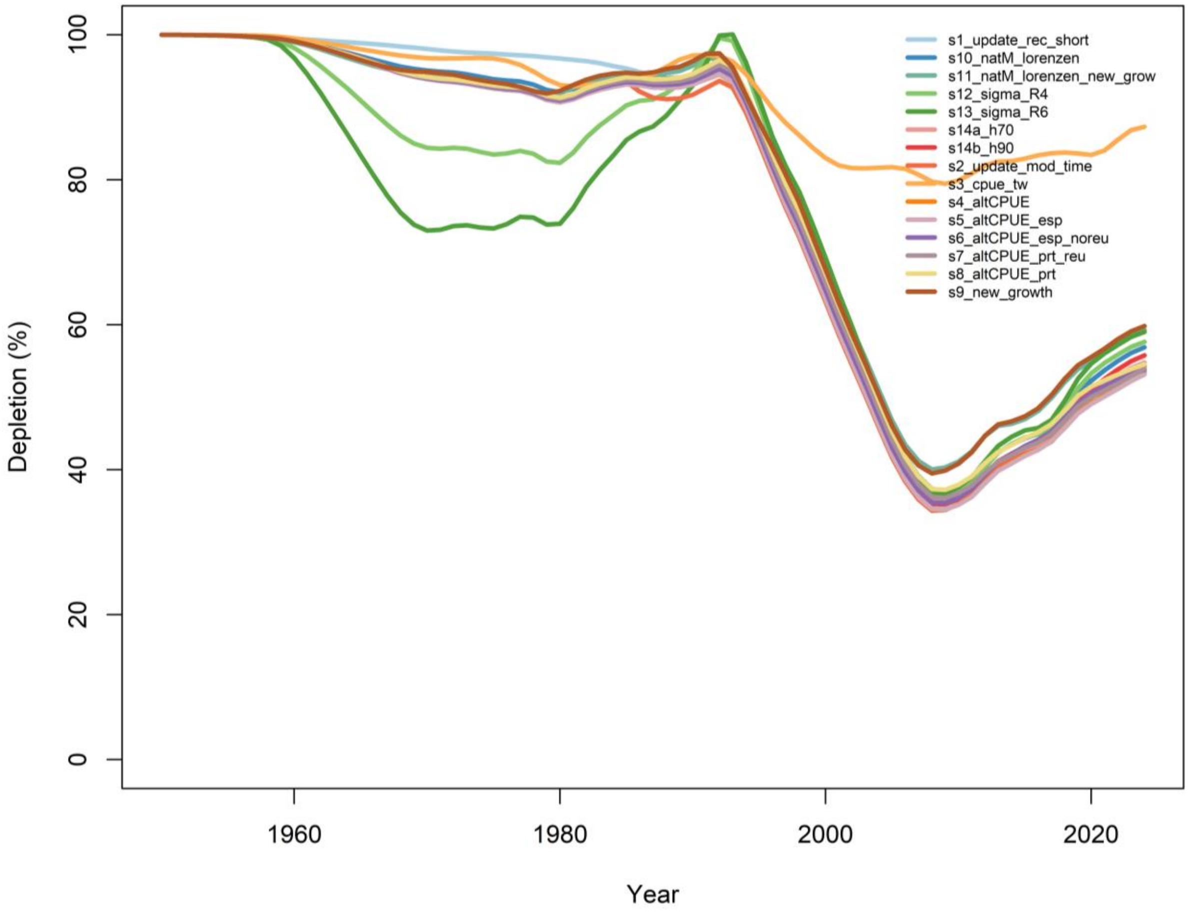

Figure 32: Depletion (% biomass or status) estimates from sensitivity runs

Table 9 (next page): Estimates of management quantities for the sensitivity testing from the base model options. Current catch (2024) is estimated at 28,112 t.

	SSB_{1950} (t)	SSB_{MSY} (t)	SSB_{2024} (t)	$SSB_{2024}SSB_{1950}$	$SSB_{1950}SSB_{MSY}$	F_{MSY}	F_{2024}	$F_{1950}F_{MSY}$	C_{MSY} (t)
s1_update_rec_short	279424	64760.2	152293	0.5450248	2.351645	0.167092	0.063839	0.382059	37036.3
s10_natM_lorenzen	231567	48256	131766	0.5690189	2.730562	0.186552	0.060972	0.326834	40502
s11_natM_lorenzen_new_grow	265887	55312	157611	0.5927744	2.84949	0.173427	0.054004	0.311391	41850.7
s12_sigma_R4	267019	61879.2	153937	0.576502	2.487702	0.167172	0.062612	0.374535	35452.6
s13_sigma_R6	256694	59481	151529	0.5903099	2.547519	0.167258	0.063229	0.378031	34140
s14a_h70	288678	79340.2	158148	0.5478353	1.99329	0.131426	0.06176	0.469922	33119.8
s14b_h90	259183	46246.1	144560	0.5577526	3.125885	0.222279	0.066747	0.300287	39572.7
s2_update_mod_time	265994	61650	144601	0.543625	2.345515	0.167256	0.066747	0.399069	35344.1
s3_cpue_tw	752183	173472	656811	0.8732064	3.786265	0.164036	0.016689	0.101741	88365.2
s4_altCPUE	265918	61705.3	142057	0.5342136	2.302185	0.166878	0.067024	0.401636	35233.1
s5_altCPUE_esp	264912	61459.9	140788	0.531452	2.290729	0.166929	0.067689	0.405494	35122.1
s6_altCPUE_esp_noreu	269543	62503.8	144987	0.5378993	2.319651	0.167028	0.066415	0.397629	35739.3
s7_altCPUE_prt_reu	273333	63432.1	147390	0.5392324	2.323587	0.166817	0.064664	0.387635	36197.6
s8_altCPUE_prt	278817	64676.8	152150	0.5456984	2.352466	0.166895	0.063258	0.379029	36923.4
s9_new_growth	292540	68137.3	175024	0.5982908	2.568696	0.164567	0.056006	0.340324	39154.4

7.3. Proposed final model options for grid / ensemble

On basis of the sensitivity analyses, further model options were configured to capture the main uncertainties in the model (Table 10). From the results of the sensitivity analyses, the model was most sensitive to changes in the inclusion or not of the Tawian,China CPUE index (relatively "flat" compared to the other indices), and changes to recruitment variability. Indeed, the model is mainly driven by the estimated recruitment (which in turn is driven by the CPUE indices). However, the biomass estimates from the model that only used the TWLL CPUE indices were significantly higher than any of the other models. Whether this should be included within the grid, as a completely alternative solution could be debated (e.g. with no independent abundance indices, the current abundance could feasibly be either represented by the TWLL CPUE indices, or the other, more variable CPUE indices). The grid was run using the TWLL CPUE index as an additional variable, however the results below do not include these runs, due to the uncertainty surrounding initial biomass estimates from these models. Depending on the assessment group's decision, these runs could be included in the final uncertainty grid, or continue to be omitted.

Therefore, the grid incorporates an alternative CPUE option (where Indonesian, South African, and Réunion indices are included), new growth, Lorenzen instantaneous rate of natural mortality (*M*), and variation in recruitment, along with uncertainty in the steepness (*h*) parameter, and growth. The final models proposed for inclusion in the ensemble of models are:

- two options for growth;
- two options for *M*;
- two options for recruitment variability;
- two options for CPUE;
- three options for *h*.

These results presented below are preliminary and will be presented to the WPB for discussion and finalisation. After running the final assessment grid, the report will be finalised, including the discussion, which will summarise the WPB(AS) discussions, and include future work proposed to improve the assessment for 2029.

Table 10: Description of the proposed final model options for the grid for the 2026 assessment. The final models consist of a full combination of options below, making a total of 48 models. The options adopted within the reference (base) model ('4_update_rec') are highlighted.

Model options	Description
Steepness (*h*) in SRR	• h70: *h* = 0.70
	• **h80: *h* = 0.80**
	• h90: *h* = 0.90
Growth	• Gnew: VB growth parameters estimated by Wang et al. (2026) • **Gold**: VB growth parameters estimated by Farley et al., (2016)
Natural Mortality	• Lorenzen: – Lorenzen functional form *M* with reference ages 5-12 yrs, and fixed M of 0.25
	• **Fixed M of 0.25 for all ages**
Recruitment variability	• **σ_r = 0.20**
	• σ_r = 0.40
CPUE	• **Only Japanese longline indices (NW, NE, SW, SE)**
	• altCPUE: Inclusion of Japanese (NW, NE, SW, SE; weight = 1.0); Indonesian (NE; weight 0.5); South African (SW; weight = 0.1); EU (Réunion; SW; weight = 0.5) indices. Based on CPUE comparison analyses.

8. STOCK STATUS

8.1. Current status and yields

MSY based estimates of stock status were determined for the final model options, including alternative assumptions on abundance indices, alternative values of SRR steepness, growth, and natural mortality. Stock status was determined for individual models (Table 11), as well as for all (48) models combined incorporating uncertainty from individual models based on estimated variance-covariance matrix of parameters (Table 12).

For the selected model options, point estimates of Catch at *MSY* ranged from 31,166 t to 48,258 t (Table 11, blue and pink highlights respectively) which are all above the current estimates of catch in 2023 and 2024 (Table 2 & Table 12). Model options with higher steepness generally yielded comparatively higher estimates of *MSY*. On average fishing mortality rates have been well above the F_{MSY} through the mid-2000s to around 2015 when fishing effort and catches declined to current levels (Figure 34). Biomass was estimated to have declined considerably from 1990 to 2005 before a steady increase to 2024 (Figure 32). The increased biomass coincides with increasing abundance indices (CPUE indices), and stable, lower catches, suggesting the stock may be rebuilding.

Models with higher σ_R values show reductions in biomass in the early "bycatch" years of the fishery, suggesting the model is allowing for reduced recruitment estimates in these years. This is not supported by length frequency data, or any other information other than the catch data, and noticeable lack of CPUE indices in these early years.

Current fishing mortality (F_{2024}) was estimated to be higher than F_{MSY} for 41 out of 48 models, and all of these were where h = 0.90 (Table 11). Current biomass (SSB_{2024}) was estimated to be between 53 % and 63 % of SSB_{MSY} (Figure 33; Table 11). In general, current stock status relative to the *MSY* based benchmarks are not fundamentally different for the range of model options, although the proximity to the *MSY* benchmarks is sensitive to the different of model assumptions. Current (2024) fishing mortality was estimated to be below the F_{MSY} level (F_{2024}/F_{MSY} < 1.0) for all models; current spawning biomass was estimated to be above the SB_{MSY} level (SB_{2024}/SB_{MSY} > 1.0) for all models.

Estimates were combined across from the 48 models to generate the final KOBE stock status plot (Figure 34). For individual models, the uncertainty is characterised using the multivariate lognormal Monte-Carlo approach (Walter et al. 2019, Walter & Winker 2019, Winker et al. 2019), based on the maximum likelihood estimates and variance-covariance of the untransformed quantities F/F_{MSY} and SSB/SSB_{MSY}. Thus, estimates of stock status included both within and across model uncertainty. Combined across the model ensemble, SSB_{2024} was estimated to be 2.81 times SSB_{MSY} (1.97–3.64), and F_{2024} was estimated 0.34 F_{MSY} (0.23 – 0.45) (Table 11). Critically, the current catch (28,112 t) is below all estimates of C_{MSY}. Taking all the available information into account, the stock is considered to be **not overfished,** and **not subject to overfishing** in 2024.

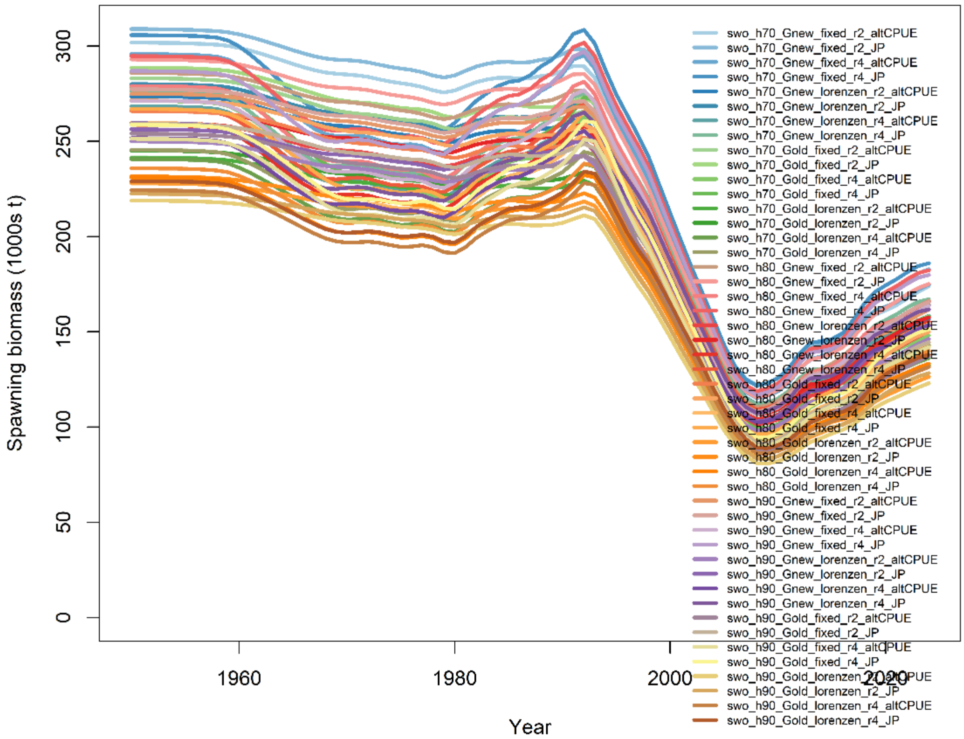

Figure 32: Spawning biomass trajectories from the proposed final model options in the grid

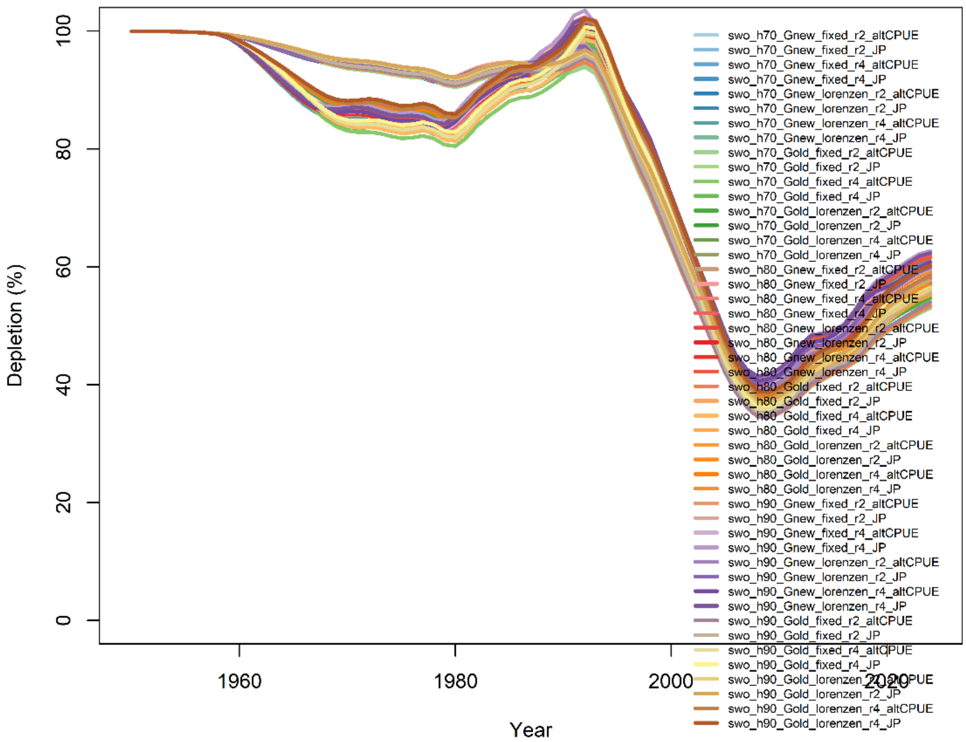

Figure 33: Spawning biomass depletion (% SSB_0) from the proposed final model options in the grid

Table 11 Estimates of management quantities for the stock assessment model options. Current yield (mt) represents yield in 2024 corresponding to fishing mortality at the FMSY level.

	SSB_0	SSB_{MSY}	SSB_{2024}	$SSB_{2024}SSB_0$	$SSB_{2024}SSB_{MSY}$	F_{MSY}	F_{2024}	$F_{2024}F_{MSY}$	C_{MSY}
swo_h70_Gnew_fixed_r2_altCPUE	301821	83409.6	174007	0.5765238	2.086175	0.129958	0.05594146	0.430458	34954.8
swo_h70_Gnew_fixed_r2_JP	308942	85299.7	182863	0.5919007	2.143771	0.130106	0.05391176	0.414368	35811.3
swo_h70_Gnew_fixed_r4_altCPUE	295780	81749.4	174817	0.5910373	2.13845	0.130093	0.05466794	0.420222	34317.2
swo_h70_Gnew_fixed_r4_JP	305766	84417.2	186003	0.6083181	2.203378	0.130256	0.0521743	0.400552	35505.9
swo_h70_Gnew_lorenzen_r2_altCPUE	273643	69882.1	156719	0.5727134	2.24262	0.134635	0.05388779	0.400251	36646.3
swo_h70_Gnew_lorenzen_r2_JP	280054	71530.2	164318	0.5867368	2.297184	0.134543	0.05212747	0.387441	37498.4
swo_h70_Gnew_lorenzen_r4_altCPUE	268367	68543.9	158437	0.5903744	2.311468	0.134658	0.05196479	0.385902	35978.8
swo_h70_Gnew_lorenzen_r4_JP	276157	70537	167100	0.6050906	2.368969	0.134581	0.05005296	0.371917	37019.8
swo_h70_Gold_fixed_r2_altCPUE	283100	77886.6	150128	0.5303002	1.92752	0.131228	0.06391827	0.487078	32458.8
swo_h70_Gold_fixed_r2_JP	288678	79340.2	158148	0.5478353	1.99329	0.131426	0.06175997	0.469922	33119.8
swo_h70_Gold_fixed_r4_altCPUE	271274	74627.7	148124	0.546031	1.984839	0.131337	0.06391358	0.486638	31166.2
swo_h70_Gold_fixed_r4_JP	278738	76594.6	157781	0.5660549	2.059949	0.131559	0.061289	0.465867	32047.1
swo_h70_Gold_lorenzen_r2_altCPUE	241495	61577.4	132389	0.548206	2.149961	0.144061	0.06001624	0.416603	35914.9
swo_h70_Gold_lorenzen_r2_JP	245165	62519.8	137923	0.5625721	2.206069	0.14399	0.05864785	0.407305	36477.4
swo_h70_Gold_lorenzen_r4_altCPUE	240642	61361.5	136229	0.5661065	2.220105	0.144027	0.05775209	0.400981	35801.7
swo_h70_Gold_lorenzen_r4_JP	245478	62598	142946	0.5823169	2.283555	0.143978	0.0561818	0.390211	36544.9
swo_h80_Gnew_fixed_r2_altCPUE	285901	66647.8	166356	0.5818658	2.496046	0.164429	0.05817153	0.353779	38226.3
swo_h80_Gnew_fixed_r2_JP	292966	68236.4	175097	0.59767	2.566035	0.164561	0.05600669	0.34034	39208.7
swo_h80_Gnew_fixed_r4_altCPUE	279036	65024.3	165858	0.5943964	2.550708	0.164679	0.0572169	0.347445	37392.5

swo_h80_Gnew_fixed_r4_JP	294741	68639	182306	0.6185295	2.656012	0.164659	0.05309479	0.322453	39485.9
swo_h80_Gnew_lorenzen_r2_altCPUE	259553	53971.6	150142	0.5784637	2.78187	0.173652	0.05585985	0.321677	40864.3
swo_h80_Gnew_lorenzen_r2_JP	265887	55312	157611	0.5927744	2.84949	0.173427	0.05400361	0.311391	41850.7
swo_h80_Gnew_lorenzen_r4_altCPUE	258587	53780.2	155258	0.6004091	2.886899	0.173614	0.05284515	0.304383	40737.4
swo_h80_Gnew_lorenzen_r4_JP	266366	55412.7	163853	0.6151423	2.956958	0.173414	0.05088244	0.293416	41957.1
swo_h80_Gold_fixed_r2_altCPUE	265918	61705.3	142057	0.5342136	2.302185	0.166878	0.06702421	0.401636	35233.1
swo_h80_Gold_fixed_r2_JP	271449	62914	149921	0.552299	2.382951	0.167094	0.0646851	0.387118	35995.3
swo_h80_Gold_fixed_r4_altCPUE	259612	60244.6	144415	0.5562724	2.397144	0.166909	0.06532101	0.391357	34436.6
swo_h80_Gold_fixed_r4_JP	267019	61879.2	153937	0.576502	2.487702	0.167172	0.06261177	0.374535	35452.6
swo_h80_Gold_lorenzen_r2_altCPUE	227966	47494.5	126380	0.5543809	2.66094	0.186789	0.06241237	0.334133	39856.1
swo_h80_Gold_lorenzen_r2_JP	231567	48256	131766	0.5690189	2.730562	0.186552	0.06097154	0.326834	40502
swo_h80_Gold_lorenzen_r4_altCPUE	231076	48152.1	133316	0.5769357	2.768644	0.186717	0.05881922	0.315018	40397.3
swo_h80_Gold_lorenzen_r4_JP	235851	49154.2	139911	0.5932178	2.846369	0.186507	0.05721979	0.306797	41257.7
swo_h90_Gnew_fixed_r2_altCPUE	275003	49340.1	161712	0.5880372	3.277496	0.216898	0.05961463	0.274851	42285
swo_h90_Gnew_fixed_r2_JP	277346	49696.6	165581	0.5970196	3.331838	0.217141	0.05880417	0.270811	42744.7
swo_h90_Gnew_fixed_r4_altCPUE	271320	48652.7	163588	0.6029338	3.362362	0.217124	0.05789503	0.266645	41795
swo_h90_Gnew_fixed_r4_JP	286923	51421.8	179884	0.6269417	3.498205	0.216998	0.05371525	0.247538	44189.2
swo_h90_Gnew_lorenzen_r2_altCPUE	249986	37186.5	146251	0.5850368	3.932906	0.236882	0.05709543	0.241029	46494.6
swo_h90_Gnew_lorenzen_r2_JP	256288	38154.3	153639	0.5994779	4.026781	0.236342	0.05518137	0.233481	47647.6
swo_h90_Gnew_lorenzen_r4_altCPUE	251670	37443.7	153196	0.6087178	4.091369	0.236754	0.05343135	0.225683	46822.6
swo_h90_Gnew_lorenzen_r4_JP	259444	38621.5	161748	0.6234409	4.18803	0.236253	0.05143488	0.217711	48257.7

swo_h90_Gold_fixed_r2_altCPUE	254030	45386.8	137146	0.5398811	3.021716	0.222144	0.06906857	0.310918	38741.9
swo_h90_Gold_fixed_r2_JP	259183	46246.1	144560	0.5577526	3.125885	0.222279	0.06674749	0.300287	39572.7
swo_h90_Gold_fixed_r4_altCPUE	251302	44908.3	141995	0.5650373	3.161888	0.222082	0.06627304	0.298417	38346.2
swo_h90_Gold_fixed_r4_JP	258657	46141.1	151412	0.5853775	3.2815	0.222345	0.06351196	0.285646	39516.2
swo_h90_Gold_lorenzen_r2_altCPUE	218913	32941.2	123027	0.5619904	3.734746	0.257217	0.06383637	0.248181	45158.8
swo_h90_Gold_lorenzen_r2_JP	222503	33493.8	128341	0.5768057	3.831784	0.256569	0.06235012	0.243015	45914.3
swo_h90_Gold_lorenzen_r4_altCPUE	224344	33772.2	131500	0.5861534	3.893735	0.257095	0.05950412	0.231448	46262
swo_h90_Gold_lorenzen_r4_JP	229090	34493.9	138022	0.6024794	4.001345	0.256473	0.05788519	0.225697	47267.8

Table 12: STOCK STATUS INDICATORS FROM MODEL ENSEMBLE

Catch in 2024:	28112
Average catch 2019–2024:	27076
MSY (1000 t) (plausible range):	39 (32-46)
F_{MSY}	0.06 (0.05-0.06)
SSB_0(1000 t) (80% CI):	264 (226-302)
SSB_{2024} (1000 t) (80% CI):	152 (119-185)
SSB_{MSY}	58 (38-77)
SSB_{2024}/SSB_0 (80% CI):	0.58 (0.55-0.61)
SSB_{2024} / SSB_{MSY}	2.81 (1.97-3.64)
F_{2024} / F_{MSY}	0.34 (0.23-0.45)

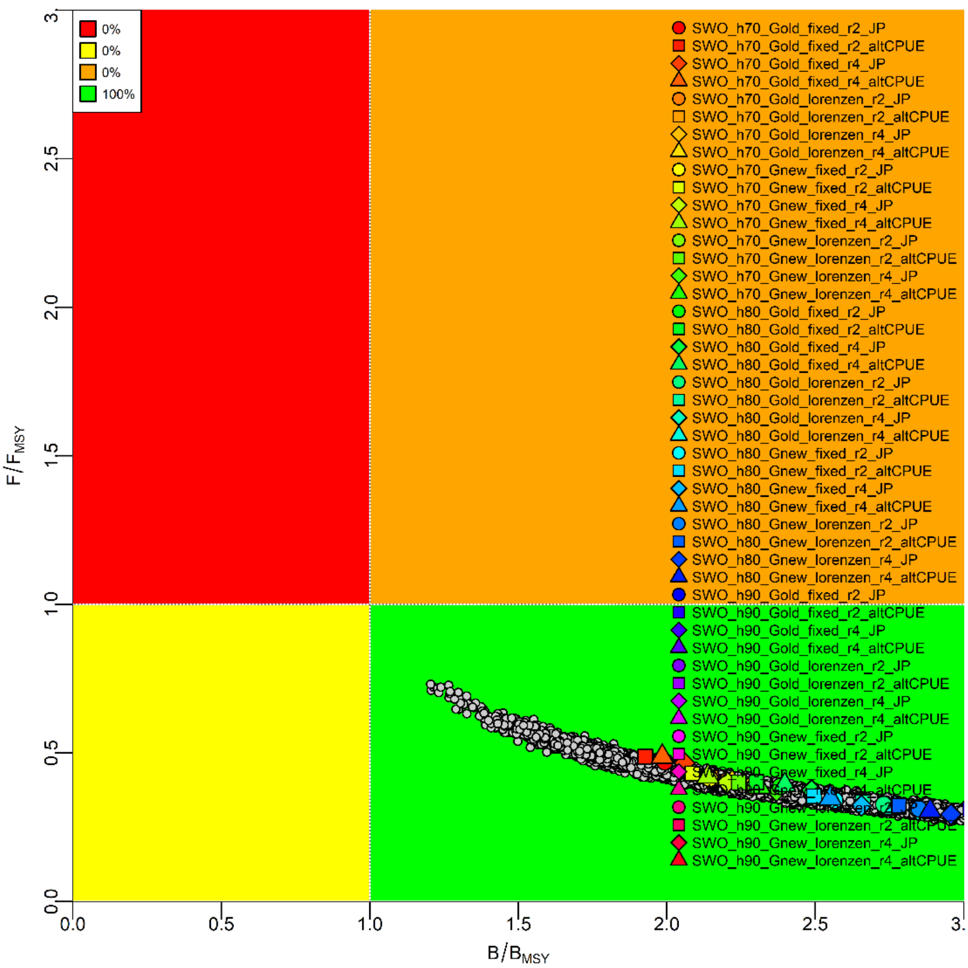

Figure 34: KOBE PLOT FROM GRID RUNS

In the 2023 assessment (using data up to 2021) the model ensemble estimated that the stock was **not overfished** and **not subject to overfishing** in 2021, this was the same in the 2019 assessment when the stock was estimated to be **not overfished** and **not subject to overfishing**.

The estimated biomass trajectory shows a decline from exploited but equilibrium spawning stock biomass levels in 1975 to 2019 (Figure 35). Biomass levels appear to have stabilised and are increasing in the final years of the model, providing a more positive outlook for the stock, despite several years of increased catches that are estimated to be at or above MSY. However, a period of lower catches in the prior 5 years has helped to continue to rebuild the stock. Fishing mortality has been consistently below that of F/F_{MSY} (Figure 35). As there is a significant lack of representative biological data (length data, and representative ages), the model is forced to fit closely to the main abundance indices from the longline fleets. As there have been increases in these indices in the three most recent years (2022-2024 inclusive), alongside stable catches, it is likely that the CPUE indices are driving the increase in estimated biomass in the model, rather than any biological parameters.

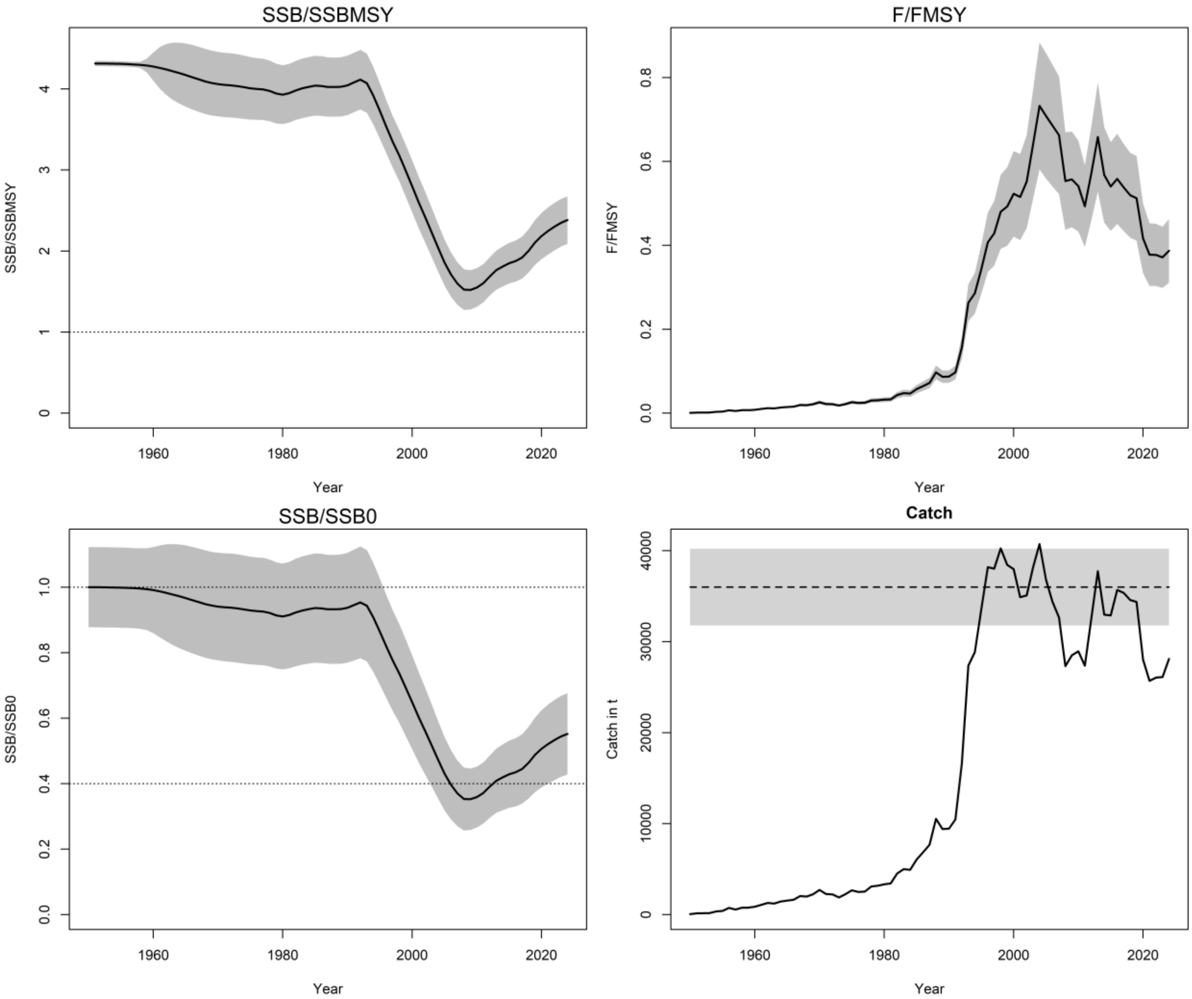

Figure 35: Management outputs from the ensemble of models (grid) used in 2024. Bounds around the main darker line represent the highest and lowest values from the grid of models. The grey band on the catch graph represents estimated optimal catch at MSY (80 % confidence interval). The horizontal red lines indicate limit or reference points for SSB/SSB_{MSY} and F/F_{MSY}.

9. DISCUSSION

This report presents a preliminary stock assessment for Indian Ocean swordfish using a spatially explicit, age structured model. It represents an update and revision of the 2023 assessment model with newly available information. There are no fundamental changes in the structure of the current assessment models compared to the previous assessment, with most revisions concerning observational data, e.g., the inclusion of specific CPUE indices, and the incorporation newly available biological information including growth and natural mortality. A range of exploratory models are also presented to explore the impact of key data sets and model assumptions.

The overall stock status estimates obtained from a range of model options is similar to the previous assessment: current spawning biomass remains above SSB_{MSY} (SSB_{2024}/SSB_{MSY} = 2.81), and fishing mortality is estimated to be below F_{MSY} (F_{2024}/F_{MSY} = 0.34). (Current SSB (SSB_{2024}) is estimated to be above the estimated SSB_{MSY} in the 2023 assessment, and the 2019 assessment).

The Indian Ocean swordfish fisheries present a number of unique problems in the development of a stock population model: there is a lack of good information on recruitment; there is considerable uncertainty on growth, maturity, and natural mortality; there are good time series of CPUE, but their reliability to track abundance is highly uncertain, given the conflicts between these time series; there is also a large amount of data on size structure, but the sampling may be not random. As with earlier assessments, the models presented here, while fairly representing some of the data (e.g., the biomass indices), also show some signs of poor fit. The assessment tested various combinations of assumptions to explore the sensitivity and describe the uncertainty in stock status. It is unlikely the estimates of historical stock size are accurate, given assumptions about annual recruitment and the reliance on the historical catch-effort indices of abundance. Current stock status as estimated here should thus be treated with caution.

The model estimates are driven primarily by the recruitment deviates, which in turn are driven by the CPUE indices ("abundance" indices). As the model contains no true fishery independent survey data, it remains (as in the previous assessment of swordfish), that the trends in recruitment (e.g. a large spike in recruitment just prior to the start of the target fishery, that is unsupported by any length data) are suspicious. The impact of assuming the CPUE indices are true reflections of regional abundance is clearly demonstrated when the TWLL CPUE indices are included as the main "abundance" indices in the model. In these sensitivity runs, the model was unable to generate similar trends in biomass, as the CPUE indices do not display the same variation through time. The TWLL fleet represents the largest fleet in terms of swordfish catch in the Indian Ocean (40 % total catch in 2024).

The Japanese and Taiwanese longline fleets have traditionally been used to generate the abundance indices for Indian Ocean swordfish stocks. These fleets have an extensive history, broad spatial coverage, and substantive logbook programmes. However, the operations of these fleets have changed historically, with large shifts in targeting that are poorly quantified. Conventional fisheries theory suggests that the depletion estimated by the Japanese series has been more consistent with the swordfish exploitation history than the Taiwanese series, and this interpretation has generally been given more weight in the assessment and management advice (Kolody et al. 2011). It is widely known that the catch efficiency of swordfish has experienced dramatic changes in the late 1980s and early 1990s with the deveopment of fresh-chill longline fleets which have further improved on catch rates through refinements to fishing gear such as the the introduction of light sticks and monofilament longlines in this period (Ward & Elscot 2000).

The recent trend in the Japanese CPUE in the northern regions is also suspicious: the very large increase in the index coincided with the period when vessels returned to old fishing grounds that had been avoided for several years due to the threat of piracy. The increase may be related to a combination of factors including increase in abundance and major changes in catchability, implying a possible nonlinear relationship between CPUE and abundance. As such, the Taiwanese indices can provide an alternative possibility of relative abundance trend in recent years.

Biological data are major sources of uncertainty in the model. The current growth models in the reference model (Gnew, Farley et al., 2016) are from estimates of age and length from the South Pacific Ocean. It is known within both oceans that differential growth is likely in many species of pelagic fish, let alone between oceanic basins. The alternative growth parameters (Wang et al., 2010, 2026), while from the Indian Ocean, were sampled in 2008, nearly 20 years ago. True age-structured assessment models require age cohorts, which requires both length and age data from fish from representative samples (e.g. across time and space within the entire Indian Ocean) to be aged annually. This would then provide the model with critical information on whether fishing is affecting growth, whether fish grow at different rates across the Indian Ocean, and provide true information on age cohorts that the model can then use to provide more accurate population dynamics. The assessment model would then be running as a true population dynamics model.

There is no information on rates of natural mortality for Indian Ocean swordfish. There are no tagging data available that could inform estimates of M. Additionally, good estimates for maximum age for swordfish, and better estimates for ages of adult fish (through increases in biological data collection) would allow for more accurate estimates of M. This is particularly important as most integrated models are sensitive to misspecification of M.

The assessment is assuming a single IO stock disaggregated into 4 areas with shared spawning and foraging grounds site fidelity. More research and information on the movement rates of adult and sub-adult swordfish in the Indian Ocean would go some way to improving our understanding of the movement of individuals between areas of the Indian Ocean. Additionally, biological data from the putative two stocks of Indian Ocean swordfish (Chevrier et al., 2025), would allow for biological disaggregation of data into biologically relevant areas.

The assessment of Indian Ocean swordfish is due to be revisited in 2029. We strongly encourage CPCs to provide additional data, and research to support an updated stock assessment in 2029.

9.1. Recommendations for future assessments:

- **Improved quality and quantity of length composition data**: The model is relatively sensitive to the length-frequency data. It is recommended that improvements in both quantity and quality of length frequency data are provided to the Secretariat prior to the next assessment of swordfish in 2029, and that any length data omitted in this assessment are reassessed for suitability and inclusion in 2029. Of particular interest would be sex-specific measurements, considering the model is sex-specific with regards to growth, and currently the model does not assume different length frequencies for individual sexes.
- **Development of independent abundance indices**: as with other assessments in the IOTC, there are no fishery-independent abundance indices included in the stock assessment. Two of the CPC's CPUE indices (Spain (European Union), and Taiwan (China)) show very flat trajectories compared to the other indices – this could be a plausible representation of regional swordfish abundance, which would mean that biomass is extremely high. However, with no independent abundance indices, it is currently not possible to know which of the indices trajectories is biologically accurate. Additionally, as with other IOTC assessments, the CPUE indices are driving the assessment, and the model is estimating recruitment trends based on the estimates of biomass (that are being driven by the CPUE indices). The model is heavily influenced by the estimated recruitment.
- **Ageing data**: It is strongly recommended that more fish are aged, encompassing both male and female fish, from all length-bins across the spatial extent of the fishery, to build a reasonable timeseries of biologically informative data. Age data should be accompanied by detailed information on the source of the fish (e.g. time, date, location, sex, fishing gear, vessel flag etc.) if the data are to be used to either estimate age-at-length within the model (as data need to be allocated to appropriate timesteps, model areas, and model fleets) or to account for changes in age-at-length over time or space (due to population dynamics, environmental factors, such as climate change or high fishing effort). Estimating age within the model allows for more accurate diagnosis of the cause of potential model misspecification. Fish could be aged on a yearly basis, to provide additional information.
- **Transition to a biologically relevant population dynamics model**: Currently the SS3 stock assessment model for Indian Ocean swordfish is partitioned and structured based on fleet dynamics (e.g. data are aggregated into métiers) with an underlying assumption that similar fleets are targeting a similar biological portion of the stock. However, there are little, if any, biological data to support these assumptions, other than fishery-dependent size measurements. As with other IOTC stock assessments, the model would benefit from fishery-independent biological data to support a biologically plausible population dynamics model (e.g. structured based on the biological characteristics of the species, rather than fishery behaviours). This is particularly important if we want to avoid fishing sensitive portions of the stock(s) – e.g. spawning aggregations, or juvenile 'nursery' areas.
- **Incorporation of climate variables**: As stipulated under Resolution 25/01 the IOTC "Commission should support further research into the relationship between climate change, fisheries for IOTC fisheries…and the ecosystems…". Currently the assessment does not incorporate any information on potential changes in population distribution due to climate change. This part of the assessment could benefit from targeted research from CPCs or research organisations.

10.REFERENCES

Abascal, F.J., Mejuto, J., Quintans, M., García-Cortés, B., Ramos-Cartelle, A. 2015. Tracking of the broadbill swordfish, *Xiphias gladius*, in the central and eastern North Atlantic. *Fisheries Research*, 162, 20-28. doi: 10.1016/j.fishre.2014.09.011.

Abecassis, M., Dewar, H., Hawn, D., Polovina, J. 2012. Modeling swordfish daytime vertical habitat in the North Pacific Ocean from pop-up archival tags. *Marine Ecology Progress Series*, 452, 219-236. doi: 10.3354/meps/09583.

Arocha., F. 2002. Oocyte development and maturity classification of swordfish from the north-western Atlantic. *Journal of Fish Biology*, 60 (1), 13-27. doi: 10.1111/j.1095-8649.2002.tb02385.x.

Bigelow, K.A., Boggs, C.H., Xi, H. 1999. Environmental effects on swordfish and blue shark catch rates in the US North Pacific longline fishery. 1999. *Fisheries Oceanography*, 8 (3), 178-198. doi: 10/1046/j.1365-2419.1999.00105.x.

Bourjea, J., Le Couls S., Grewe P., Evano H. and Muths D. 2011. Preliminary results of the Indian Ocean swordfish stock structure project – IOSSS – focus on the population genetic approach. IOTC-2011-WPB-09-info-5.

Bradman, H., Grewe, P. and Appleton, B. 2010. Direct comparison of mitochondrial markers for the analysis of swordfish population structure. Fisheries Research 109: 95–99.

Brawn., C.D., Gaube, P., Afonso, P., Fontes, J., Skomal, G.B., Thorrold, S.R. 2019. Assimilating electronic tagging, oceanographic modelling, and fisheries data to estimate movements and connectivity of swordfish in the North Atlantic. *ICES Journal of Marine Science*, 76 (7), 2305-2317. doi: 10.1093/icesjms/fsz106.

Brunel, T., Mosqueira, I. 2024. Proposal for amending the management procedure adopted for the Indian Ocean swordfish and practical aspect for its first implementation. IOTC-2024-WPM-11rev2.

Campbell, R. 1998. Longline effort in the eastern AFZ. Unpublished paper presented at the Eastern Tuna and Billfish Fishery Effort Setting Workshop, Canberra, 20 November 1998.

Carey, F.G., Robinson, B.H. 1981. Daily patterns in the activities of swordfish, Xiphias gladius, observed by acoustic telemetry. Fisheries Bulletin 79(2), pp.277-292.

Cartelle, A.R., Costa, F.J., A., Mejuto, J. 2020. Updated Standardized Catch Rates of Swordfish (*Xiphias Gladius*) Caught by the Spanish Surface Longline Fleet in the Indian Ocean During the 2001-2018 Period. IOTC–2020–WPB18–12.

Chevrier, T., Cowart, D.A., Nieblas, A-E., Charrier, G., Bernard, S., Evano, H., Brisset, B., Chanut, J., Bonhommeau, S. 2025. Population structure of the swordfish, *Xiphias gladius*, across the Indian Ocean using next generation sequencing. *ICES Journal of Marine Science*, 82 (5), fsae179, doi: 10.1093/icesjms/fsae179.

Coelho, R., Rosa, D., Lino, P.G. 2023. Update of the swordfish catch, effort and standardized CPUEs by the Portuguese pelagic longline fleet operating in the Indian ocean, between 1998 and 2022. IOTC–2023–WPB21–xx.

Davies, N., Pilling, G., Harley, S., Hampton, J. 2013. Stock assessment of swordfish (*Xiphias gladius*) in the southwest Pacific Ocean. WCPFC-SC9-2013/SA-WP-05.

DeMartini, E. E., James H. Uchiyama ,Robert L. Humphreys Jr. ,Jeffrey D. Sampaga, Happy A. Williams (2007)Age and growth of swordfish (Xiphias gladius) caught by the Hawaii-based pelagic longline fishery Fish. Bull. 105:356–367.

Dewar, H., Prince, E.D., Musyl, M.K., Brill, R.W., Sepulveda, C., Luo, J., Foley, D., Orbesen, E.S., Domeier, M.L., Nasby-Lucas, N., Snodgrass, D., Laurs, R.M., Hoolihan, J.P., Block, B.A., Mcnaughton, L.M. 2011. Movements and behaviours of swordfish in the Atlantic and Pacific Oceans examined using pop-up satellite archival tags. *Fisheries Oceanography*, 20 (3), 219-241. doi: 10.1111/j.1365-2419.2011.00581.x.

Evans, K., Abascal, F., Kolody, D., Sippel, T., Holdsworth, J., Maru, P. 2014. The horizontal and vertical dynamics of swordfish in the South Pacific Ocean. *Journal of Experimental Marine Biology and Ecology*, 450, 55-67. doi: 10.1016/j.jembe.2013.10.025.

Farley, J., Clear, Naomi., Kolody, D., Krusic-Golub, K,. Eveson, Paige., Young, Jock. 2016. Determination of swordfish growth and maturity relevant to the southwest Pacific stock. R 2014/0821.

Francis, R.I.C.C. 2012. Data weighting in statistical fisheries stock assessment models. Canadian Journal of Fisheries and Aquatic Sciences, 2011, 68(6): 1124-1138.

Fu. 2017. An age-, sex- and spatially-structured stock assessment of the Indian ocean swordfish fishery 1950-2015, using stock synthesis. IOTC–2017–WPB15–20_Rev1.

Fu. 2020. Preliminary Indian Ocean swordfish stock assessment 1950-2018 (stock synthesis). IOTC-2020-WPB18-16.

Geehan, J. 2018. Revision to the IOTC scientific estimates of Indonesia's fresh longline catches. IOTC-2018-WPDCS14-23.

Geehan, J, Seyyadji, B. 2018. Revision to the IOTC Scientific Estimates of Indonesia's Fresh Longline Catches. IOTC-2018-WPB16-22

ISSF 2011. Report of the 2011 ISSF stock assessment workshop, Rome, Italy, March 14-17. Unpublished report. 18pp.

Kadagi, N.I., Harris, T., and Conway, N. 2011. East Africa billfish Conservation and Research: Marlin, Sailfish and Swordfish Mark-Recapture field studies. IOTC-2011-WPB09-10.

Kikuchi, A., Mourato, B., Sant'Ana, R., Gillespie, K., Cardoso, L.G. 2026. South Atlantic swordfish (*Xiphias gladius*) preliminary assessment using Stock Synthesis, 1950-2024. SCRS/2026/166 (ICCAT).

Kolody, D. 2009. Exploratory Modelling of the Indian Ocean Swordfish Fishery, using an age-structured, sex-structured and spatially-disaggregated implementation of Stock Synthesis software.

Kolody, D. 2010. A Spatially-Structured Stock Synthesis Assessment of the Indian Ocean Swordfish Fishery 1950-2008, including Special Emphasis on the SW Region. Working paper for the IOTC Billfish Working Party July 2010: IOTC-2010-WPB-05.

Kolody, D. 2011. Review of CPUE Issues for the 2011 Indian Ocean Swordfish Stock Assessment. IOTC-2011-WPB09-13.

Kolody, D.; Herrera, M. 2011. An Age-, Sex- and Spatially-Structured Stock Assessment of the Indian Ocean Swordfish Fishery 1950-2009, including Special Emphasis on the South-West Region. OTC-2011-WPB-17.

Lu, C,P., Chen, C.A., Hui, C.F., Tzeng, T.D., Yeh, S.Y. 2006. Population genetic structure of the swordfish, *Xiphias gladius* (Linnaeus 1758), in the Indian Ocean and West Pacific inferred from the complete DNA sequence of the mitochondrial control region. Zoological studies 45(2): 269-279.

Martell, S. 2010. SCAM Swordfish Stock Assessment. Working Party IOTC-2010-WPB-14.

Methot Jr, R.D., Wetzel, C.R. 2013. Stock synthesis: A biological and statistical framework for fish stock assessment and fishery management. Fisheries Research, 142(0): 86-99.

Methot Jr, R.D., Taylor, I.G., Doering, K. 2020. 2020. Stock Synthesis User Manual Version 3.30.15. U.S. Department of Commerce, NOAA Processed Report NMFS-NWFSC-PR-2020-05.

Muths, D., Le Couls, S., Evano, H., Grewe, P. , Bourjea, J. 2013. Multi-Genetic Marker Approach and Spatio-Temporal Analysis Suggest There Is a Single Panmictic Population of Swordfish Xiphias gladius in the Indian Ocean. IOTC-2013-WPB11-10

Neubauer, P., Kim, K., Amar, T., Large, K. 2023. Addressing uncertainty in WCPFC stock assessments: Review and recommendations from WCPFC Project 113. WCPFC-SC19-2023/SA-WP-12.

Nishikawa, Y., Honma, M., Ueyanagi, S., Kikawa, S. 1985. Average distribution of larvae of

oceanic species of scombrid fishes, 1956–1981. Far Seas Fisheries Research Laboratory, Shimizu. S Series 12. WPTT-04-06.

Nishida, T. 2008. Notes on the standardized swordfish CPUE of tuna longline fisheries (Japan and Taiwan) in WPB6 (1980-2006 and 1992-2006). IOTC-2008-WPB-INF04.

Parker, D., Kerwath, S.E. Standardized Catch per Unit Effort of Swordfish (*Xiphias Gladius*) for the South African Longline Fishery. IOTC–2020–WPB18–13.

Poisson, F., Fauvel, C. 2009. Reproductive dynamics of swordfish (*Xiphias gladius*) in the southwestern Indian Ocean (Réunion Island). Part 2: fecundity and spawning pattern. *Aquatic Living Resources*, 22, 59-68. doi: 10.1051/alr/2009012.

Potier, M., Marsac, F., Cherel, Y., Lucas, V., Sabatié, R., Maury, O., Ménard, F. 2007. Forage fauna in the diet of three large pelagic fishes (lancetfish, swordfish and yellowfin tuna) in the western equatorial Indian Ocean. *Fisheries Research*, 83(1), 60-72. doi: 10.1016/j.fishres.2006.08.020.

Potier, M., Romanov, E., Cherel, Y, Sabatié, R., Zamarov, V., Ménard, F. 2008. Spatial distribution of *Cubiceps pauciradiatus* (Perciformes : Nomeidae) in the tropical Indian Ocean and its importance in the diet of large pelagic fishes. *Aquatic Living Resources*, 21, 123-134. doi: 10.1051/alr:2008026.

Preti, A., Stohs, S.M., DiNardo, G.T., MacKenzie, K., Noble, L.R., Jones, C.S., Pierce, G.J. 2023. Feeding ecology of broadbill swordfish (*Xiphias gladius*) in the California current. *PLOS One,* 18 (2), e0258011. doi: 10.1371/journal.pone.0258011.

Setyadji, B., Parker, D., Wang, S.P. Fahmi, Z. 2020. Standardized CPUE of swordfish (*Xiphias Gladius*) from Indonesian tuna longline fleets in the north-eastern Indian Ocean. IOTC–2020–WPB18–20.

Sharma, R., Herrera, M. 2016. An Age-, Sex- and Spatially-Structured Stock Assessment of the Indian Ocean Swordfish Fishery 1950-2012, USING STOCK SYNTHESIS. IOTC–2014–WPB12–26_Rev2.

Taki, K., Ijima, H., Semba.Y. 2020. Japanese Longline CPUE Standardization (1979-2018) for Swordfish (Xiphias gladius) in the Indian Ocean using zero-inflated Bayesian hierarchical spatial model. IOTC–2020–WPB18–12.

Ward, P., Elscot, S. 2000. Broadbill swordfish: Status of world fisheries: Bureau of Rural Sciences, Canberra.

Wang, S.P. 2020. CPUE Standardization of Swordfish (*Xiphias gladius*) Caught by Taiwanese Large Scale Longline Fishery in the Indian Ocean. IOTC–2020–WPB18–15.

Wang, S.P. 2026. Updated sex-specific growth parameters for swordfish (*Xiphias gladius*) in the tropical Indian Ocean for the 2026 IOTC stock assessment. IOTC-2026-WPB24-16.

Wang, S.P., Chi-Hong, L., Chiang, W.C. 2010. Age and growth analysis of swordfish (*Xiphias gladius*) in the Indian Ocean based on the specimens collected by Taiwanese observer program. Working paper IOTC-2010-WPB-08 (revision 1).

Walter, J., Hiroki, Y., Satoh, K., Matsumoto, T., Winker, H., Ijurco, A.U., Schirripa, M., 2019. Atlantic bigeye tuna stock synthesis projections and kobe 2 matrices. Col. Vol. Sci. Pap. ICCAT 75, 2283–2300.

Walter, J., Winker, H., 2019. Projections to create Kobe 2 Strategy Matrices using the multivariate log-normal approximation for Atlantic yellowfin tuna. ICCAT-SCRS/2019/145 1–12.

Winker, H., Walter, J., Cardinale, M., Fu, D. 2019. A multivariate lognormal Monte-Carlo approach for estimating structural uncertainty about the stock status and future projections for Indian Ocean Yellowfin tuna. IOTC–2019–WPTT21–xx.

Young, J., Drake, A. 2004. Age and growth of broadbill swordfish (*Xiphius gladius*) from Australian waters. Final report for project 2001/014, Fisheries Research Development Corporation, Canberra, Australia.

11.APPENDIX A: CPUE COMPARISON

Analysis of Indian Ocean CPUE - 2026 Swordfish Assessment

11.1. Introduction

This document presents a comparison of the thirteen catch per unit of effort (CPUE) series submitted for consideration in the 2026 IOTC swordfish (*Xiphias gladius*) assessment in the Indian Ocean using methods developed for CPUE comparisons for stock assessment models within ICCAT. The goals of this analysis are 1) to investigate any relative differences between model inputs so that data conflict is not introduced into the model via indices of abundance (CPUE series) that imply different, conflicting states of nature (i.e. do alternative indices of abundance indicate that the stock is increasing or the stock is decreasing); and 2) to understand which abundance indices should be included in each region in the stock assessment.

11.2. Data

A full description of the thirteen CPUE indices can be found in section 3.6 of this document. Briefly:

11.2.1. Japan longline

- Two series previously used (1979–1993 and 1994–2022), but only the later period (1994–2024) was supplied this time; the earlier segment was shown in 2020 to be uninformative about stock depletion, so its exclusion has little effect on results.
- NW region: stable index, rising 2004–2012 then declining.
- NE region: rose to a high plateau from 2012 through 2024.
- SE region: increasing since 2016, diverging from the declining Taiwan (China) trend.
- SW region: broadly consistent with Portuguese, South African, and Taiwan (China) indices.

11.2.2. Taiwan (China) longline

- Standardised from 2004 to 2023 in each region.
- NE: fluctuates around the mean with relatively high variability, possibly due to inconsistent effort.
- NW: rose 2004–2012, then flat through 2024.
- SE: declining since 2016, in contrast to Japan's rising trend there.
- SW: increasing, consistent with other SW indices.

11.2.3. South Africa longline

- Based on a swordfish-targeted fishery off the west and east coasts.
- Declined 1994–2014, rose 2015–2017, then stable at a lower level from 2018–2024.
- Assigned to the SW region; trend contrasts with the rising Portuguese/Réunion/Japan indices there.

11.2.4. Portugal (European Union) longline

- Pelagic longline fishery (mainly swordfish, with shark bycatch) operating since the late 1990s.
- Declined 2000–2021, but has risen markedly since the last assessment, matching the Réunion index trend.
- Assigned to the SW region.

11.2.5. Indonesia

- Derived from observer data, 2006–2024, assigned to the NE region.
- Stable from 2006–2020, then a marked increase in recent years, similar to the Taiwan (China) NE index.

11.2.6. Réunion (European Union, France)

- Assigned to the SW region; trend rising in line with Portugal and Japan there (limited detail otherwise provided in this excerpt).

11.2.7. Spain (European Union)

- Series covers 2000–2023, assigned to the SW region despite the fleet operating over a wider area.
- Shifting targeting between shark and swordfish is significant, but excluding/including a species-ratio adjustment barely changes the series, suggesting no major consistent bias.
- Overall trend is relatively flat with some variation around the mean.

11.3. Methods

The CPUE time series for swordfish (*Xiphias gladius*) in the Indian Ocean are plotted (**Figure 1**) along with a lowess smoother fitted to the CPUE each year using a general additive model (GAM) to compare trends for the submitted CPUEs. Residuals from the smoother fits to CPUE are compared to identify deviations from the overall trends. This allows conflicts between indices (e.g. highlighted by patterns in the residuals) to be identified.

Correlations between indices are evaluated in **Figure 3** via pairwise scatter plots for CPUE indices where they overlap. The lower triangle shows the pairwise scatter plots between indices with a regression line, the upper triangle provides the correlation coefficients, and the diagonal provides the range of observations along with a linear model fit between them.

A hierarchical cluster analysis was used to evaluate the indices using a set of dissimilarities and the results are plotted in **Figure 4**. This analysis can identify similar and dissimilar trends. If indices represent the same stock components, then it is reasonable to expect them to be correlated. If indices are not correlated or are negatively correlated, i.e. they show conflicting trends, then this may result in poor fits to the data and bias in the parameter estimates obtained within a stock assessment model. Therefore, correlations can be used to select groups of indices that represent a common hypothesis about the evolution of the stock.

Cross-correlations for the region are plotted with a lag from -10 to 10 in **Figure 5** (i.e., the correlations between series when they are lagged by -10 to 10 years) which can help determine whether there is relationship between two time-dependent variables at different time lags. This approach can be particularly useful when comparing indices of abundance for bycatch species derived from fleets targeting different species (i.e. swordfish vs blue shark) or aggregated at different levels (trips *vs* sets).

If all CPUE series are thought to represent the overall dynamics of the stock, careful examination of how one index may lead or lag another, temporal shifts or delays in population dynamics may become apparent (e.g. migration patterns, or the effects of environmental drivers). For example, a strong correlation at a positive lag might indicate that changes in one index precedes changes in another, possibly suggesting sampling of separate part of the stock (e.g. juvenile vs adult).

Conversely, correlations at negative lags may reflect delayed responses in one component of the population to changes in another. Overall, lagged cross-correlation helps clarify potential lead-lag relationships between datasets, offering insights into the relative similarity of the CPUE series. Careful interpretation of the results is suggested given the potential bycatch nature of this stock and the changes fleet dynamics and potential gear or technological creep within the purse seine fisheries.

The diagonals in **Figure 5** show the auto-correlations of an index lagged against itself. This can help identify whether a relationship exists between the CPUE series and earlier years, which would be identified by a large correlation, with the correlations on both sides that quickly become small.

All analyses were conducted using R and FLR, including the *diags* package which provides a set of common methods for reading these data into R, plotting and summarising them (e.g., see: http://www.flr-project.org/).

11.4. Results and conclusions

11.4.1. Overall trend and residual patterns (Figures A1/A2)

Most standardised CPUE series show a broadly similar overall pattern: a decline from the start of each series through to a low point around 2010–2015, followed by a marked increase toward the end of the time series (2020–2024). This recent upward trend is particularly strong for sw_jap, sw_zaf, sw_twn, sw_eu_reu, and ne_idn. The residual plots (**Figure A2**) support this, showing a run of negative residuals (observed CPUE below the smoothed trend) through the mid-2000s to mid-2010s across many series, switching to consistently positive residuals in the most recent years — most notably for sw_jap, sw_zaf, sw_eu_reu, and ne_idn, indicating recent CPUE has increased faster than the long-term smoothed expectation.

Some series depart from this general pattern: nw_jap and nw_twn are comparatively flat with no strong directional trend, aside from an early spike (nw_twn, ~2006–2008); se_twn shows a decline in the final years rather than an increase, in contrast to most other SE/SW series; and sw_eu_esp (Spain) remains relatively flat throughout, fluctuating around the mean without a strong trend in either direction.

11.4.2. Correlations between indices (Figures A3 and A4)

Pairwise correlations (**Figure A3**) and the correlation matrix (**Figure A4**) indicate that most series are positively correlated, though the strength varies considerably. The strongest relationships include:

se_jap and sw_zaf (Corr ≈ 0.71)

sw_eu_reu and sw_twn (Corr ≈ 0.70)

ne_idn and sw_eu_reu (Corr ≈ 0.69)

sw_eu_reu and sw_jap (Corr ≈ 0.64)

ne_idn and sw_eu_esp (Corr ≈ 0.65)

se_jap and sw_eu_reu (Corr ≈ 0.57)

ne_jap and sw_jap (Corr ≈ 0.57)

These strong associations, particularly those involving sw_eu_reu (Réunion), suggest that several fleets across the SE, SW, and NE regions are tracking a common underlying abundance signal in recent years, consistent with the shared upward trend noted above.

A small number of pairings show weak or negative correlations. Notably, nw_twn and sw_eu_esp are significantly negatively correlated (Corr ≈ -0.47), and ne_idn and ne_jap are essentially uncorrelated (Corr ≈ -0.01), suggesting these indices may be capturing different components of the stock or are influenced by differing local fishing dynamics.

The hierarchical clustering (**Figure A4**) broadly separates the indices into two groups: a smaller cluster (se_twn, nw_jap, sw_eu_esp) that correlates relatively weakly with the rest, and a larger cluster (se_jap, sw_zaf, ne_jap, sw_jap, nw_twn, sw_eu_reu, sw_twn, ne_twn, ne_idn, sw_eu_prt) that shows generally stronger positive correlations among its members, particularly among the SW-region and Réunion/Portugal indices.

11.4.3. Lagged cross-correlations (Figure A5)

The lagged cross-correlation matrix shows that for most pairs of indices, correlation peaks at or near zero lag, indicating the series are tracking the same underlying signal contemporaneously rather than with a substantial time offset. This is consistent with the pairwise correlation results and supports the interpretation that many of these fleets/regions are sampling overlapping components of the stock without a strong lagged relationship between them.

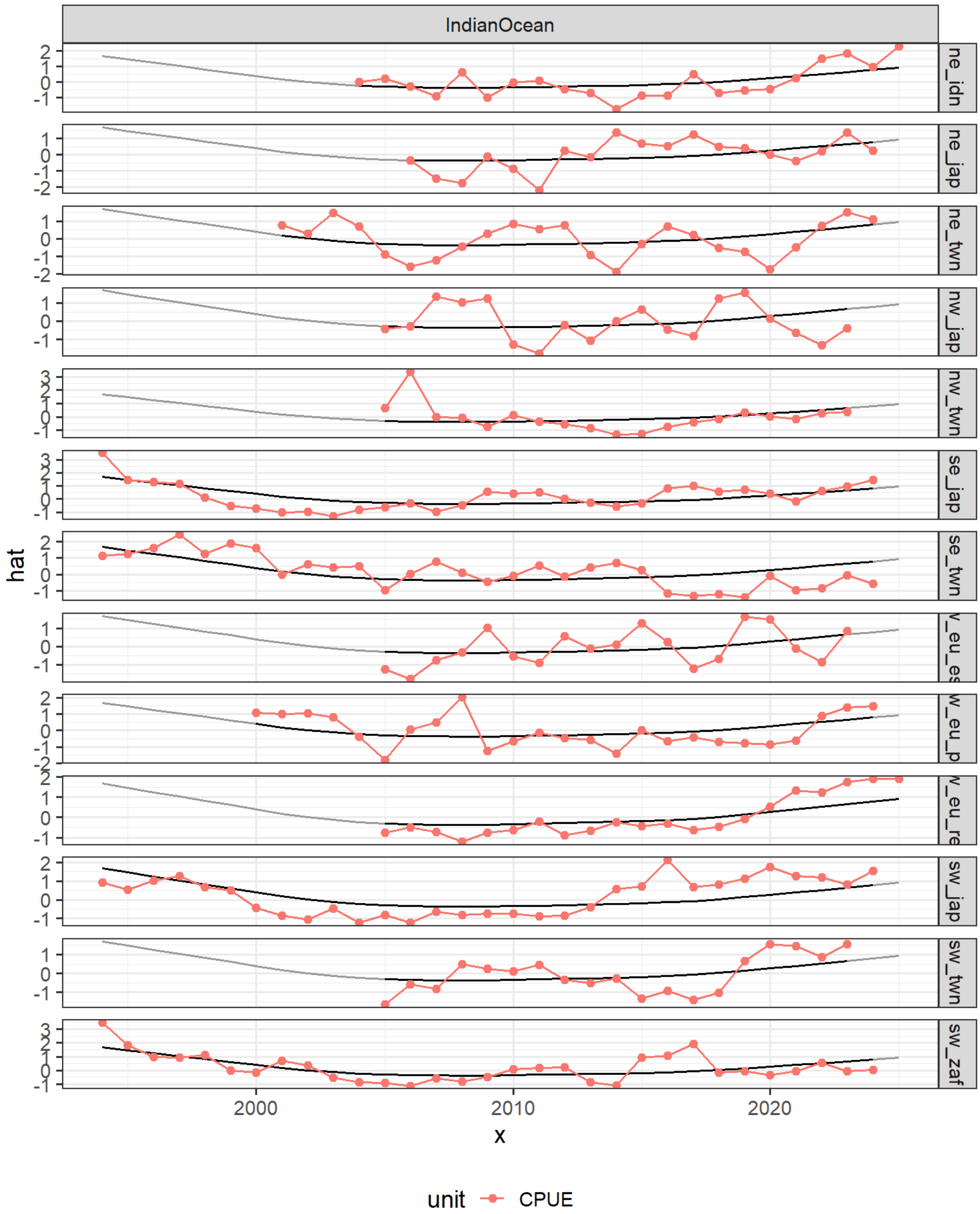

Figure A1. Indian Ocean time series of CPUE indices; Points are the standardized values, continuous black lines are a lowess smoother showing the average trend by area (i.e. fitted to year for each area with series as a factor). X-axis is time, Y-axis are the scaled indices.

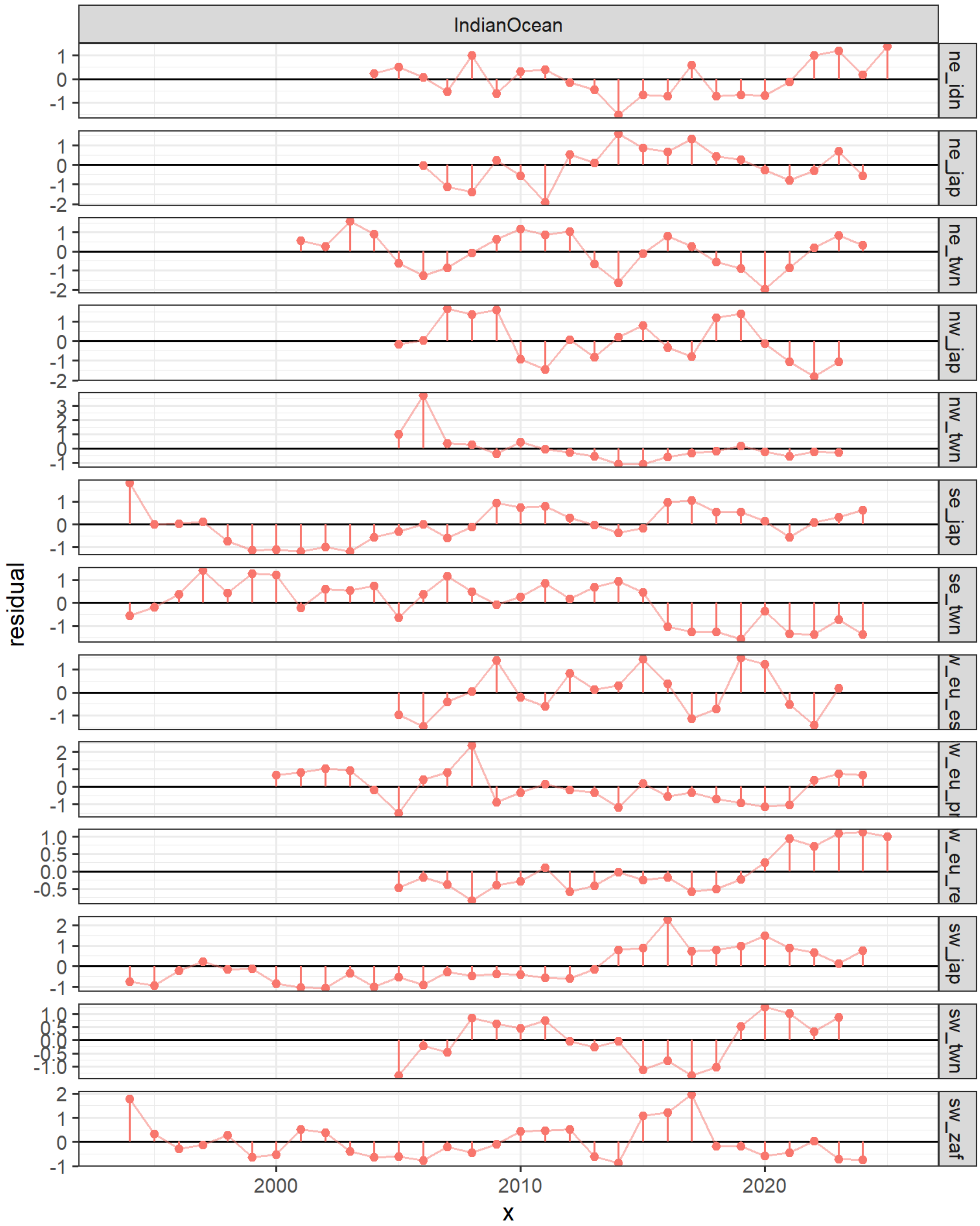

Figure B2. Time series of residuals from the smooth fit to CPUE indices. X-axis is time, Y-axis are the scaled indices.

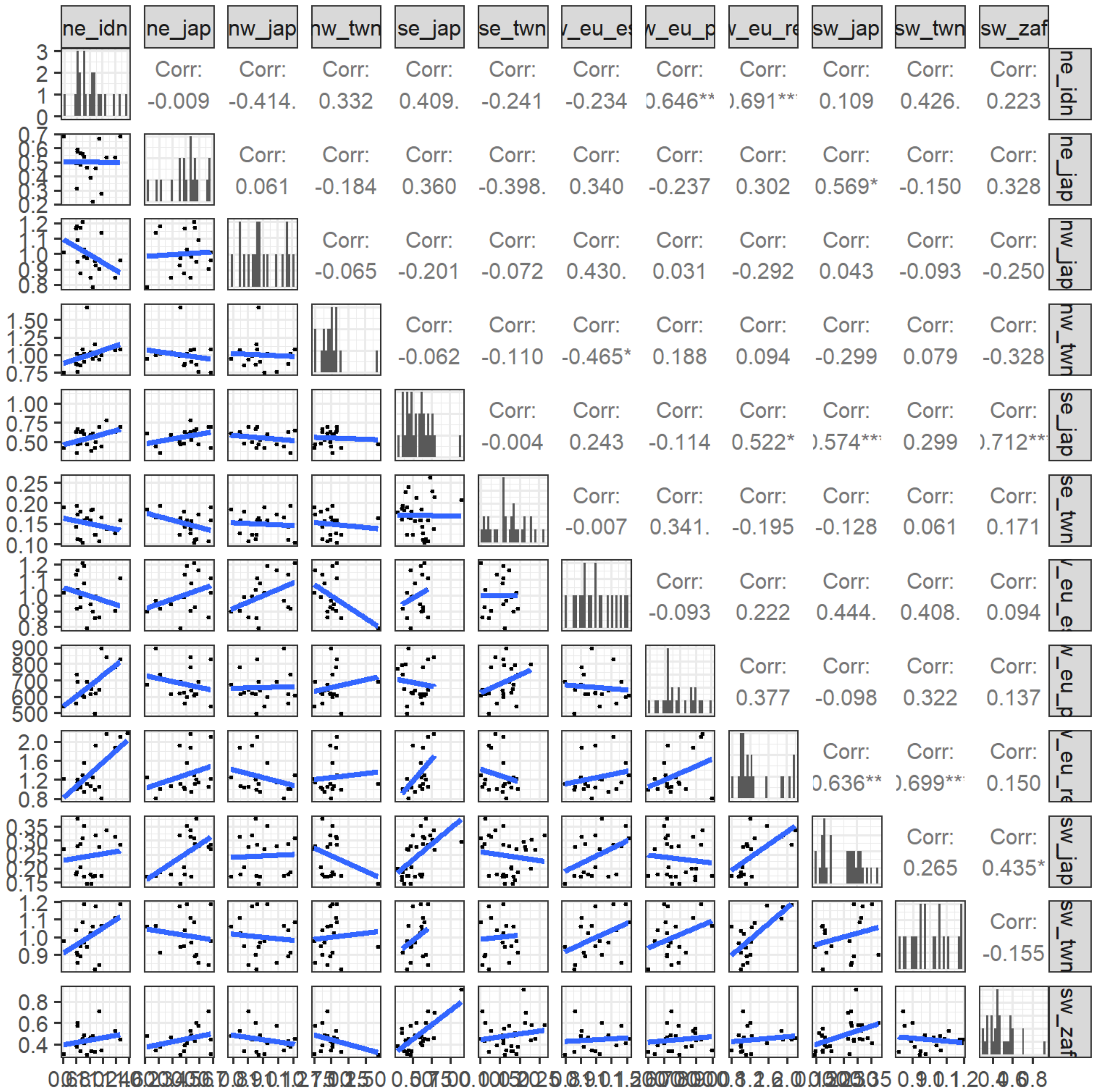

Figure B3. Pairwise scatter plots for CPUE indices. X- and Y-axis are scaled indices.

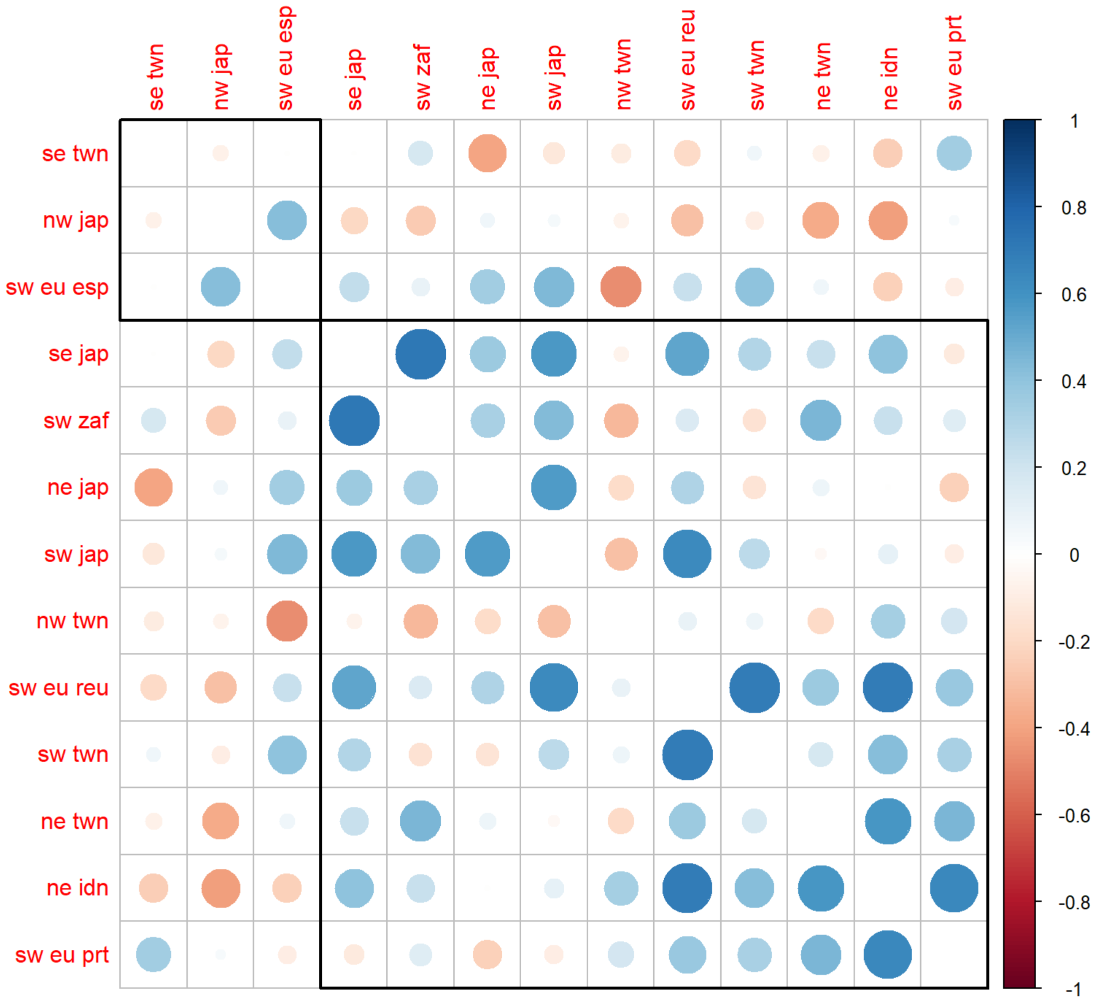

Figure B4. Correlation matrix for CPUE indices; blue indicates positive and red negative correlations, the order of the indices and the rectangular boxes are chosen based on a hierarchical cluster analysis using a set of dissimilarities.

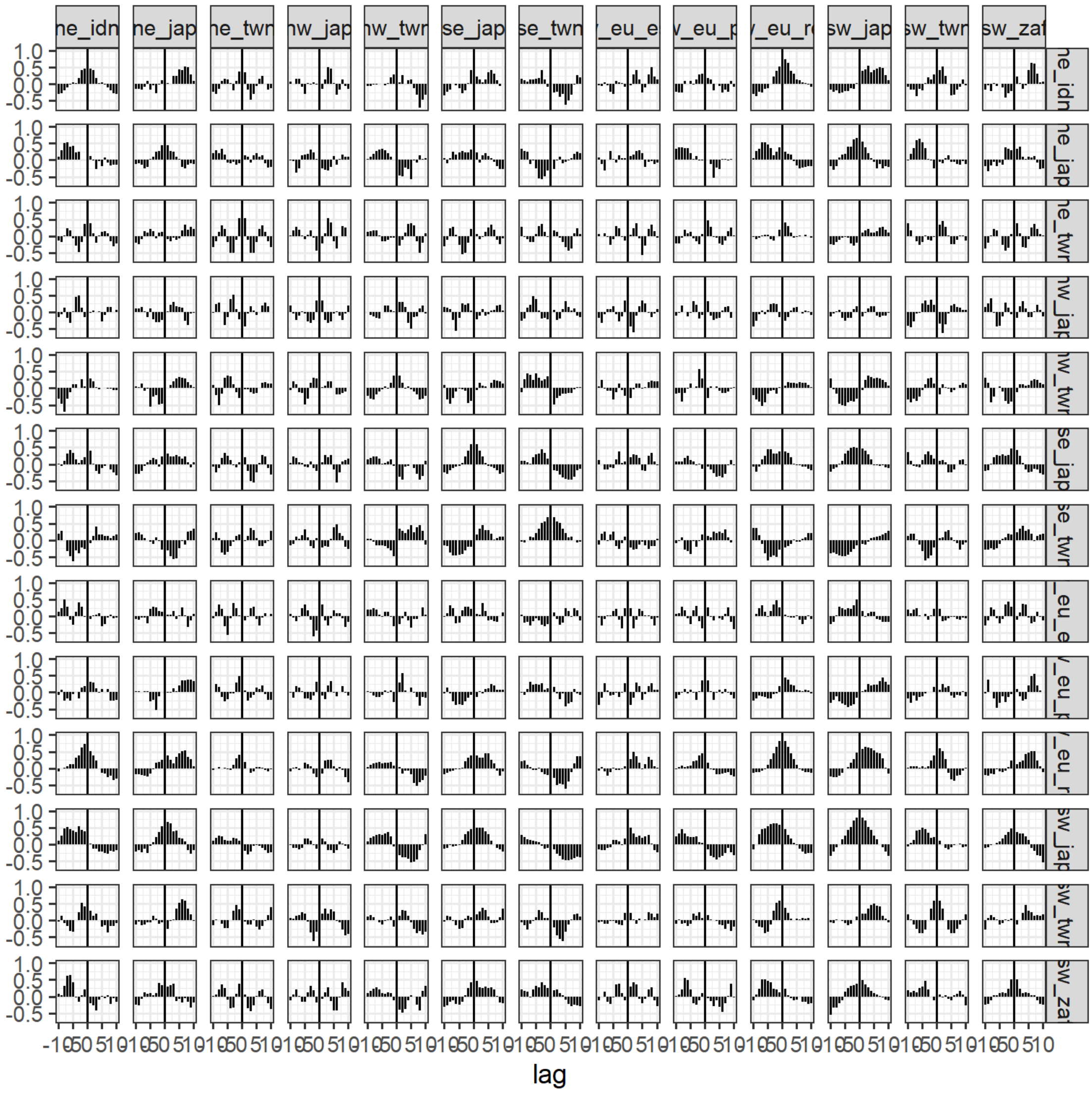

Figure A5 Cross-correlations between CPUE indices to identify lagged correlations (e.g., due to year-class effects). X-axis is lag number, and y-axis is cross-correlation.

12. APPENDIX B

12.1. Fits to length composition data for model sensitivity runs

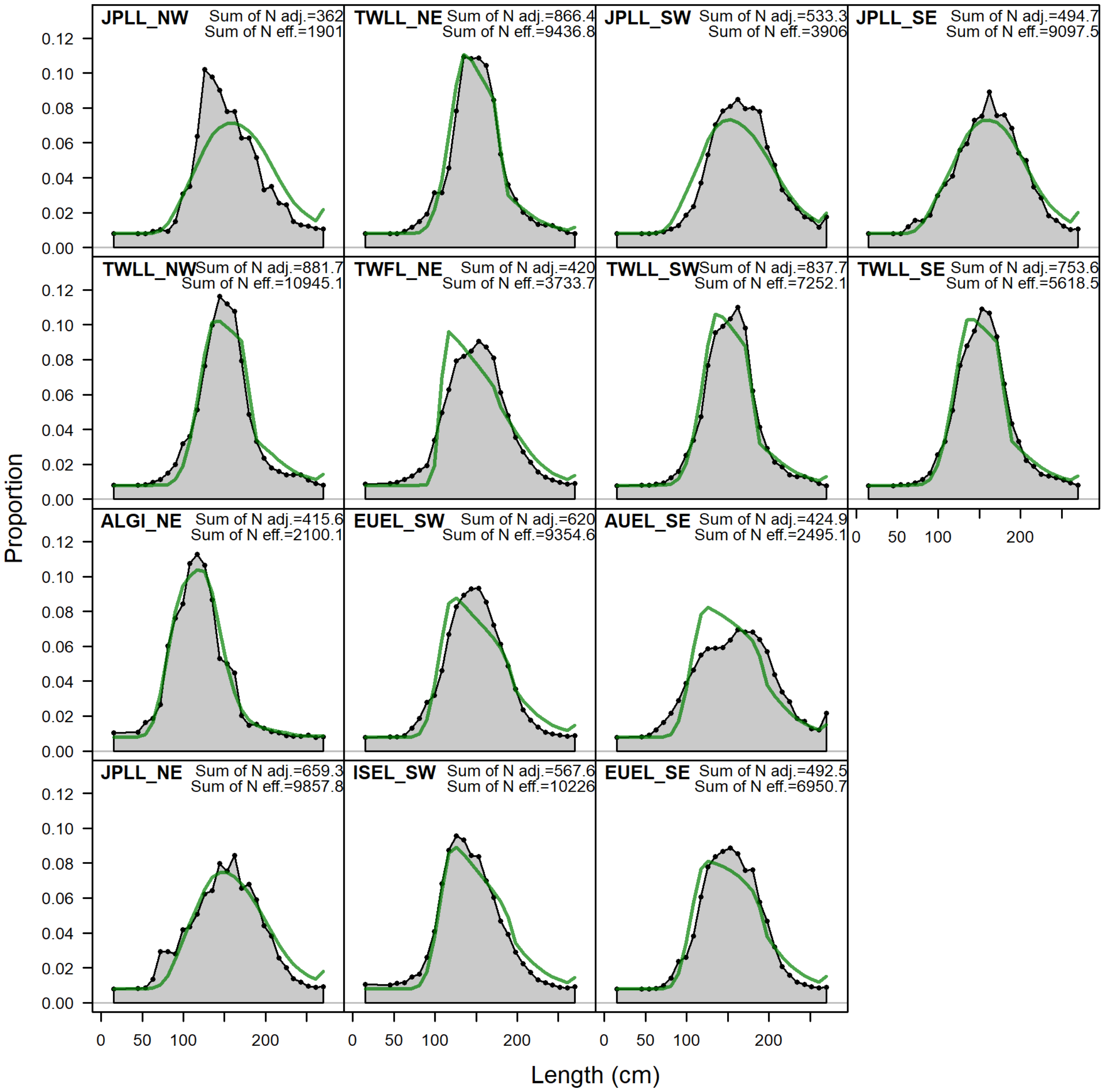

Figure B1: Model estimated fits (green line) to length composition data for the sensitivity run "s3_cpue_tw"

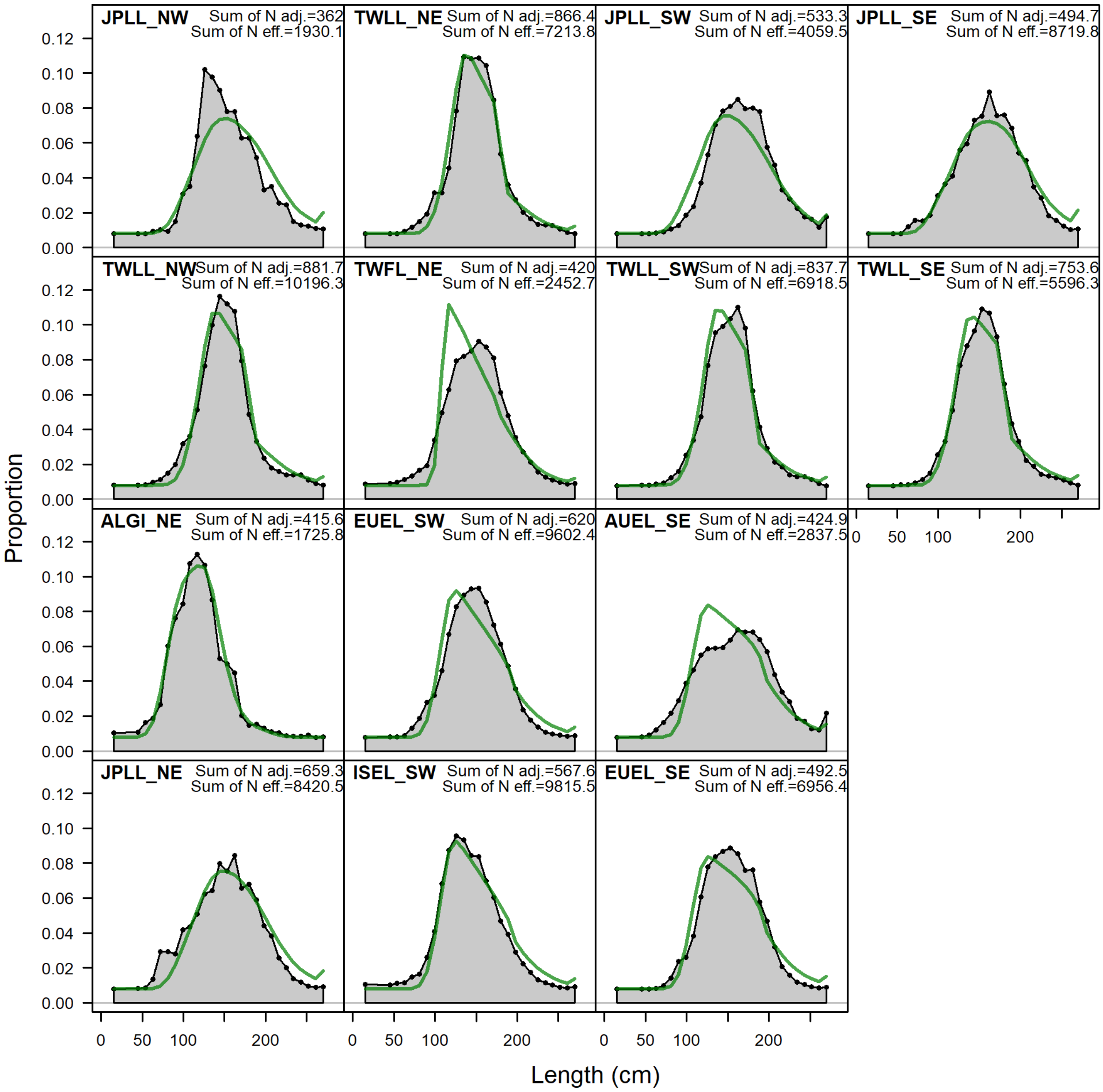

Figure B2: Model estimated fits (green line) to length composition data for the sensitivity run "s4_altCPUE"

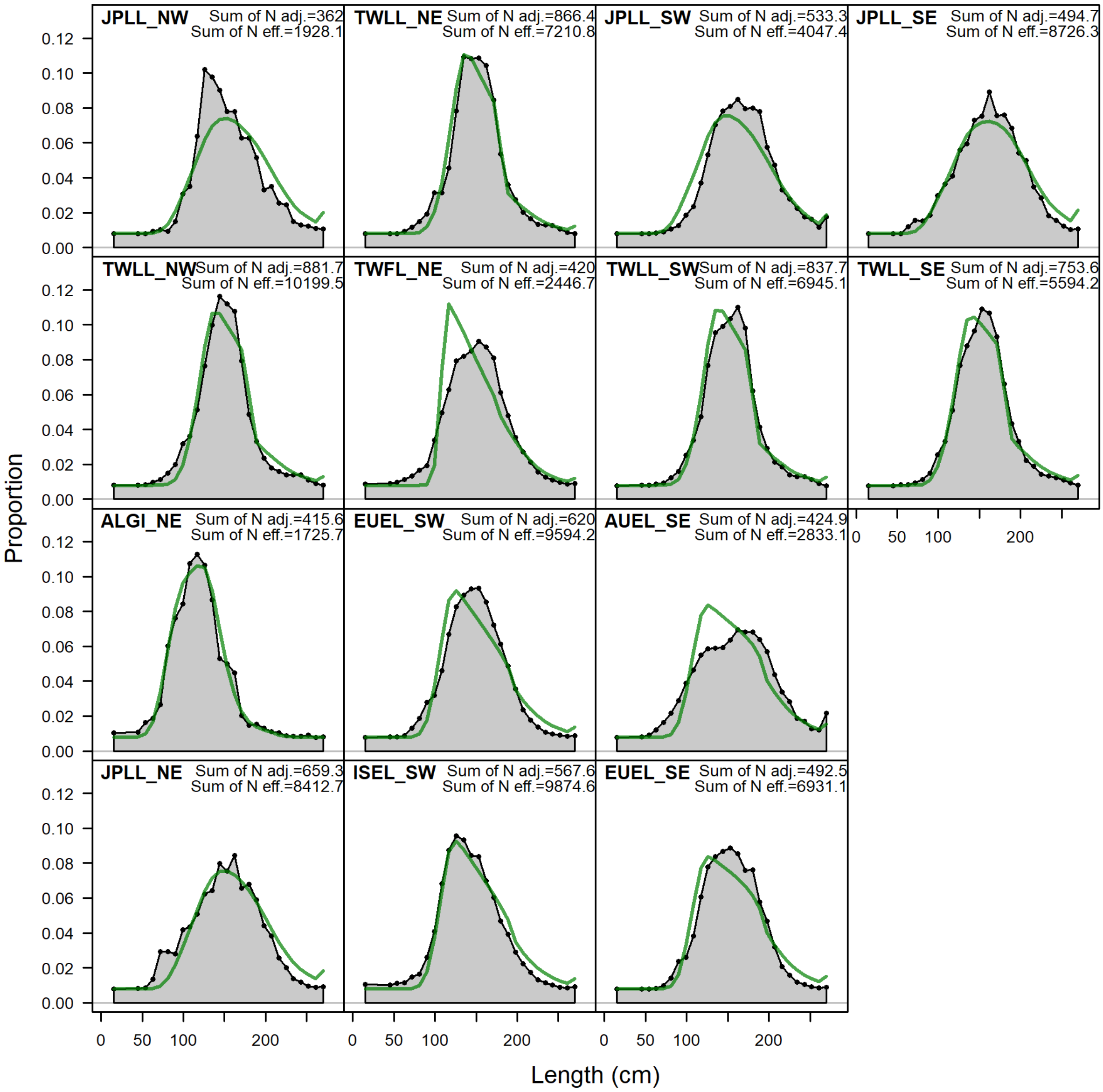

Figure B3: Model estimated fits (green line) to length composition data for the sensitivity run "s5_altCPUE_esp"

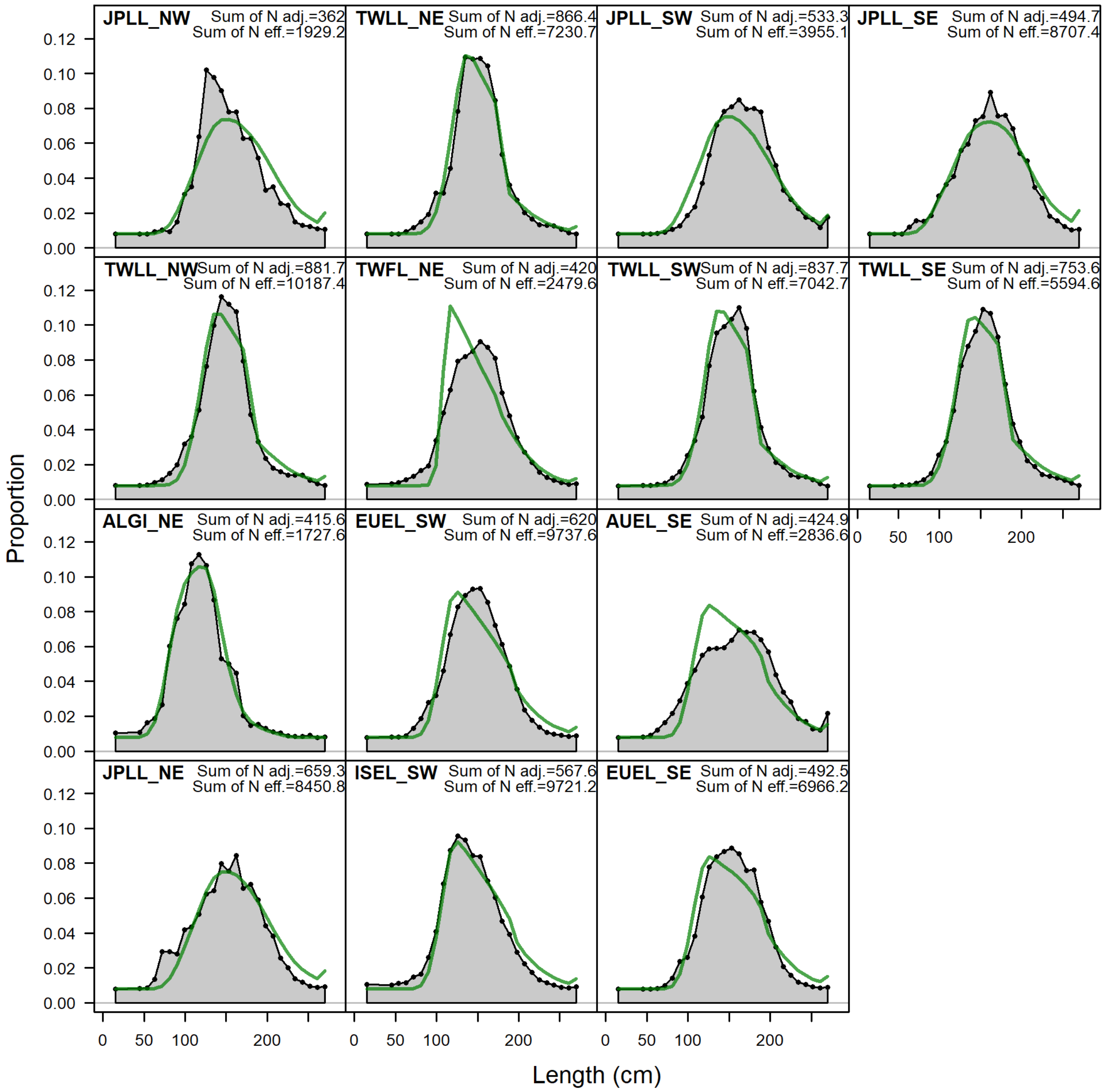

Figure B4: Model estimated fits (green line) to length composition data for the sensitivity run "s6_altCPUE_esp_noreu"

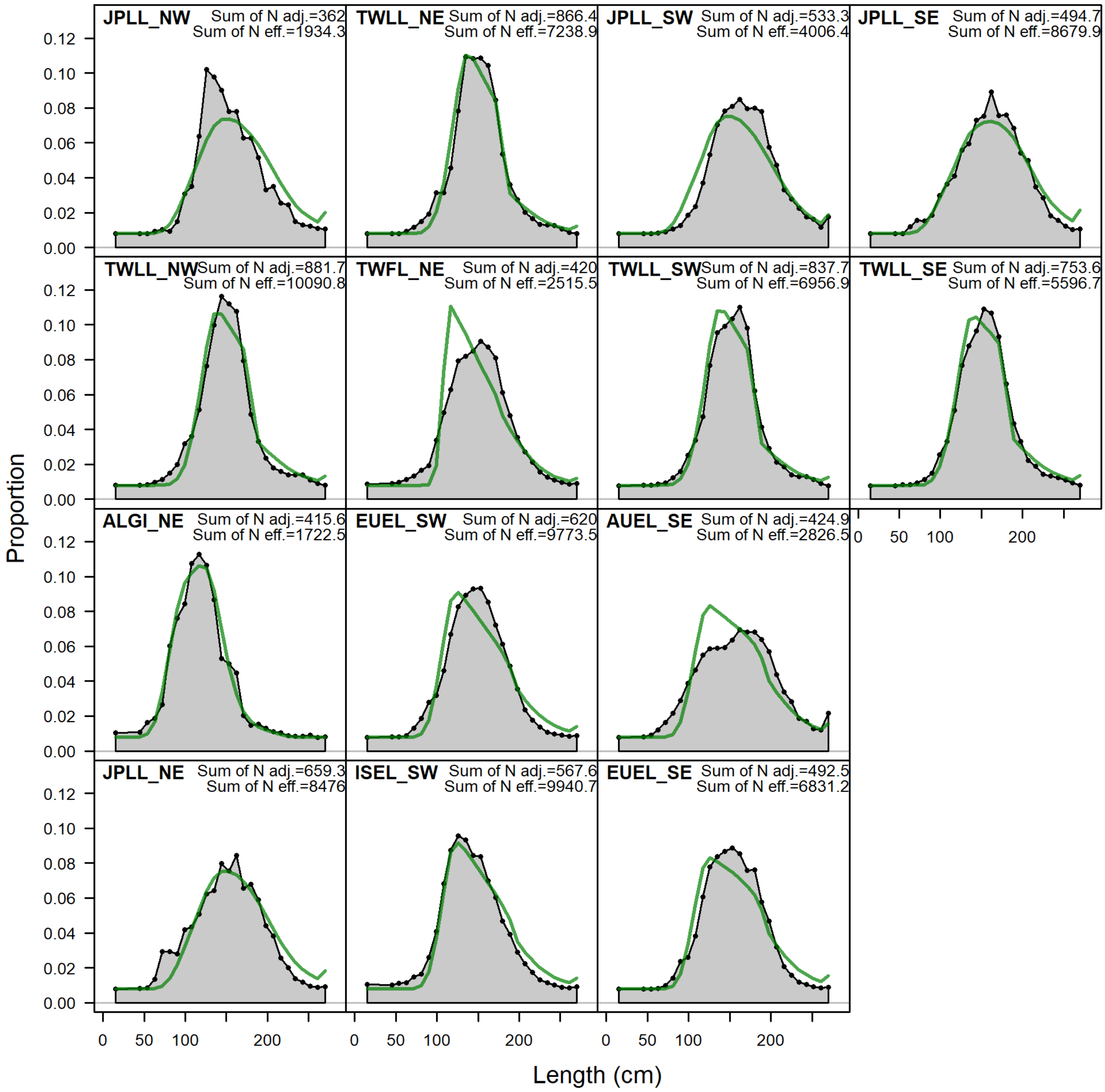

Figure B5: Model estimated fits (green line) to length composition data for the sensitivity run "s7_altCPUE_prt_reu"

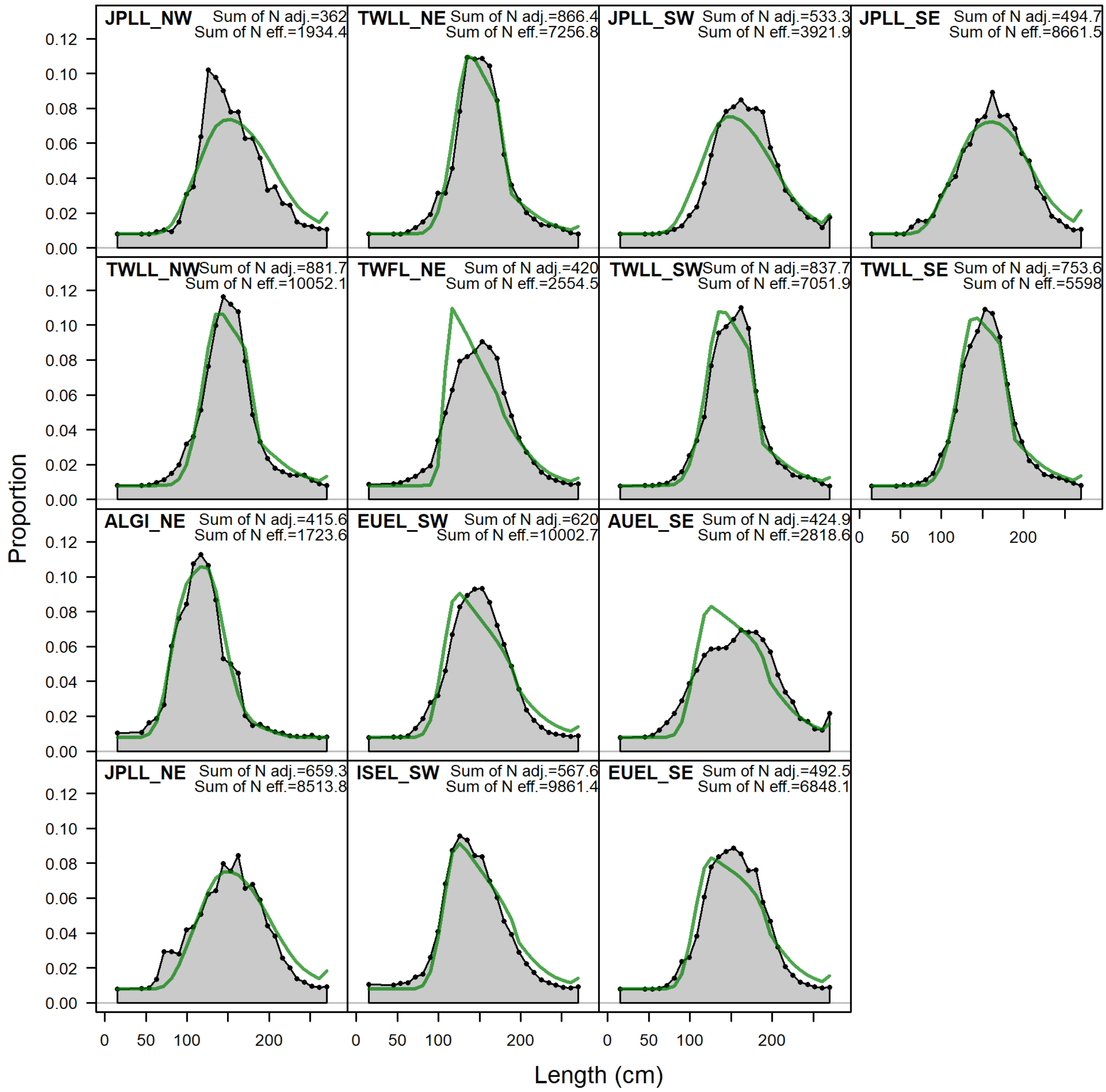

Figure B6: Model estimated fits (green line) to length composition data for the sensitivity run "s8_altCPUE_prt"

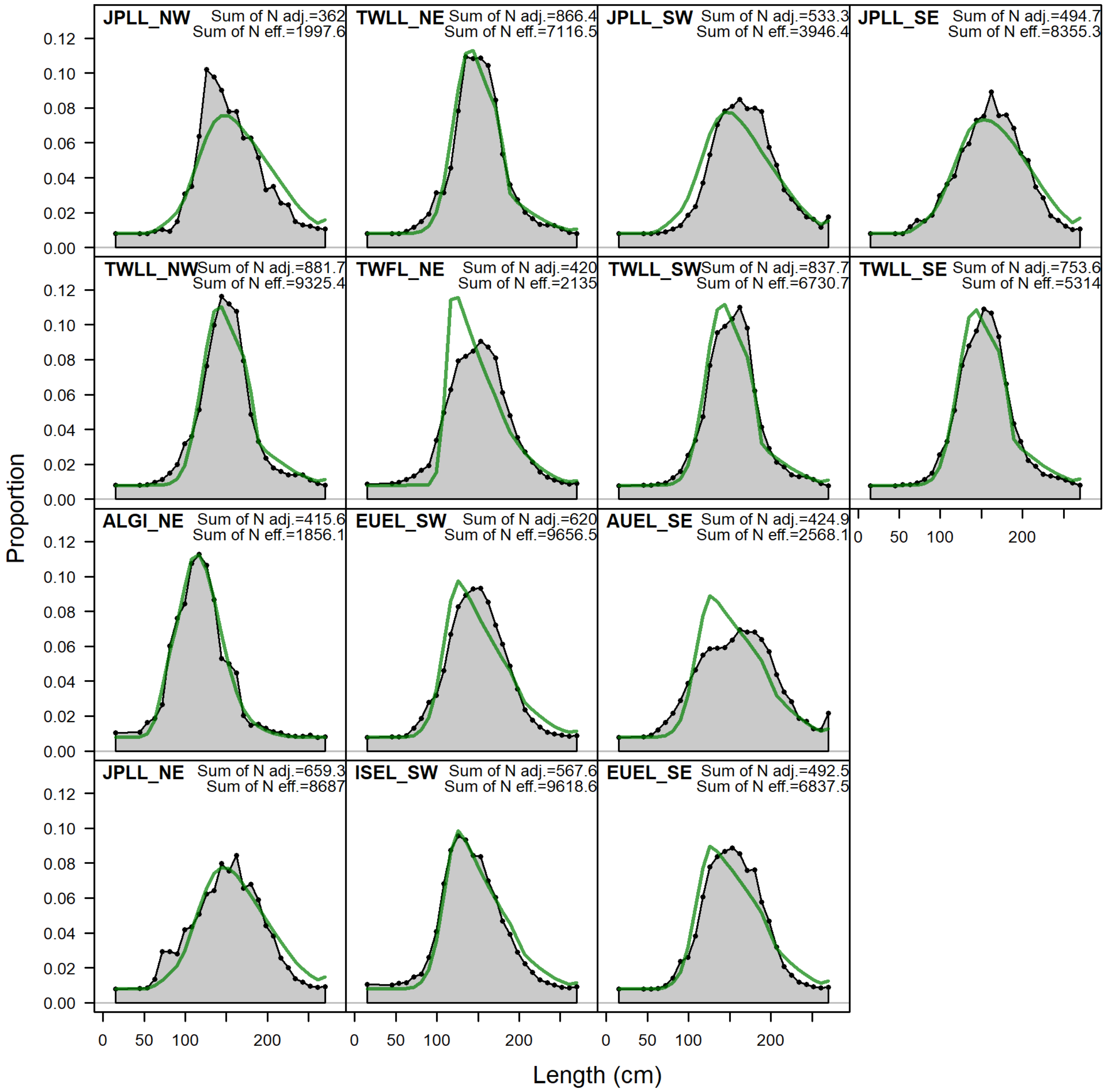

Figure B7: Model estimated fits (green line) to length composition data for the sensitivity run "s9_new_growth"

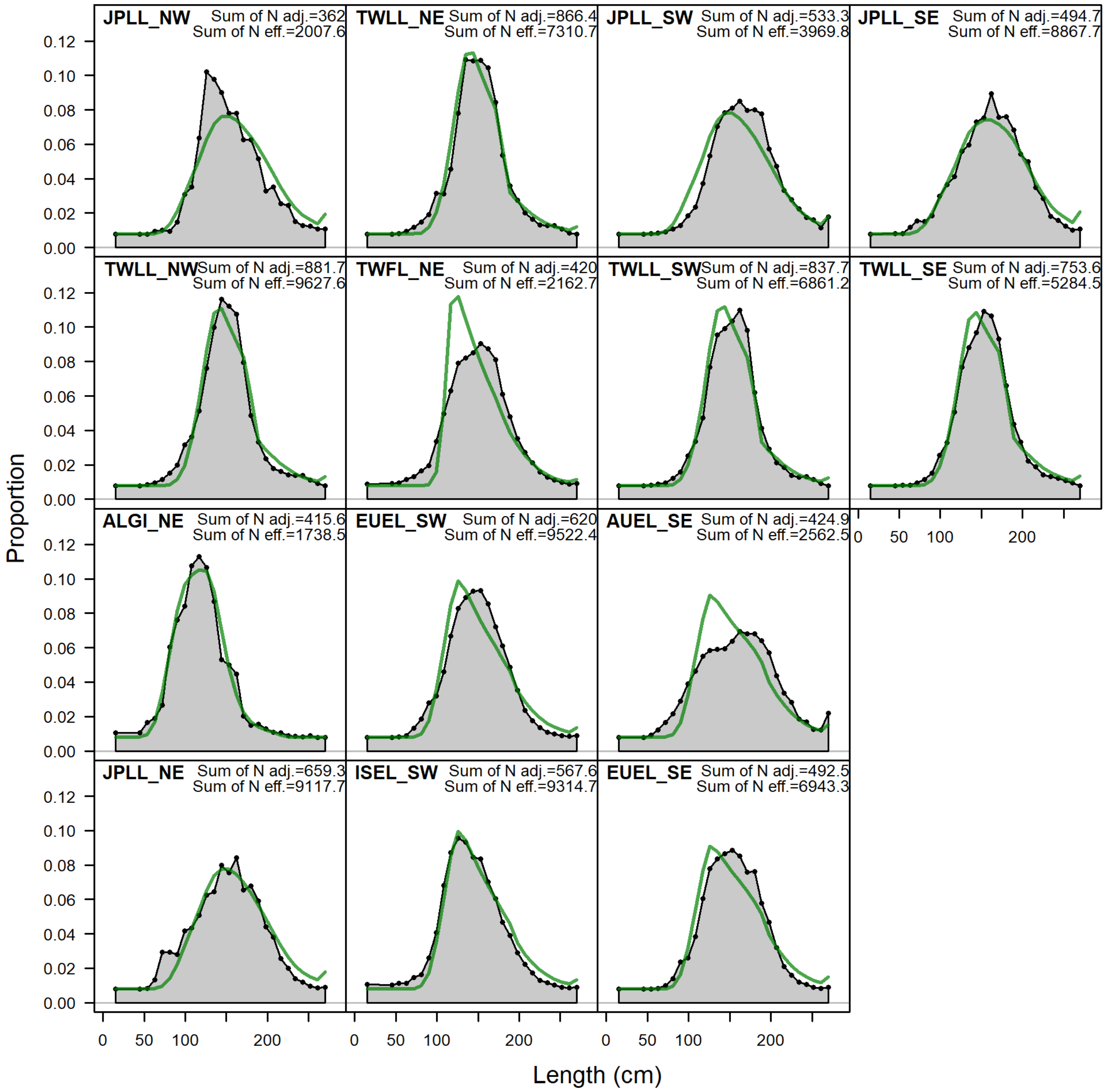

Figure B8: Model estimated fits (green line) to length composition data for the sensitivity run "s10_natM_lorenzen"

12.2. Fits to CPUE data for model sensitivity runs (upweighted CPUE indices)

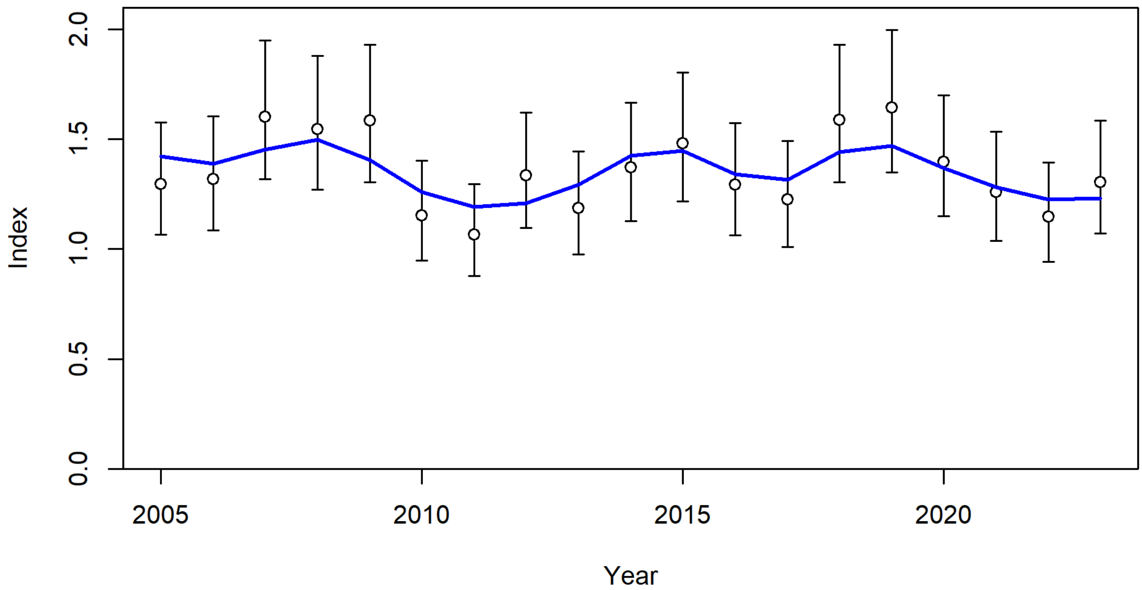

Figure B9: Estimated fit to the TWLL(NE) CPUE index for the model "s3_cpue_tw"

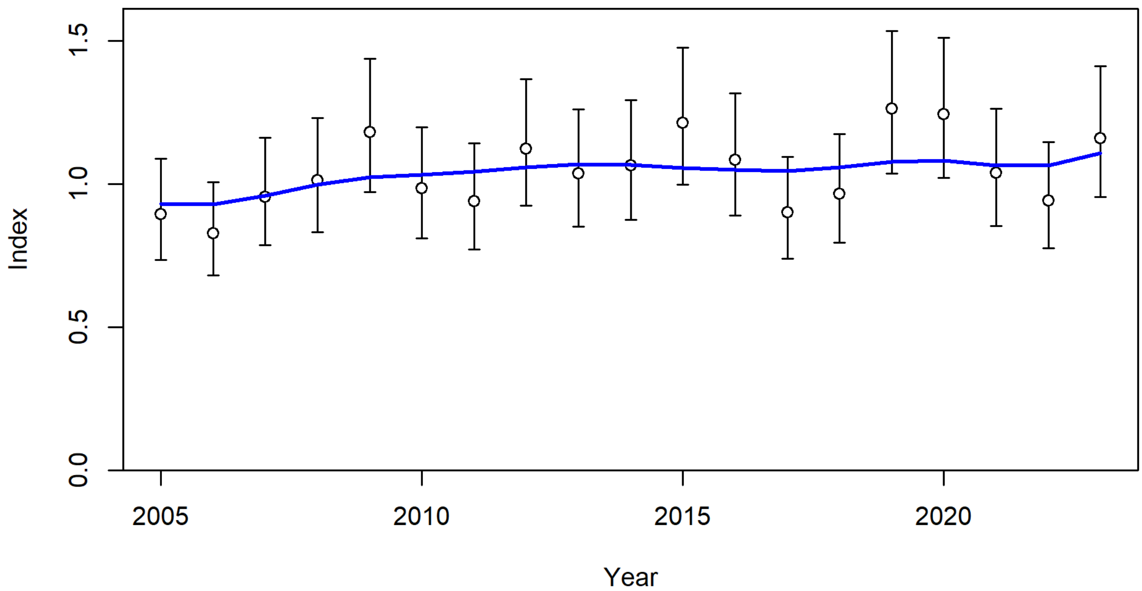

Figure B10: Estimated fit to the TWLL(NW) CPUE index for the model "s3_cpue_tw"

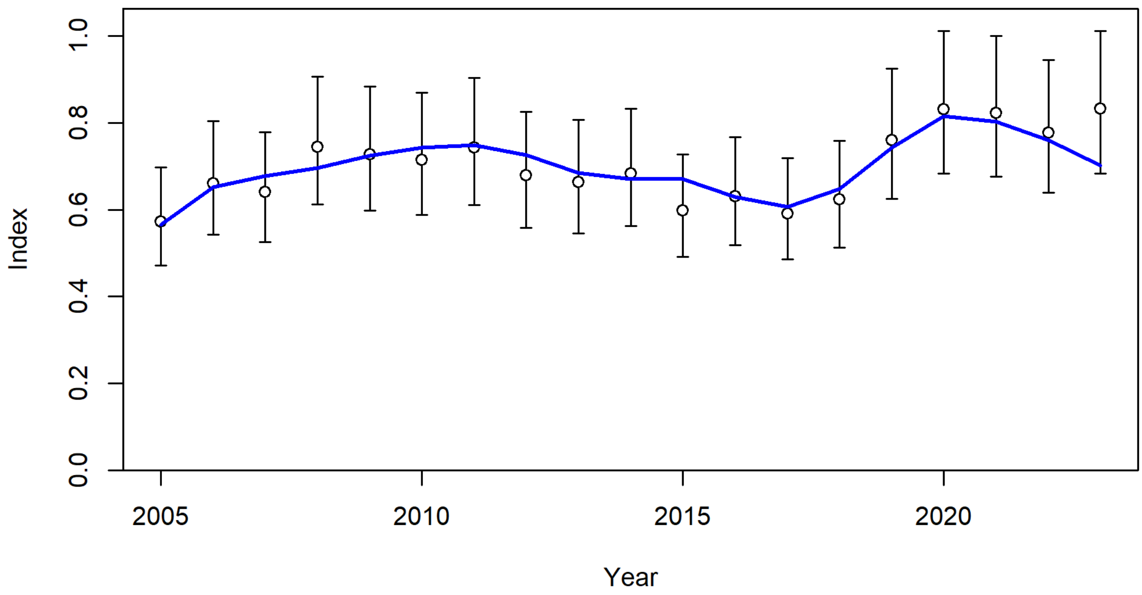

Figure B11: Estimated fit to the TWLL(SW) CPUE index for the model "s3_cpue_tw"

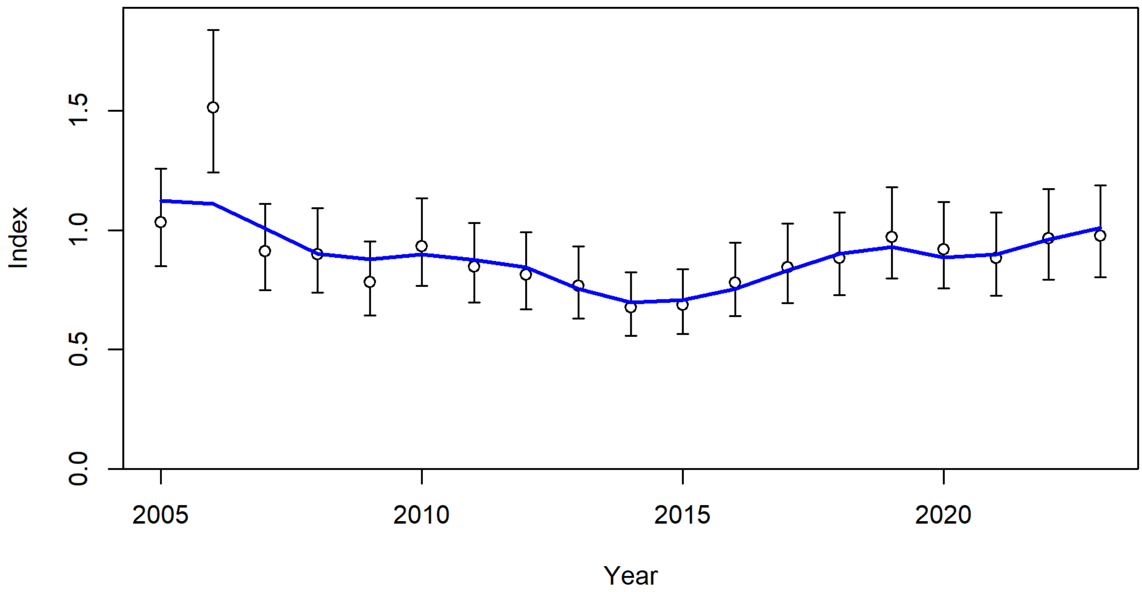

Figure B12: Estimated fit to the TWLL(SE) CPUE index for the model "s3_cpue_tw"

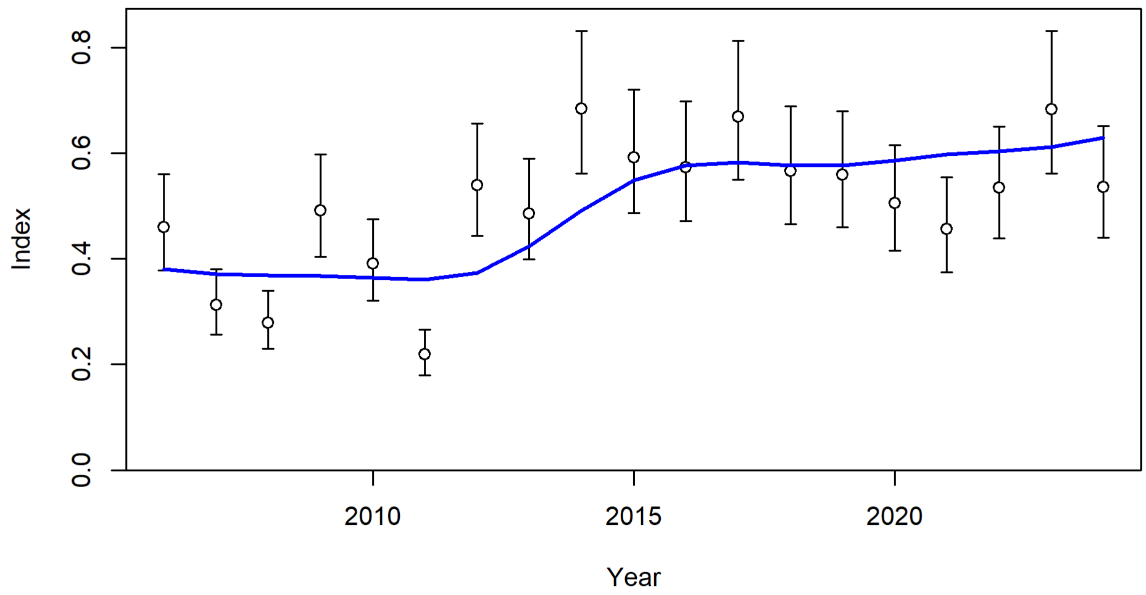

Figure B13: Estimated fit to the IDN(NE) CPUE index for the model "s4_altCPUE". This index had weighting 0.5, compared to 1.0 for JPLL and 0.5 to REU.

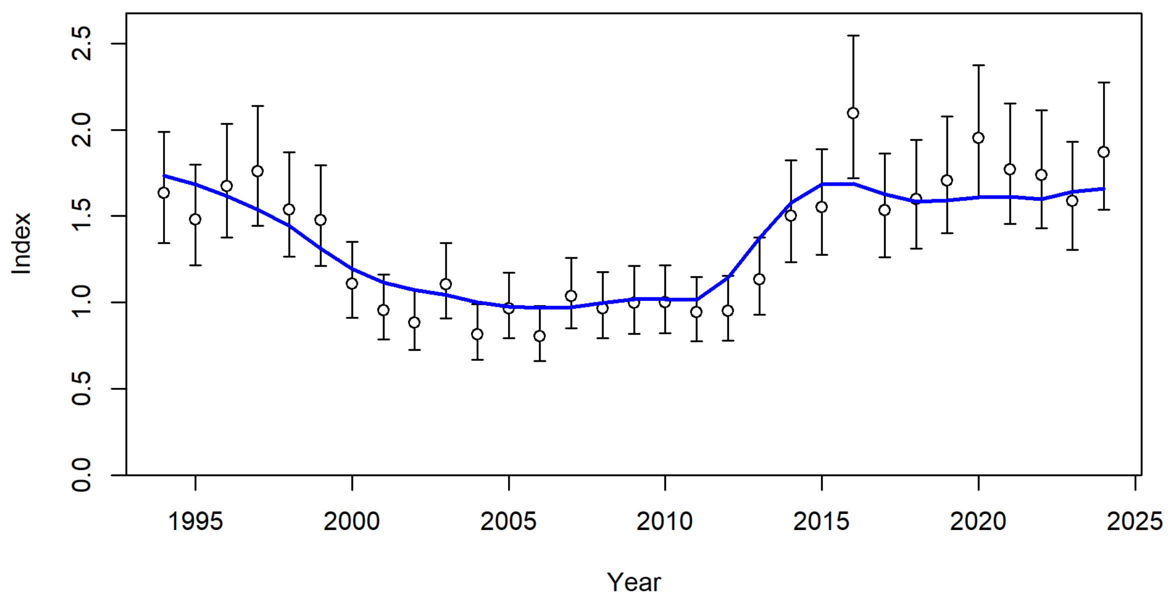

Figure B14: Estimated fit to the JPLL(NE) CPUE index for the model "s4_altCPUE". This index had weighting 1.0, compared to 0.5 for IDN and 0.5 to REU.

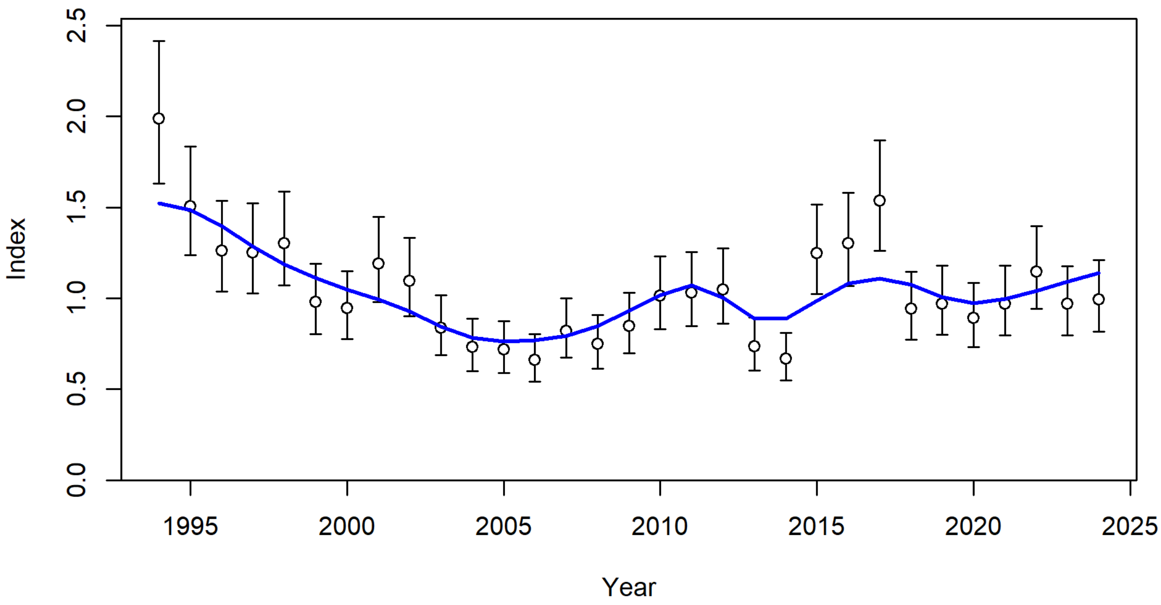

Figure B15: Estimated fit to the JPLL(NW) CPUE index for the model "s4_altCPUE". This index had weighting 1.0, compared to 0.5 for IDN and 0.5 to REU.

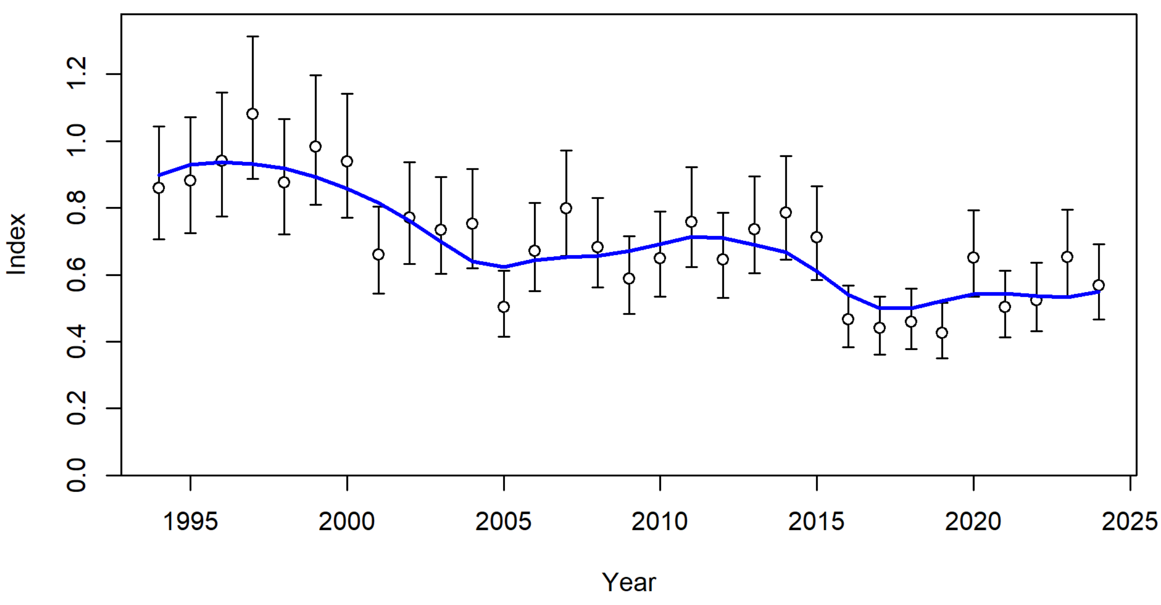

Figure B16: Estimated fit to the JPLL(SW) CPUE index for the model "s4_altCPUE". This index had weighting 1.0, compared to 0.5 for IDN and 0.5 to REU.

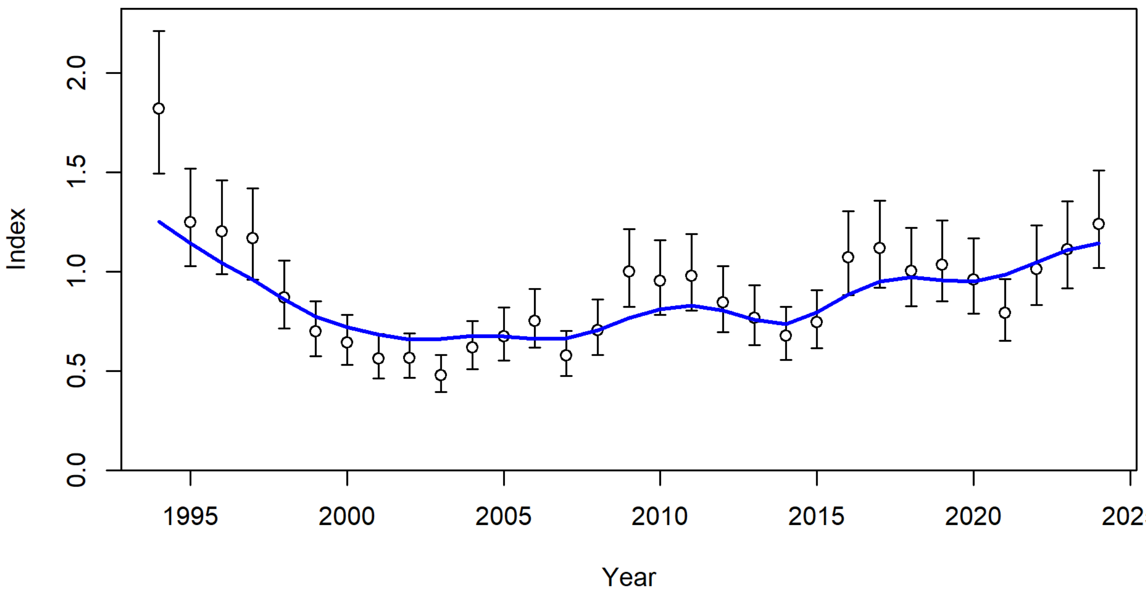

Figure B17: Estimated fit to the JPLL(SE) CPUE index for the model "s4_altCPUE". This index had weighting 1.0, compared to 0.5 for IDN and 0.5 to REU.

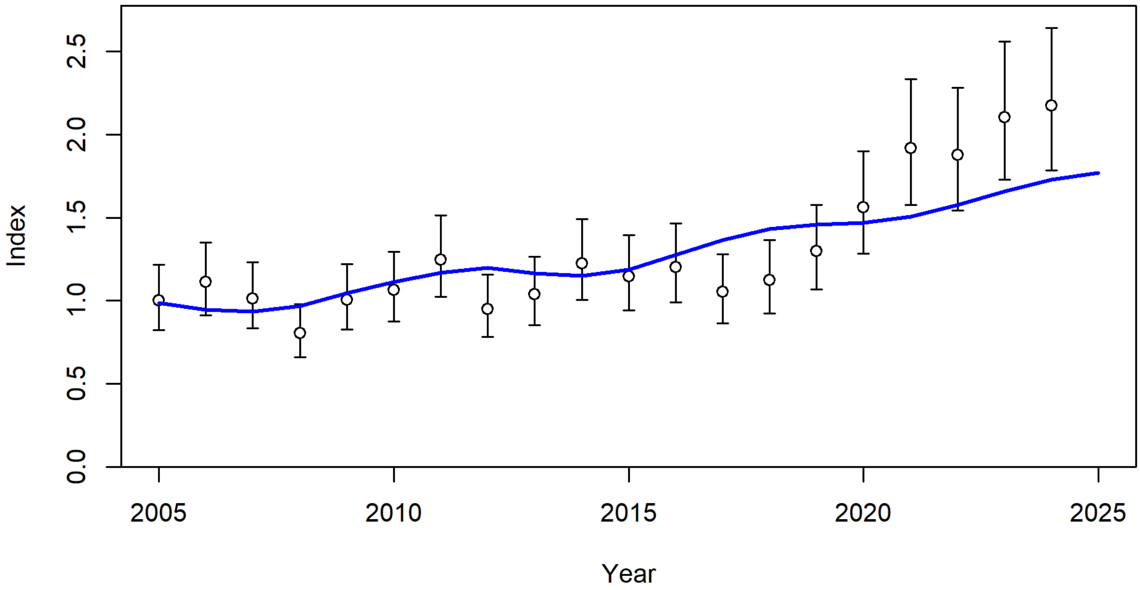

Figure B17: Estimated fit to the REU(SW) CPUE index for the model "s4_altCPUE". This index had weighting 0.5, compared to 0.5 for IDN and 1.0 to JPLL.